# Molecular Characterization of the RING E3 Ubiquitin Ligase LIN41/TRIM71 in Early Neurogenesis

Inaugural-Dissertation
to obtain the academic degree
Doctor rerum naturalium (Dr. rer. nat.)
submitted to the Department of Biology, Chemistry and Pharmacy of
Freie Universität Berlin.

by

**Anna Maria Rohde**

from Berlin, Germany.

Berlin, 2014

April 2010 – March 2014
Institute for Cell and Neurobiology, Charité. Berlin

1st Reviewer: Dr. F. Gregory Wulczyn
2nd Reviewer: Prof. Dr. Florian Heyd
Defense: 1st July 2014

# ACKNOWLEGDEMENTS

Here, I would like to thank my supervisor Dr. Gregory Wulczyn for giving me the opportunity to join his lab and to work on this interesting project. Greg, thank you for the fruitful discussions, the support and great opportunities.

Also, I would like to thank all members of AG Wu: Eli, Fred, Duong, Ele, Daniel and Marlis. Thanks for all the support, the nice atmosphere and good times; science-wise and else. You all make this group as special as it is. I could not have wished for a better. Especially Eli, thank you for being my last-minute-Postdoc, but much more for being with me through everything in the last years, for being my friend.

Thanks to everyone in the Institute of Cell and Neurobiology; thanks for making it a nice place to work at, with a friendly and helpful atmosphere (and the one or the other BBQ and party).

Moreover, I would like to thank my mentors from University: Prof. Dr. Matthias Dobbelstein at the University of Göttingen and Dr. Lars Holmgren at Karolinska Institutet, Stockholm, for their support and advice.

I would like to thank my friends from Goslar, Göttingen, Stockholm and Berlin, for being with me on this incredible journey.

But mostly, I want to thank my whole family; especially my aunt Margrit for inspiring me since I have been a 5-year-old and my parents for always understanding me, for being with me all my life, supporting all my decisions.

# TABLE OF CONTENTS

# TABLE OF FIGURES

# ABBREVIATIONS

| | |
|---|---|
| A | alanine |
| aa | amino acid |
| ADHD | attention deficit hyperactivity disorder |
| AGO | Agonaute |
| amp | ampicillin |
| ASD | autism spectrum disorder |
| ATP | adenosine triphosphate |
| BERP | Brain-expressed RING |
| bp | basepair |
| BRAT | brain tumor |
| BSA | bovine serum albumin |
| C | cysteine |
| *C. elegans* | Caenorhabditis elegans |
| CBL | Casitas B-lineage lymphoma |
| cDNA | coding DNA |
| CNS | central nervous system |
| d | day |
| *D. melanogaster* | Drosophila melanogaster |
| DAPI | 4',6-diamidino-2-phenylindole |
| DGCR8 | DiGeorge syndrome critical region gene 8 |
| DNA | desoxyribonucleic acid |
| ds | double-stranded |
| E | embryonic day |
| *E. coli* | Escherichia coli |
| E1 enzyme | ubiquitin activating enzyme |
| E2 enzyme | ubiquitin-conjugating enzyme |
| E3 enzyme | ubiquitin-protein ligase |
| ECL | enhanced chemiluminescence |
| EHV | equine herpes virus |
| ESC | embryonic stem cells |
| FACS | fluorescence assisted cell sorting |
| FBS | fetal bovine serum |
| g | gram |
| G418 | geneticin |
| GABA | γ aminobutyric acid |
| GFP | green fluorescent protein |
| GKAP | guanylate kinase-associated protein |
| gMyo | myosin globular domain |
| GW182 | N-terminal glycin (G) - tryptophane (W) rich protein of 182 kDa |
| H | histidine |
| h | hours |
| H3K9me3 | histone 3 lysine 9 trimethylation |
| HBS | HEPES buffered saline |
| HEK293T | human embryonic kidney 293T cells |
| HMGA2 | high mobility group AT hook 2 |
| hsa | homo sapiens |
| HT2A | human immunodeficiency virus transactivator of transcription interacting protein 2A |
| Ig | immune globulin |
| iLin41 cells | Flag-Lin41 inducible cells |

| | |
|---|---|
| IMP1 | insulin-like growth factor 2 mRNA binding protein 1 |
| IP | immunoprecipitation |
| ISG15 | interferon-stimulated gene 15 |
| IZ | intermediate zone |
| kana | kanamycin |
| kbp | kilo base pairs |
| kDa | kiloDalton |
| L | larval stage |
| LB | lysogeny broth |
| let-7 | lethal 7 |
| LGMD | Limb-girdle muscular dystrophy |
| LIN28 | abnormal cell lineage protein 28 |
| LIN41 | abnormal cell lineage protein 41 |
| Luci | luciferase |
| M | molar |
| m | milli |
| min | minutes |
| miR | microRNA |
| ml | Milliliter |
| MOV10 | Moloney leukemia virus 10 |
| mRNA | messenger RNA |
| mut | mutant |
| MYC | myelocytomatosis oncogene |
| MZ | mantle zone |
| NARF | neural activity-related RING finger |
| NE | neuroepithelium |
| NEDD8 | neural precursor cell expressed developmentally downregulated 8 |
| NF-L | neurofilament light chain |
| NGF | nerve growth factor |
| NHL | Nhl HT2A Lin41 |
| nm | nanometer |
| NMDA | N-methyl-D-aspartate |
| OCT4 | octamer-binding transcription factor 4 |
| P body | processing body |
| PB | phosphate buffer |
| PBS | phosphate buffered saline |
| PCR | polymerase chain reaction |
| PFA | paraformaldehyde |
| PML | promyelocytic leukemia |
| pre-miR | precursor microRNA |
| pri-miR | primary microRNA |
| PTBP | Polypyrimidine tract binding protein |
| PTZ | pentylenetetrazol |
| qRT-PCR | quantitative real-time PCR |
| RA | retinoic acid |
| RARα | retinoic acid receptor α |
| REST | RE1-silencing transcription factor |
| RING | really interesting new gene |
| RISC | RNA-induced silencing complex |
| RNA | ribonucleic acid |
| rpm | revolutions per minute |
| RT | room temperature |
| SDS | Sodium dodecyl sulfate |

| | |
|---|---|
| sec | seconds |
| shRNA | small hairpin RNA |
| siRNA | small interfering RNA |
| SOX2 | sex determining region Y – Box 2 |
| ss | single-stranded |
| STM | sarcotubular myopathy |
| SUMO | small ubiquitin-like modifier |
| SVZ | subventricular zone |
| TBE | Tris-borate-EDTA buffer |
| TEMED | N,N,N',N'-Tetramethylethylenediamine |
| TLX | tailless gene homologue protein |
| TRBP | human immunodeficiency virus 1 transactivating response RNA binding protein |
| TRIM | tripartite motif |
| Trim | tripartite motif |
| Ub | ubiquitin |
| UTR | untranslated region |
| VZ | ventricular zone |
| WB | western blot |
| wt | wild type |
| zn | zinc |
| µl | microliter |
| µm | micrometer |

## SUMMARY

The RING E3 ubiquitin ligases TRIM2, TRIM3, TRIM32 and LIN41/TRIM71 form the mammalian TRIM-NHL protein family. They contain a characteristic domain structure consisting of an N-terminal **tri**partite **m**otif (TRIM) and a C-terminal NHL domain. The TRIM-NHL proteins have reciprocal expression patterns in development: LIN41 is highly expressed in stem cells and early embryos and is downregulated during development, while expression of the other family members TRIM2, TRIM3 and TRIM32 increases. Relatively little was known about the function of TRIM-NHL proteins at the beginning of this thesis. In pluripotent cells, LIN41 was shown to target ARGONAUTE2, the effector protein in the RNA-induced silencing complex, for proteasomal degradation resulting in a repression of microRNA activity. During differentiation, *Lin41* is efficiently downregulated at the transcriptional and at the post-transcriptional levels, the latter by the combined action of let-7 and miR-125 (two differentiation-associated microRNA). Homozygous *Lin41* gene trap mice showed embryonic lethality. Knockout mice of the other TRIM-NHL proteins were viable and displayed various central nervous system phenotypes.

The goal of the thesis was to investigate potentially shared functions of TRIM-NHL proteins. Therefore it was determined if TRIM32 and LIN41 interact with MYOSIN V (like TRIM2 and TRIM3) and if LIN41 influences endosomal trafficking (like TRIM3). The results presented in this thesis indicate that LIN41 and TRIM32 bind MYOSIN V, but (unlike TRIM3) LIN41 does not influence endosomal trafficking. Furthermore, the question of a LIN41 effect on pluripotency and of a possible regulation of microRNA activity by the other TRIM-NHL proteins was addressed. The results suggest that LIN41 affects pluripotency only indirectly and that TRIM32, but not TRIM2 or TRIM3, is able to mimic LIN41 function in a microRNA sensor assay.

The major focus of this thesis was to investigate the potential interplay between LIN41 and the other TRIM-NHL family members in early neurodevelopment. In *C. elegans*, loss of the *Trim32* ortholog was reported to rescue the heterochronic phenotype of a hypomorphic *lin-41* mutant, demonstrating a

genetic interaction between the two. To date, the idea that mammalian TRIM-NHL proteins may directly and functionally interact has been largely neglected. Using co-immunostaining, co-localization of all three other TRIM-NHLs with LIN41 in cytoplasmatic foci of transfected cells was observed. In sections of E11.5 embryos, co-staining of the four TRIM-NHL proteins in the neuroepithelium was shown. Unexpectedly, the four TRIM-NHL proteins were also co-expressed in pluripotent embryonic stem cells. Co-immunoprecipitation employing E11.5 head extracts revealed an RNA-independent physical interaction of TRIM2, TRIM3 and TRIM32 with LIN41. As all four TRIM-NHL proteins are functional RING E3 ubiquitin ligases, this result indicates that they may act in a combinatorial fashion. Mutual ubiquitination or change of target specificity upon interaction of LIN41 and TRIM32 (which showed an almost complete co-localization) was hypothesized. Indeed, LIN41 overexpression in embryonic stem cells led to downregulation of TRIM32. Analysis of the global ubiquitination landscape of embryonic stem cells revealed LIN41-driven ubiquitination of TRIM32. TRIM32 is a pro-differentiation factor in neural stem cells and enhances retinoic acid signaling. This suggests that LIN41 may prevent premature differentiation of pluripotent cells at least in part by regulating TRIM32 activity. Together, this research provides novel insight into the developmental roles of LIN41 by elucidating its functional interaction with other members of the TRIM-NHL family during mammalian neurodevelopment.

# ZUSAMMENFASSUNG

Die RING E3 Ubiquitinligasen TRIM2, TRIM3, TRIM32 und LIN41/TRIM71 bilden mit ihrer charakteristischen Domänenstruktur, einer N-terminalen TRIM (**tri**partite **m**otif) und einer C-terminalen NHL-Domäne, die TRIM-NHL Proteinfamilie. In der Säugetierentwicklung weisen TRIM-NHL Proteine entgegengesetzte Expressionsmuster auf: LIN41 ist in Stamzellen und in frühen Entwicklungsstadien stark exprimiert. Diese Expression wird im Verlauf der Entwicklung herunterreguliert, während die Expression von TRIM2, TRIM3 und TRIM32 ansteigt. Die Funktion der TRIM-NHL Proteine war zu Beginn der hier vorliegenden Dissertation weitestgehend unbekannt. Für LIN41 war bereits beschrieben, dass es in pluripotenten Zellen ARGONAUTE2 (das Mediatorprotein für microRNA-Funktion) für proteasomalen Abbau markiert und dadurch zu verringerter microRNA Aktivität führte. Während der Differenzierung wird nicht nur die Transkription von *Lin41* verringert, auch bereits bestehende *Lin41* mRNA wird durch let-7 (eine differenzierungs-assoziierte microRNA) reprimiert. Homozygote Tiere des *Lin41* "gene trap knockout" Mausmodells sind nicht überlebensfähig und sterben in der Embryonalphase. Mäuse, die homozygot für die Deletion des TRIM2, TRIM3 oder TRIM32 Gens sind, sind hingegen überlebensfähig; jedoch weisen die Tiere Missbildungen und Fehlfunktionen im Zentralnervensystem auf.

Ziel der hier vorliegenden Doktorarbeit war es herauszufinden ob TRIM-NHL Proteine generell ähnliche Funktionen ausführen können. Es wurde untersucht ob TRIM32 und LIN41 mit MYOSIN Va interagieren (so wie TRIM2 und TRIM3) und ob LIN41, wie TRIM3, den Transport von Endosomen steuert. Die Ergebnisse, die in dieser Arbeit vorgestellt werden, deuten darauf hin, dass LIN41 und TRIM32 MYOSIN Va binden, aber LIN41 den endosomalen Transport nicht reguliert. Weiterhin war von Interesse ob der Verlust von LIN41 Auswirkung auf die Pluripotenz der Zellen hat und ob die gesamte TRIM-NHL Familie in der Lage ist die Aktivität von microRNAs zu regulieren. Die Ergebnisse zeigen, dass der LIN41-Verlust nur indirekte Auswirkung auf Pluripotenzfaktoren hat und dass TRIM32, nicht aber TRIM2 oder TRIM3, in der Lage ist die LIN41-Funktion im microRNA Sensorversuch zu übernehmen.

Der Fokus der vorliegenden Arbeit lag auf einer potentiellen Wechselwirkung der TRIM-NHL Proteine untereinander in den frühen Phasen der Nervensystementwicklung im Säugetier. Im Wurm *C. elegans* wurde bereits ein genetischer Zusammenhang zwischen den orthologen Proteinen von TRIM32 und LIN41 gezeigt: eine zusätzliche Deletion des *Trim32* Orthologs kompensierte den Phänotyp der *Lin-41* Mutante. Aufgrund dieser genetischen Interaktion sollte in dieser Doktorarbeit die Möglichkeit einer direkten Interaktion geprüft werden. Mittels Doppelfärbung transfizierter Zellen konnte gezeigt werden, dass die anderen drei TRIM-NHL Proteine in den gleichen zytoplasmatischen Aggregaten auffindbar sind wie LIN41. Färbungen von E11.5 Mausembryonen bestätigten, dass alle vier TRIM-NHL Protein im Neuroepithel exprimiert werden. Immunfärbungen verschiedener Stammzelllinien zeigten überrasschenderweise, dass alle TRIM-NHL Proteine, nicht nur LIN41, in pluripotenten Zellen exprimiert werden. TRIM2, TRIM3 und TRIM32 befinden sich nicht nur zufällig in denselben Aggregaten wie LIN41, die Proteine interagieren physikalisch miteinander. Diese Interaktion konnte sowohl in Überexpressionsversuchen als auch mit Proteinlysaten von E11.5 Embryoköpfen gezeigt werden. Alle TRIM-NHL Proteine sind funktionale E3 Ubiquitinligasen, daher liegen funktionelle Folgen der Interaktion Nahe. Die Hypothese war, dass LIN41 und TRIM32 (das die exakteste Übereinstimmung im Lokalisationsexperiment aufwies) sich möglicherweise gegenseitig ubiquitinieren oder ihre Zielproteinspezifität beeinflussen. In Übereinstimmung mit dieser Hypothese führte die Induktion von LIN41 in Stamzellen zu einer verringerten TRIM32 Expression. Eine Analyse des globalen Ubiquitinierungsprofils von Stammzellen deutet darauf hin, dass TRIM32 Ubiquitinierung tatsächlich von LIN41 hervorgerufen werden kann. TRIM32 hat einen positiven Einfluss auf die Differenzierung, in dem es Retinolsäuresignale verstärkt. Somit verhindert LIN41 eventuell eine frühzeitige Differenzierung von Stammzellen, indem es TRIM32 ubiquitiniert und dadurch seinen Abbau einleitet. Durch die Untersuchung der TRIM-NHL Proteinwechselwirkung liefert die hier vorliegende Doktorarbeit neue Erkenntnisse über die Funktion von LIN41 in der Entwicklung des zentralen Nervensystems.

# 1 INTRODUCTION

## 1.1 Neurogenesis

The mammalian brain is a highly complex organ. The fundamental architecture of the rodent brain (apart from the substantially reduced gyrification) is similar enough to monkey and human to serve as a useful model. As in all mammals, neurons of the rodent cortex are organized in six layers. Within one layer neurons have similar identity and form functional units, projecting to the same distant brain regions (Molyneaux *et al.*, 2007)

### 1.1.1 Embryonic brain development

Embryonic brain development is a tightly controlled process following a strict spatio-temporal sequence of events. Neurogenesis, the generation of neurons in the central nervous system, starts at embryonic day (E) 8.5 in the spinal cord and progresses rostrally, when multipotent neuroepithelial cells start to differentiate. Mid and forebrain neurogenesis starts at E10.5, peaks at E14.5 and is widely completed at E16.5, with ongoing neurogenesis in the adult brain restricted to a few adult neural stem cells residing in neurogenic niches of the brain (Götz and Huttner, 2005). At first, multipotent neuroepithelial cells that line the lateral ventricles undergo symmetric, proliferative divisions to increase the progenitor cell pool. The neuroepithelium appears layered but is actually only pseudo-stratified: all cells span the distance between the apical surface of the neural tube and the outer basal membrane, only their nuclei migrate during the cell cycle. Then, between E10.5 and E12.5 in the cortex, neuroepithelial cells transform into radial glia cells, which loose some epithelial features (tight junctions) and gain glial properties (adherence junctions and glial marker expression). Radial glial cells still span the whole cortical thickness with their basal process, but their cell body resides in the ventricular zone. They initially divide symmetrically to enlarge the progenitor pool (see Figure 1.1). As neurogenesis progresses they undergo more and more asymmetric divisions. These can be either neurogenic to produce one radial glial cell and one neuron or non-neurogenic to form a radial glial cell and a basal progenitor that will reside in the subventricular zone. Division of basal progenitors is always symmetric, it can give rise to two basal progenitors or (if neurogenic) to two

terminally differentiated neurons (reviewed in Götz and Huttner, 2005; Kriegstein and Alvarez-Buylla, 2009).

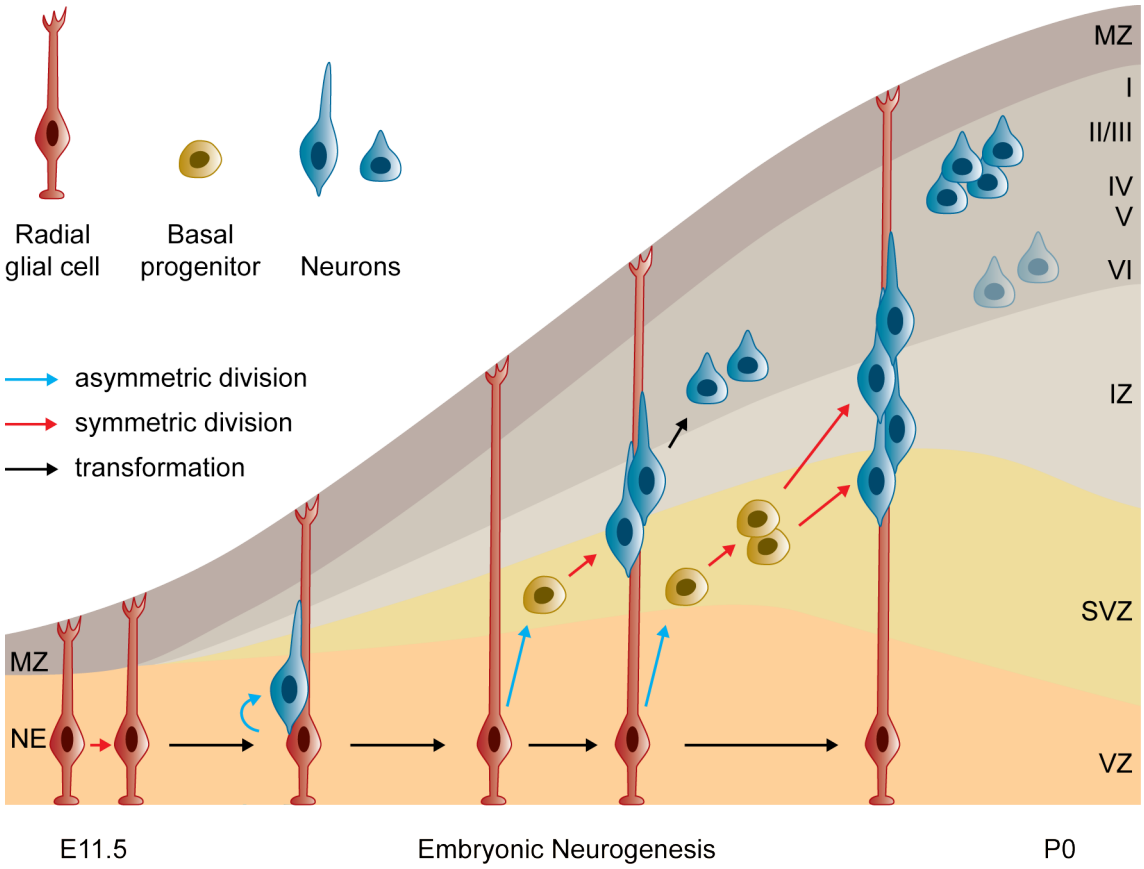


**Figure 1.1 Neurogenesis during cortical development.**
In early neurogenesis, radial glial cells divide symmetrically to form the neuroepithelium (NE). Their basal process projects to the marginal zone (MZ), but (also in later stages) their cell body resides in the ventricular zone (VZ). During neurogenesis, radial glial division mode switches to asymmetric. Product can be multipotent basal progenitor cells, which reside in the subventricular zone (SVZ) or neurons that migrate along the basal process through the intermediate zone (IZ) to form the deeper cortical layers (IV-VI). Basal progenitor division is always symmetric. It can enlarge the progenitor pool or (if neurogenic) result in two terminally differentiated neurons, which migrate through IZ and deeper cortical layers to form the upper layers of the cortical plate (I-III). The picture was adapted from Kriegstein and Alvarez-Buylla, 2009.

Neurons destined to form one layer are born at the same time in the ventricular zone (early-born, deep layer neurons) or in the subventricular zone (late-born, upper layer neurons). Newborn neurons migrate along the basal processes of radial glial cells to the basal end of the cortical thickness and form a new layer, a new functional unit, thereby adding layer to layer in an inside out fashion (Molyneaux *et al.*, 2007).

### 1.1.2 Embryonic stem cell differentiaton

Development of the nervous system is a complicated process that is not easily studied. *In vitro* embryonic stem cell differentiation provides a complimentary model to *in vivo* neurodevelopment methods like *in utero* electroporation. As additional benefit, the *in vitro* system can be more easily manipulated (Muguruma and Sasai, 2012). *In vitro* culture of stem cells depends on various factors and basically on how well the artificial stem cell niche simulates *in vivo* conditions. If vertebrate embryonic stem cells are deprived of growth factors, they differentiate to neural progenitors, indicating that neural induction is a default program (Hemmati-Brivanlou and Melton, 1997). Defined media and also physiological stimuli like retinoic acid are frequently used to induce neural differentiation (Bain *et al.*, 1994). However, choosing a protocol should be an informed decision, as different protocols give rise to different cell fates. There is increasing evidence that the enzyme "RING E3 ubiquitin ligase" **LIN41/TRIM71** (hereafter only named LIN41) and microRNAs play an important role in early development and stem cell differentiation (introduced in section 1.2 and 1.3).

## 1.2 The stem cell TRIM-NHL protein LIN41

Mammalian LIN41 (abnormal cell **lin**eage protein **41**) is a member of the TRIM-NHL (**tri**partite **m**otif - NHL) proteins, which are important in stem cell differentiation (LIN41) and neuronal function in the central nervous system (CNS; TRIM2, TRIM3 and TRIM32) (Balastik *et al.*, 2008; Hung *et al.*, 2010; Kudryashova *et al.*, 2009; Rybak *et al.*, 2009). Based on a precocious phenotype observed in mutants, *lin-41* was identified as a heterochronic gene (involved in developmental timing) in *C. elegans*. Progression through the larval stages one to four (L1-L4) was faster in *lin-41* mutant nematodes: they showed precocious terminal differentiation of the seam cells (that express LIN-41 in wild type) at L3 (Slack and Ruvkun, 1998a). Overexpression of LIN-41 showed the opposite phenotype: reiteration of L3 larval stages in L4 and adult (Slack and Ruvkun, 1998a; Slack *et al.*, 2000). LIN-41 expression was tightly regulated by let-7 (lethal-7), a differentiation-associated microRNA (see section 1.3.2). let-7 was found to bind the 3' untranslated region (UTR) of *lin-41* messenger RNA (mRNA) and targets it for translational repression and mRNA decay in wild type

animals (Bagga *et al.*, 2005; Ding and Grosshans, 2009; for a preview on microRNA function see Figure 1.3). This targeting was found to be evolutionary conserved and LIN41 and let-7 showed reciprocal expression patterns in the developing embryo and in adult tissues (Lin *et al.*, 2007; O'Farrell *et al.*, 2008; Rybak *et al.*, 2009). Zou and colleagues found the let-7/LIN-41 axis also to be important in *C. elegans* axon regeneration: in L1 and L2, LIN-41 was expressed in the anterior ventral microtubule neuron and was required for axon regeneration capacity observed at this stage. Upregulation of let-7 at L3 reduced both LIN-41 levels and axon regeneration capacity (Zou *et al.*, 2013).

In mammals, LIN41 is highly expressed in early embryonic development and in various stem cells both *in vivo* and *in vitro* (Rybak *et al.*, 2009; Schulman *et al.*, 2005), while the other members of the TRIM-NHL family (TRIM2, TRIM3 and TRIM32) are expressed in later stages (Balastik *et al.*, 2008; Hung *et al.*, 2010; Schwamborn *et al.*, 2009, detailed description in section 1.4.5). Using a gene trap mutation in *Lin41*, the promoter activity was shown to be ubiquitous in early development until E9.5, became restricted to the limb buds and midbrain/hindbrain border at E10.5/E11.5 and was shut down towards E12.5, when only the hind limb buds showed residual *Lin41* promoter activity (Maller Schulman *et al.*, 2008). In accordance with the promoter activity recorded, the *Lin41* mRNA was found by in situ hybridization to be highly expressed at E8.5 and to decrease until being lost at E12.5 (Schulman *et al.*, 2005). At E10.5 the *Lin41* mRNA was present in neuroepithelium, dorsal root ganglia, branchial arches, all limb buds, and the tail bud (Maller Schulman *et al.*, 2008). The mammalian LIN41 protein has a molecular mass of 95 kDa and consists of a RING, two B boxes, two short coiled-coil (49 aa and 38 aa), one filamin (101 aa) and a C-terminal NHL domain formed by six NHL repeats (see section 1.4.2 for detailed introduction of the domains). It was shown to be expressed in stem cells and E7 mouse embryos, where it co-expressed with the pluripotency marker OCT4 (**oct**amer-binding transcription factor **4**). LIN41 protein expression declined with development and was absent from E12.5 on. In the postnatal mouse, LIN41 was present in spermatogonial stem cells during postnatal testis development and after postnatal day ten (P10) in ependymal cells of all four ventricles in the brain (Rybak *et al.*, 2009; Elisa Cuevas García, PhD thesis).

Knock out animals from the published *Lin41* gene trap mouse lines have a lethal phenotype and display a neural tube closure defect at E9.5, directly before the embryos start being reabsorbed (Maller Schulman *et al.*, 2008). Chen and colleagues reported that *Lin41*$^{-/-}$ neuroepithelial cells proliferate less and differentiate prematurely, hampering closure of the neural tube at E9.5 (Chen *et al.*, 2012). Recently LIN41 was shown to influence proliferation also in additional contexts. LIN41 overexpression in embryonic stem cells shortened their cell cycle by LIN41 cooperating with miR-302 to diminish levels of cyclin-dependent kinase inhibitor 1A (CDKN1a), a factor mediating cell cycle arrest at the G1-S checkpoint. RNA interference with *Lin41* in embryonic stem cells increased the number of cells in G1 phase by 25-31% and decreased growth rates to 65% compared to control (Chang *et al.*, 2012). This indicates a role for LIN41 in promoting G1 to S phase transition. In biopsies of hepatocellular carcinoma patients, LIN41 expression was found upregulated compared to non-tumorous liver parenchyma and correlated with high tumor grade and poor long term survival for patients (Chen *et al.*, 2013). Despite this evidence for the involvement of LIN41 in stem cell growth control, *Lin41*-deficient mice are viable until day E9.5 (Maller Schulman *et al.*, 2008). This is difficult to reconcile with an essential role for LIN41 in pluripotent embryonic stem cells. Along these lines, a role for LIN41 in cellular reprogramming has recently been described. LIN41 facilitates the transition to the pluripotent state by helping to overcome the barrier to reprogramming posed by microRNA populations expressed in fibroblast state (Worringer *et al.*, 2014).

As described before, LIN41 and let-7 display reciprocal expression patterns in terms of space and time and *Lin41* translation is downregulated by the microRNA let-7 in differentiation. On the other hand, LIN41 was also found to be able to regulate let-7 activity. LIN41 localized to P bodies and bound **A**R**GO**NAUTE **2** (AGO2), as well as other **A**R**GO**NAUTE (AGO) family members found in somatic cells. AGO proteins are the major mediators of microRNA function. Wild type LIN41, but not a C12LC15A RING point mutant, ubiquitinated AGO2 for proteasomal degradation (Rybak *et al.*, 2009). Control of the steady-state AGO levels were reported to limit microRNA activity by two mechanisms: microRNAs bound to AGO were protected from degradation, and

levels of AGO were limiting for the activity of the **R**NA-**i**nduced **s**ilencing **c**omplex (RISC) (Diederichs *et al.*, 2008; Winter and Diederichs, 2011). Consistent with this, LIN41 overexpression was found to block the positive effect of ectopic AGO expression on the activity of let-7 and miR-124 (another differentiation-associated microRNA). Furthermore, ectopic LIN41 reduced microRNA-mediated post-transcriptional silencing activity in sensor assays (Rybak *et al.*, 2009). By cooperating with the pluripotency factor LIN28 (abnormal cell **lin**eage protein **28**) to reduce let-7 activity, LIN41 is part of a double negative feedback loop controlling pluripotency and differentiation (see Figure 1.2). It should be pointed out that several groups have failed to detect physiologically relevant reduction in steady-state AGO levels by Lin41 (Chang *et al.*, 2012; Loedige *et al.*, 2012).

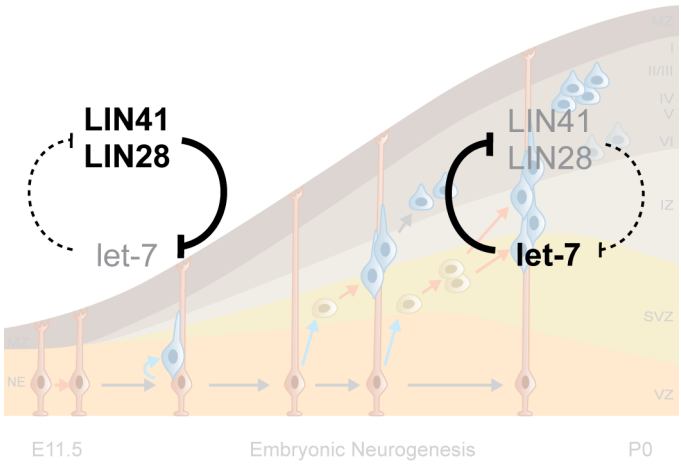


**Figure 1.2 A negative feedback loop between LIN41, LIN28 and let-7 controls pluripotency and differentiation.**
In stem cells, the pluripotency factor LIN28 largely prevents let-7 maturation. In addition, the LIN41 E3 ubiquitin ligase downregulates AGO2 and thereby reduces residual let-7 activity. Upon (neuro)differentiation, LIN41 and LIN28 are transcriptionally downregulated and mature let-7 levels rise immediately. By repressing *Lin41* and *Lin28* translation, let-7 accelerates the reduction of LIN41 and LIN28 protein expression. By additionally targeting other pluripotency factors let-7 promotes neurogenesis (see section 1.3.2).

At the same time, there is increasing evidence that LIN41 functions as an RNA-binding protein (Kwon *et al.*, 2013; Loedige *et al.*, 2012). mRNA-binding and subsequent translational repression was mediated by the LIN41 NHL domain and abrogated in swapping experiments using the TRIM32 NHL domain (Loedige *et al.*, 2012). This leaves LIN41 as a major effector of microRNA activity, acting as a post-transcriptional and post-translational regulator. The

other members of the TRIM-NHL family are introduced in more detail in section 1.4.3 - 1.4.5.

## 1.3 MicroRNAs – post-transcriptional regulation in neurogenesis

MicroRNAs are endogenous small RNAs (usually 21-22 nucleotides in length) that play an important role in post-transcriptional regulation thereby influencing various biological processes (Bartel, 2004). It was shown that a single microRNA can target complementary sequences in the 3'UTR of hundreds of mRNAs and repress protein production by either translational repression or mRNA decay. Affected protein levels are reduced by about 50% (Selbach *et al.*, 2008)

The first microRNAs (the miR-125 homologue lin-4 and let-7) were discovered as heterochronic genes in *C. elegans*. Their expression increases in development, interestingly in a reciprocal fashion to other heterochronic genes, namely *lin-28* and *lin-41* (see Figure 1.2). Sequence analysis of lin-4 and let-7 showed complementary regions in the 3'UTR of *lin-28* and *lin-41*, which suggested direct regulation of the mRNAs (Moss *et al.*, 1997; Reinhart *et al.*, 2000). Expression and temporal regulation of let-7 was found to be highly conserved throughout bilateral animal phyla (Pasquinelli *et al.*, 2000). Deep Sequencing analysis later showed that about 50% of the *C. elegans* microRNAs have homologues in *Drosophila* and humans (Ibáñez-Ventoso *et al.*, 2008). This implies that microRNAs execute important functions in biology. Most microRNAs have multiple isoforms. These isoforms share identical nucleotides at position 2-7, the so-called seed region, and form microRNA families. The seed region is crucial for base pairing with complementary sites in 3'UTRs of target mRNAs. Ventura and colleagues reported the other nucleotide positions contribute to target recognition as well, but may form bulges (Ventura *et al.*, 2008). MicroRNAs in general showed tissue specific expression patterns (Lagos-Quintana *et al.*, 2002). Distinct expression patterns of isoforms were suggested to allow them to serve distinct roles (Ventura *et al.*, 2008). The maturation of microRNAs is a multistep process and will be discussed in the next section.

### 1.3.1 MicroRNA biogenesis and function

As mentioned before, the LIN41 substrate AGO2 is the major effector of microRNA function, therefore microRNA biogenesis and function are introduced here in more detail (see a schematic overview in Figure 1.3). All microRNAs are transcribed by RNA polymerase II and III (Borchert *et al.*, 2006; Lee *et al.*, 2004). These **pri**mary **mi**cro**R**NA (pri-miR) transcripts can be several kilobases long and contain a cap structure and a poly-A tail. Sequences destined to become microRNAs are characterized by local stem-loop hairpin structures (Lee *et al.*, 2004). DROSHA, an RNase III enzyme, cleaves the secondary pri-miR structure into about 70 nucleotide long hairpin precursor microRNAs (Lee *et al.*, 2003). Single-stranded (ss) regions flanking the precursor microRNA hairpin are essential for processing (Zeng and Cullen, 2005). DROSHA requires **D**i**G**eorge syndrome **c**ritical **r**egion gene 8 (DGCR8) as co-factor in the cleavage reaction (Denli *et al.*, 2004; Gregory *et al.*, 2004; Han *et al.*, 2004; Landthaler *et al.*, 2004). DGCR8 is able to bind the ssRNA flanking region while DROSHA binds the double-stranded RNA stem prior to cleavage at the base of the stem (Zeng and Cullen, 2005). Precursor microRNAs are shuttled to the cytoplasm (Yi *et al.*, 2003). The cytoplasmic RNase III enzyme DICER is responsible for the next processing step. It recognizes precursor microRNAs and cleaves the hairpin structure 22 nucleotides from the site of DROSHA cleavage (Bernstein *et al.*, 2001). DICER interacts with its co-factors (e.g. TRBP, the human immunodeficiency virus 1 **t**ransactivating response **R**NA **b**inding **p**rotein) for the assembly of the **R**NA-**i**nduced **s**ilencing **c**omplex (RISC) to load the double-stranded microRNA (Chendrimada *et al.*, 2005). RISC then is able to differentiate between the two microRNA strands and preferentially loads the guide strand while the passenger strand is disassembled (Gregory *et al.*, 2005). The loaded RISC complex co-localizes with targeted mRNAs and proteins related to mRNA decay to specific cytoplasmic structures, so called **p**rocessing bodies (P bodies) (Cougot *et al.*, 2004; Liu *et al.*, 2005a). Within the RISC, AGO proteins are the major component. They directly bind the microRNA and facilitate the interaction with semi-complementary sites in mRNAs (see Figure 1.3). AGOs require accessory proteins like GW182 (N-terminal glycin (**G**) - tryptophane (**W**) rich protein of 182 kDa) and MOV10 (**Mo**loney leukemia virus **10**) for mRNA silencing. While MOV10 is a putative RNA helicase, yet of

unknown function, GW182 interacts with AGO2 and is essential for P body maintenance (Jakymiw *et al.*, 2005; Liu *et al.*, 2005a).

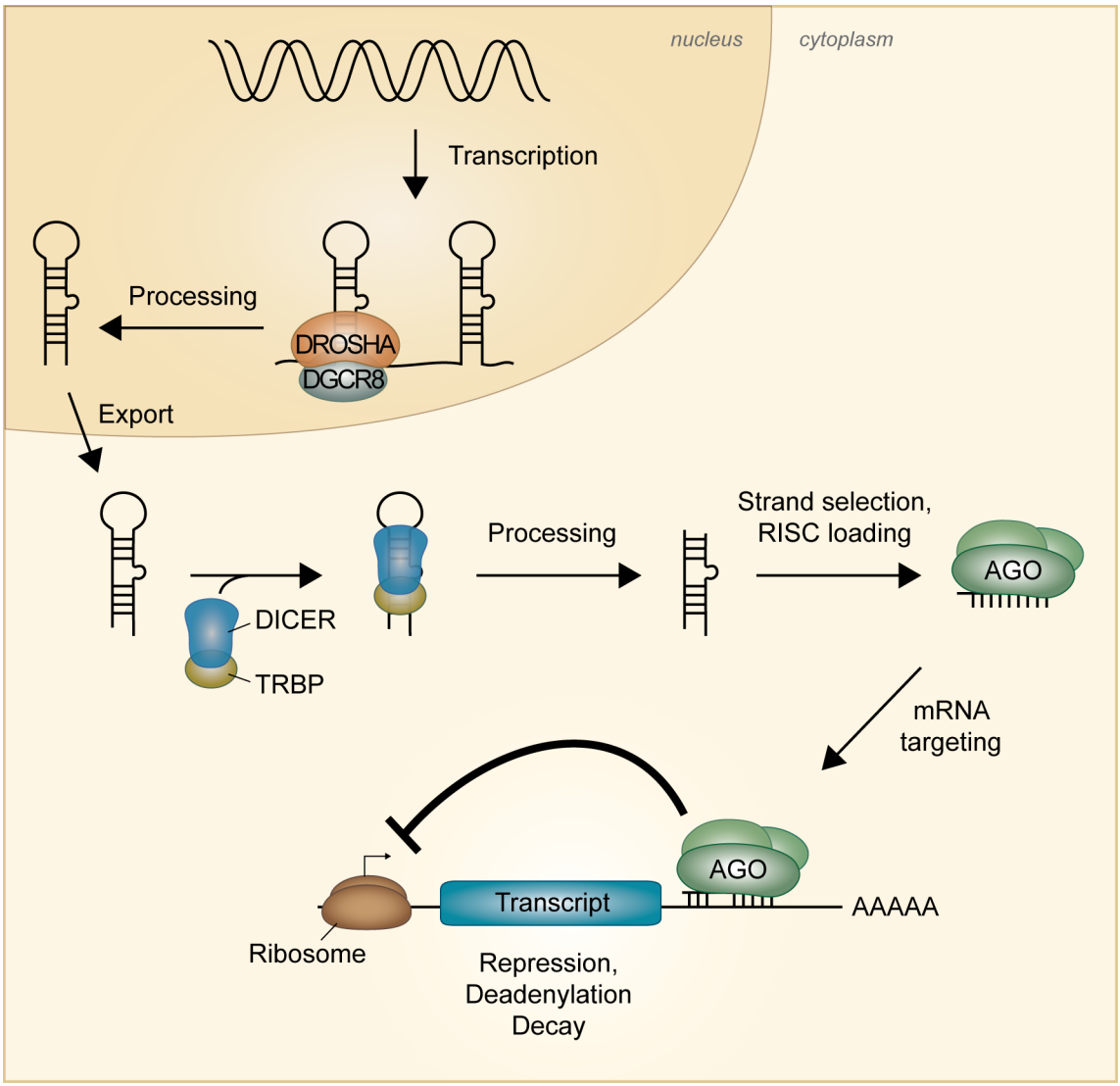


**Figure 1.3 The microRNA biogenesis pathway.**
Primary microRNAs are transcribed by RNA polymerase II and III. The transcripts form imperfectly base-paired hairpin structures. The RNase III enzyme DROSHA and its co-factor DGCR8 process primary microRNAs at the stem of the hairpin already in the nucleus. The cleavage products are about 70 nucleotides long precursor microRNAs, which are exported to the cytoplasm. The RNase III DICER and its co-factors (e.g. TRPB) bind precursor microRNAs and cleave the loop structure The resulting about 22 nucleotide long double-stranded microRNA is bound by AGO, the major effector protein of the RISC and the passenger strand is disassembled. The microRNA sequence guides loaded RISC to complementary sequences in the 3'UTR of target mRNAs, where it executes its function: translational repression, induction of mRNA deadenylation and decay.

Lowered mRNA levels account for >84% of decreased protein production (Guo *et al.*, 2010). But microRNA-mediated target silencing is established without mRNA cleavage (an AGO function in plants) (Bartel, 2004). Translational

repression mediated by AGO and subsequent mRNA deadenylation and decay cause the lowered mRNA levels (Bazzini *et al.*, 2012; Djuranovic *et al.*, 2012). In general, translation is facilitated by mRNA circularization, which is driven by interaction of proteins that bind the 5' mRNA cap with proteins that interact with the 3' mRNA poly-A tail. This conformation protects the 5' and 3' mRNA ends from degradation (reviewed in DERRY *et al.*, 2006). In addition to AGO function, the RISC component GW182 abrogates the circular mRNA conformation essential for efficient translation and exposes the 5' cap and poly-A tail for mRNA degradation (reviewed in Huntzinger and Izaurralde, 2011).

Recently, studies of the Carthew and Voinnet groups showed localization of RISC proteins (AGO2 and GW182) to the late endosomal compartment (Gibbings *et al.*, 2009; Lee *et al.*, 2009). Endosomes are membranous vesicles inside the cell, which are formed by endocytosis, a process used to internalize segments of plasma membranes and material from the extracellular space. During endocytosis, MYOSIN VI (a minus end directed motor protein) is known to support invagination of the cell membrane by interaction with the membrane (via scaffolds) and movement towards the cell center along actin filaments. Subsequent membrane scission then forms a vesicle, the endosome (reviewed in Mooren *et al.*, 2012). Other unconventional MYOSINs, like MYOSIN Va, MYOSIN Vb were also reported to transport endosomes along actin filaments with movement towards the cell periphery (Provance *et al.*, 2004; Rudolf *et al.*, 2003). Their association with RAB GTPases characterizes endosomes. RAB5 positive early endosomes are located in the cell periphery. On their way through the cell, the surface proteins of endosomes are exchanged. Late endosomes (also called multivesicular bodies) are RAB7 positive and localize more centrally (reviewed in Spang). Lee and colleagues found active RISCs to be associated with late endosomes and suggest that late endosomes promote RISC protein turnover to enhance the dynamic of RNA silencing (Lee *et al.*, 2009). These findings are important for the presented thesis, as other members of the TRIM-NHL family were shown to interact with class V MYOSINs and TRIM3 was reported to influence endosome trafficking (El-Husseini and Vincent, 1999; Ohkawa *et al.*, 2001; Yan *et al.*, 2005).

### 1.3.2 MicroRNA function in neurogenesis

The RNase III enzyme DICER is essential in the microRNA biogenesis cascade. *Dicer* depletion leads to accumulation of precursor microRNAs and a global downregulation of mature microRNA levels (Bernstein *et al.*, 2001; Hutvagner *et al.*, 2001). Andersson and colleagues established Dicer-null neural stem cell lines from *Dicer* null embryos. These neural stem cells do not differentiate into neurons and glia at all, a phenotype that was rescued by reintroducing *Dicer* cDNA, suggesting that the biogenesis of functional microRNAs is essential for neurogenesis and gliogenesis (Andersson *et al.*, 2010).

There is increasing evidence that microRNAs help to promote neurogenesis; their expression shows temporal restriction as well as lineage specific patterns. During embryonic brain development and neural differentiation microRNA expression is upregulated in terms of diversity and abundance (Miska *et al.*, 2004; Sempere *et al.*, 2004; Smirnova *et al.*, 2005; Wulczyn *et al.*, 2007), likely at the transcriptional level as well as through the loss of LIN41's negative regulation of AGO (Rybak *et al.*, 2009). The levels of most neurogenic **mi**cro**R**NAs (miRs) increase continuously during **c**entral **n**ervous **s**ystem (CNS) development and neural stem and progenitor cell differentiation (e.g. miR-9, miR-125 and the let-7 family) while the expression of others peaks at specific time points (e.g. miR-124 at E14.5 and E17.5) (Landgraf *et al.*, 2007; Smirnova *et al.*, 2005; Wulczyn *et al.*, 2007).

The microRNA let-7 was the second one discovered in *C. elegans* and is widely studied as a paradigm microRNA. Maturation of let-7 is subject of intense regulation. Primary let-7 is already transcribed in pluripotent stem cells, but (as briefly mentioned in section 1.2) its maturation is stalled by its repressor LIN28, another important stem cell factor (Heo *et al.*, 2008; Newman *et al.*, 2008; Rybak *et al.*, 2008; Viswanathan *et al.*, 2008). Upon neurodifferentiation, let-7 maturation proceeds, therefore it is among the earliest upregulated mature microRNAs in neurogenesis. The mature form of let-7 immediately targets its repressor *Lin28*, creating a feed forward loop for differentiation (see Figure 1.2). This is reinforced by miR-125 also targeting *Lin28* (Moss and Tang, 2003; Reinhart *et al.*, 2000; Rybak *et al.*, 2008; Wu and Belasco, 2005). As already

described in section 1.2, LIN41 is essential for stem cell proliferation and self-renewal throughout species. By targeting *Lin41*, let-7 enhances the feed forward loop even further (see Figure 1.2). Also *c-Myc* (**my**elo**c**ytomatosis oncogene), one of the four factors required for inducing pluripotency in somatic cells (Takahashi and Yamanaka, 2006), is repressed by let-7. In neurogenesis, this targeting was shown to be enhanced by TRIM32, another TRIM-NHL protein (Schwamborn *et al.*, 2009, for details see section 1.4.5.3). let-7 also targets factors involved neurogenesis. TLX (**t**ai**l**less gene homolog) is a transcription factor, expressed in the forebrain in early embryonic development (Monaghan *et al.*, 1995). Progenitor cells of the developing cortex are sensitive to TLX loss which results in premature differentiation (Roy *et al.*, 2004). TLX prevents transcription of other neurogenic microRNAs like miR-9 by recruiting **h**istone **d**e**ac**etylases (HDACs) and subsequent silencing of their promoter region. Upregulation of let-7 in neurodevelopment leads to Tlx down- and miR-9 upregulation, which then acts in concert with let-7 to further lower Tlx levels (Zhao *et al.*, 2009). When upregulated in neurogenesis miR-9 also downregulates the neuronal repressor REST (**RE**1-**S**ilencing **T**ranscription factor**)** plus its cofactor CoREST (both highly expressed in pluripotent stem cells), thus terminating the pluripotent state (Packer *et al.*, 2008). Another very important microRNA in neurogenesis is miR-124. It targets the mRNA of **P**olypyrimidine **t**ract **b**inding **p**rotein (PTBP) 1, a global repressor of alternative **pre**cursor (pre-) mRNA splicing. Downregulation of PTBP1 switches the dominant outcome of *Ptbp2* mRNA splicing from a form subject to nonsense-mediated decay to a productive variant. Once made, the PTBP2 protein then triggers brain-specific alternative pre-mRNA splicing (Makeyev *et al.*, 2007). Taken together, neurogenic microRNAs mediate the loss of pluripotency and promote neurogenesis.

MicroRNAs also influence the aging of progenitor cells and adult neural stem cells. In retinal development, let-7, miR-9 and miR-125 were reported to drive aging of retinal progenitor cells: overexpression of these three microRNAs in early progenitors led to production of late-born cell fates, while introduction of antagomirs (inhibiting these three neurogenic microRNAs) into late retinal progenitors rejuvenated them and led to production of early-born postmitotic cell

fates (La Torre *et al.*, 2013). In corticogenesis, let-7 was shown to repress *Imp1* (**i**nsulin-like growth factor 2 **m**RNA binding **p**rotein 1) translation and thereby drives the transition from highly proliferative embryonic neural stem cells to more quiescent adult neural stem cells (Nishino *et al.*, 2013). Additionally, endogenous upregulation of let-7 in neural stem cells from older animals led to HMGA2 (**h**igh **m**obility **g**roup **A**T hook 2) decrease and a reduced capacity to self-renew. This correlates with the reduced potency of neural stem cells as a function of age (Nishino *et al.*, 2008). The studies discussed above represent a clear demonstration of an intrinsic micro-RNA mediated clock in mammalian neural stem cells.

## 1.4 TRIM-NHL proteins - post-translational regulation in the CNS

Not only is microRNA-mediated post-transcriptional regulation important in neurogenesis and the CNS, post-translational regulation also plays an important role. The ubiquitin proteasome pathway is one of the most significant post-translational regulatory systems, to which LIN41 and the other TRIM-NHL proteins belong.

### 1.4.1 The ubiquitin proteasome pathway

The ubiquitin proteasome pathway is a major cellular system for determining the turnover rate of proteins. Protein degradation is a carefully coordinated, evolutionarily conserved multistep process. It requires a combination of three enzymes that transfer a 10 kDa **ub**iquitin (Ub) moiety to substrate proteins. The E1 enzyme activates ubiquitin in an ATP-dependent reaction and forms an E1-thiol-Ub ester. Activated ubiquitin is then transferred to the E2 enzyme. The E3 ligase then binds the E2-thiol-Ub ester intermediate as well as the substrate and the ubiquitin moiety is finally transferred (see Figure 1.4). The enzyme organization is hierarchical: only one E1 and few E2 enzymes are known, a wide variety of E3 enzymes gives the system its specificity (reviewed in Glickman and Ciechanover, 2002). Substrates can be mono- or poly-ubiquitinated. Canonically, polyubiquitination is a result of repeated transfer of ubiquitin moieties to a growing ubiquitin chain, but also the transfer of preassembled ubiquitin chains has been reported (Li *et al.*, 2007). Differential

lysine linkage in polyubiquitination leads to different outcomes: lysine 63 linked polyubiquitin chains mediate endocytosis and influence translation among other things. Lysine 48 linkage leads to recognition by specific proteins, followed by substrate translocation to the proteasome and degradation (Nathan *et al.*, 2013; Schwartz and Hochstrasser, 2003). In addition to ubiquitin there are other ubiquitin-like modifiers with diverse functions, e.g. the **s**mall **u**biquitin-like **mo**difier SUMO that plays a role in nuclear transport and transcriptional regulation or the **i**nterferon-**s**timulated **g**ene 15 ISG15, which acts in immune responses and NEDD8 (**n**eural precursor cell **e**xpressed **d**evelopmentally **d**ownregulated 8) that activates specific E3 ligases (reviewed in Schwartz and Hochstrasser, 2003). All different modifiers have distinct sets of E1, E2 and E3 enzymes.

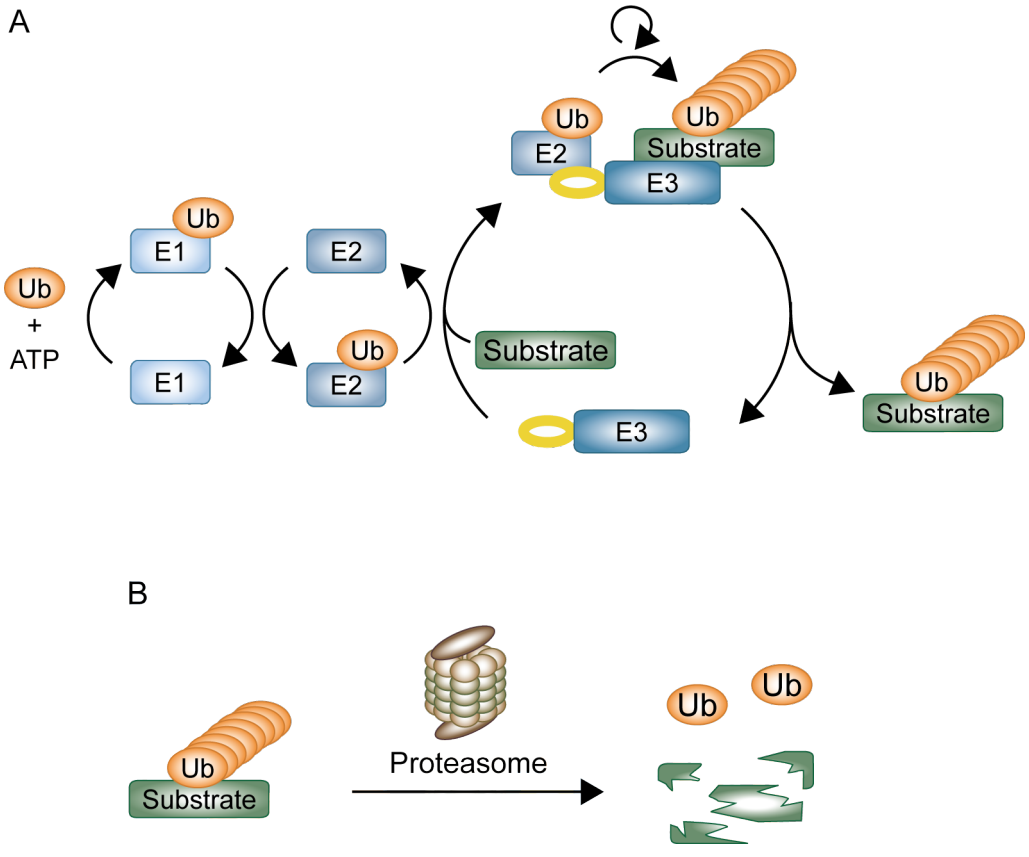


**Figure 1.4 The ubiquitin proteasome pathway.**
(A) Ubiquitin is activated by conjugation to the E1 (ubiquitin activating) enzyme in an ATP-dependent step. It is transferred to the E2 (ubiquitin conjugating) enzyme. The E2 enzyme binds to E3 ubiquitin ligases, which transfer the ubiquitin moiety to the bound substrate. The repeated ligation reaction forms a ubiquitin chain on the target proteins. (B) Proteins labeled with a lysine 48-linked poly-ubiquitin chain translocate to the proteasome, where they are degraded. Adapted from Wulczyn *et al.*, 2011

### 1.4.2 The TRIM-NHL protein domains

LIN41, as the other TRIM-NHL proteins, is defined by a distinct motif pattern. Proteins of the broader TRIM protein family share the **tri**partite **m**otif consisting of a N-terminal RING domain, followed by one or two B boxes and a coiled-coil domain. The order as well as spacing between the domains is conserved even if the protein lacks one of them (see the phylogenetic tree in Figure 1.5). This suggests that the tripartite motif is an integrated functional structure rather than a collection of separate modules. TRIM proteins are subclassified according to their C-termini. Proteins of the TRIM-NHL subfamily contain an NHL domain comprising two to six NHL repeats in their C-terminus (reviewed in Reymond *et al.*, 2001). Specifics and function of these domains are summarized in the following sections.

#### 1.4.2.1 The RING domain

By sequence alignment of proteins that contain cysteine-rich motifs a novel zinc finger motif was discovered, which was suggested to bind zinc (and other divalent metal ions). Subsequent to zinc binding this motif forms a structure that mediates protein-protein interaction (Freemont *et al.*, 1991). Further analysis refined the zinc coordination sites to be eight conserved cysteine and histidine residues with variable spacing and without additional sequence conservation. The motif is simplified called C3HC4 and the 40 amino acid long domain is called RING domain (as it is also found in *Ring1* –**r**eally **i**nteresting **n**ew **g**ene 1). A second very similar zinc finger motif was discovered later, which is abbreviated C3H2C3, as the cysteine in the fifth coordination site is replaced by histidine (Freemont, 1993). $H^1$-NMR spectroscopy provided the structures of the C3HC4 and C3H2C3 RING domains. It was shown that RING domains bind two zinc cations in a “cross-brace” conformation, where the first and third pair of zinc coordination sites bind one zinc cation and the second and fourth coordination pair bind another (Barlow *et al.*, 1994). The coordination of $Zn^{2+}$ cations was shown to be essential for autonomous folding of the RING domain (Borden *et al.*, 1995). RING domain proteins were reported to be important in the ubiquitin proteasome pathway when the C3HC4- and also C3H2C3-type were proven to bind E2 ubiquitin-conjugating enzymes and possess E3 ubiquitin

ligase activity (Joazeiro *et al.*, 1999; Lorick *et al.*, 1999). Only single cysteine mutation in the zinc-finger motif is sufficient to abrogate E3 activity and creates dominant negative forms of the E3 ligase (Waterman *et al.*, 1999). Interestingly, the activity of RING E3 ubiquitin ligases can respond to cell signaling. For example, signal-dependent phosphorylation of receptor tyrosine kinases is required for binding and ubiquitination by CBL (**C**asitas **B**-lineage **l**ymphoma; Joazeiro *et al.*, 1999).

#### 1.4.2.2 The B box domain

Sequence alignment of proteins containing a RING domain led to the discovery of another cysteine- and histidine-rich motif always situated C-terminally of the RING domain (which was called A box at the time): the B box (Reddy and Etkin, 1991). The B box domain is about 40 amino acids long and binds one $Zn^{2+}$ cation with high affinity. Tetrahedral coordination of a divalent metal cation (zinc or copper) is required for proper secondary structure, and leaves the residual cysteines and histidines free for other functions like dimerization (Borden *et al.*, 1993). Two different types of B boxes, with slightly different C-H zinc finger motifs were identified: B box type 1 and type 2. If both are present in a protein, type 1 precedes type 2, if a protein contains only a single B box it is of type 2 (reviewed in Reymond *et al.*, 2001). Resolution of the structure of tandem B boxes showed that both domains bind $Zn^{2+}$ in a cross-brace conformation, thereby revealing structural similarity to the RING domain. Moreover, the two B boxes showed a stable interaction with each other (Tao *et al.*, 2008).

#### 1.4.2.3 The coiled-coil domain

Completing the tripartite motif, the coiled-coil domain is located C-terminally of RING and B boxes. The coiled-coil domain mediates dimerization in leucine-zipper transcription factors. Parallel or antiparallel α-helices form a superhelix, with a distinctive pattern of amino acid side chains forming the core of the bundle. It requires the heptad repeat: exactly seven amino acids form two turns of the distorted α-helix. Hydrophobic amino acids face the helix interface, while hydrophilic residues form the solvent exposed surface of the superhelix. This

repeated pattern ensures the typical knobs-into-holes structure in the superhelix's core, in which two distorted α-helices intertwine and the hydrophobic residues of one α-helix (knobs) are surrounded by four residues of the opposite α-helix (hole) (reviewed in Lupas, 1996).

#### 1.4.2.4 The filamin domain

The filamin (FLM) domain is about 100 amino acids long and is mostly described in filamin and other actin binding proteins (ABP) that contain numerous repeats of the filamin domain e.g. ABP120 (a gelation factor of *Dictystelium discoidum*) contains six filamin repeats (Zhou *et al.*, 2010). Despite containing six filamin repeats, only one mediates the crucial ABP120 dimerization (McCoy *et al.*, 1999).

#### 1.4.2.5 The NHL domain

The NHL domain was first identified in three proteins – *C. elegans* **N**CL-1, *H. sapiens* **H**T2A (a TRIM32 ortholog) and *C. elegans* **L**IN-41 – and is unique to TRIM-NHL proteins (Frank and Roth, 1998; Fridell *et al.*, 1995; Slack and Ruvkun, 1998b). The domain consists of two to six repeats of NHL motifs (about 40 amino acids long) that are glycine- and hydrophobic residue-rich. The NHL domain forms a multiblade β-propeller structure, which is known to mediate protein-protein interactions (Edwards, 2003; Fridell *et al.*, 1995).

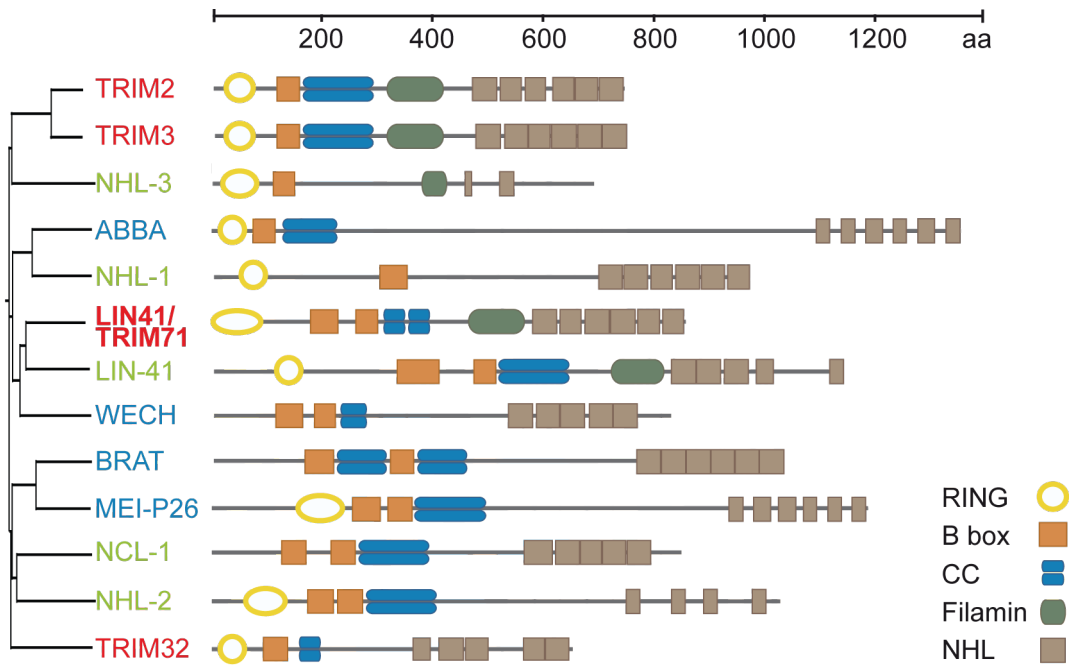


**Figure 1.5 Phylogenetic tree of the TRIM-NHL protein family.**
TRIM-NHL proteins comprise a distinct domain structure. The RING domain with E3 ubiquitin ligase activity is located N-terminally of one or two coiled-coil (CC) domains and one or two B boxes. C-terminally of this the **tri**partite **m**otif (TRIM) follow a putative Filamin and a obligatory NHL domain. Orthologues of *Mus musculus* are depicted in red, of *D. melanogaster* in blue and of *C. elegans* in green. LIN41 and TRIM71 are used synonymously. The domains were identified with e!*Ensembl.* The figure was adapted from Wulczyn *et al.*, 2011.

### 1.4.3 *C. elegans* TRIM-NHL proteins

The *C. elegans* TRIM-NHL protein family consists of five members: NCL-1, NHL-1-3 and LIN-41. NCL-1 and NHL-2 are orthologs of mammalian TRIM32, NHL-3 is the ortholog of TRIM2 and TRIM3, LIN-41 to LIN41/TRIM71, as annotated in e!*Ensembl* (see Figure 1.5). The expression and function of the C. elegans LIN-41 protein was described in detail in section 1.2. NCL-1 does not contain a RING domain, but due to overall domain structure and spacing is considered to be a TRIM-NHL protein. *ncl-1* mutants were viable and contained more protein and ribosomal RNA than wild type nematodes. They also showed increased nucleolar and cell size, both of which are linked to the amount of ribosomal RNA in the cell. Detailed examination confirmed an increase in RNA polymerase I and III transcription in *ncl-1* mutants, suggesting a role for NCL-1 in repression of RNA polymerase I and III (Frank and Roth, 1998). Hammel and colleagues investigated if other TRIM-NHL proteins are functionally related to LIN-41 by testing for genetic interactions in a *lin-41* hypomorphic backround.

The other *C. elegans* TRIM-NHL family members did not enhance the precocious phenotype of the *lin-41* mutant, which suggests NCL-1 and NHL-1-3 do not function synergistically with LIN-41. In contrast, loss of *nhl-2* (the TRIM32 ortholog) rescued the *lin-41* mutant phenotype, indicating an opposing role in developmental timing. Furthermore, NHL-2 also localized to P bodies (Hammell *et al.*, 2009).

### 1.4.4 *D. melanogaster* TRIM-NHL proteins

In *D. melanogaster* four TRIM-NHL proteins are known: ABBA, WECH/DAPPLED, BRAT and MEI-P26 (see Figure 1.5). ABBA expression is muscle-specific and required for sarcomeric integrity (Domsch *et al.*, 2013; O'Farrell *et al.*, 2008). The *D. melanogaster* LIN41 ortholog WECH/DAPPLED does not contain a RING domain but is, due to the remaining domains and their spacing, considered a member of the TRIM-NHL family. WECH/DAPPLED is expressed in embryonic muscle and is responsible for their attachment to the body wall by scaffolding talin and integrin-linked kinase (Löer *et al.*, 2008). WECH/DAPPLED expression is, as its *C. elegans* ortholog LIN-41, regulated by let-7 (O'Farrell *et al.*, 2008).

The most extensively studied *D. melanogaster* TRIM-NHL protein is the TRIM32 ortholog BRAT (**bra**in **t**umor), which lacks the RING domain. Frank and colleagues showed *brat* mutant wing disc cells have larger nucleoli and more ribosomal RNA than the wild type, while the overexpression of BRAT reduced ribosomal RNA content (Frank *et al.*, 2002). The effect on nucleolar size is shared with *C. elegans* NCL-1 and *D. melanogaster* MEI-P26 (Frank and Roth, 1998; Neumüller *et al.*, 2008). Frank and colleagues suggested the control of cell growth by Brat being the explanation for the **bra**in **t**umor phenotype of *brat* deficient fruitflies. *Brat* mRNA was reported to be expressed in the germ line and is asymmetrically inherited to differentiating cytoblasts that in turn expressed BRAT protein. In cytoblasts, BRAT repressed mRNAs of pluripotency genes (e.g. *drosophila* (d)MYC), thereby promoting differentiation (Harris *et al.*, 2011).

Another TRIM32 ortholog, MEI-P26, contains a RING domain. Herranz and colleagues found MEI-P26 to reduce dMYC protein levels but not its mRNA, suggesting a different mechanism for dMYC regulation compared to BRAT (Herranz *et al.*, 2010). Moreover, MEI-P26 was shown to influence microRNA biogenesis: a deletion mutant showed enhanced microRNA levels and MEI-P26 overexpression reduced microRNA levels. Neumüller and colleagues concluded that MEI-P26 either inhibits microRNA biogenesis or facilitates microRNA decay. MEI-P26's NHL domain interacts with AGO1, but this interaction was unlikely to precede ubiquitination as the complex was quite abundant (Neumüller *et al.*, 2008). The mechanism of microRNA level reduction by MEI-P26 has not been determined so far.

### 1.4.5 The mammalian TRIM-NHL family

The presented thesis aims at elucidating novel functions of LIN41 in early neurogenesis. Next to LIN41 (introduced in section 1.2), the mammalian TRIM-NHL family further consists of: TRIM2, TRIM3, TRIM32 (see Figure 1.5). Their expression, biochemical details and functional relevance in the central nervous system and human disorders are introduced in the following sections.

#### 1.4.5.1 TRIM2

The mammalian TRIM2 was discovered as **n**eural **a**ctivity-related **R**ING **f**inger protein (NARF). TRIM2 mRNA and protein were found to be highly expressed in the adult rodent brain, especially in hippocampus (Ohkawa *et al.*, 2001). Mouse TRIM2 has a molecular mass of 85 kDa and contains a C3HC4 RING domain, a B box, a large coiled-coil domain (100 aa) and six C- terminal NHL repeats. TRIM2 was reported to interact with MYOSIN V via its NHL domain (Ohkawa *et al.*, 2001). Homozygous *Trim2* gene trap mice are viable but show an early onset neurodegeneration – they suffer from tremor and ataxia from 1.5 months on. After five months homozygous *Trim2* gene trap mice have lost 85% of their Purkinje cells compared to equally old wild type mice. TRIM2 was shown to be an E3 ubiquitin ligase by an autoubiquitination assay and to co-purify with **n**euro**f**ilament **l**ight chain (NF-L) from transfected HeLa cells. Enhanced NF-L ubiquitination after TRIM2 expression in cells and NF-L accumulation in

homozygous *Trim2* gene trap mice led to the conclusion that TRIM2 acts as an E3 ubiquitin ligase targeting NF-L for degradation (Balastik *et al.*, 2008). Human *TRIM2* mutation was identified as the causative event for early-onset axonal neuropathy in one patient. A heterozygous mutation in the *TRIM2* coiled-coil domain resulted in a complete loss of mRNA and protein in patient's fibroblasts. Human sural nerve biopsy revealed neurofilament accumulation, implicating conservation of NF-L ubiquitination by TRIM2 (Ylikallio *et al.*, 2013). In mice, TRIM2 levels are upregulated by kainate and PTZ (**p**entylene**t**etra**z**ol)-induced seizures. This upregulation is activity-dependent and requires signalling via NMDA (**N**-**m**ethyl-**D**-**a**spartate) receptors (Ohkawa *et al.*, 2001). Moreover, TRIM2 is implicated in axon outgrowth. In neuronal cultures, TRIM2 overexpression resulted in hyperpolarization showing multiple axons, while downregulation resulted in hypopolarized neurons without axons (Khazaei *et al.*, 2010).

#### 1.4.5.2 TRIM3

The mammalian TRIM3 was identified as **B**rain-**e**xpressed **R**ING finger **p**rotein (BERP) being expressed in the soma and growth cones of neurally differentiated PC-12 cells (El-Husseini and Vincent, 1999). In rat, TRIM3 was detected in cultured hippocampal neurons and in forebrain development from E15.5 on. Its expression increased with developmental time until reaching a plateau at P7 (Hung *et al.*, 2010). TRIM3 has a molecular mass of 82 kDa and contains a C3HC4 RING domain, one B box and large coiled-coil domain (100 aa), as well as six C-terminal NHL repeats. It was reported to homomultimerize and to bind the globular domain of MYOSIN Vb with its NHL domain. This interaction was crucial for neurite outgrowth during neurodifferentiation of PC-12 cells. Endogenous TRIM3 was shown to co-precipitate with MYOSIN Vb from rat brain lysates, suggesting a physiological role for this interaction (El-Husseini and Vincent, 1999). Moreover, El Husseini and colleagues observed the interaction of the TRIM3 N-terminus with α- ACTININ-4 (El-Husseini *et al.*, 2000). Consequently, TRIM3 was proposed to act as a scaffold between MYOSIN Vb and α-ACTININ-4 to ensure transferrin receptor recycling (Yan *et al.*, 2005). *Trim3* knockout mice are viable but less susceptible to PTZ-induced

seizures than wild type mice. *Trim3*$^{-/-}$ mice displayed reduced surface expression of $GABA_A$ (**γ** **a**mino**b**utyric **a**cid) receptor raising the possibility that TRIM3 is a direct post-translational regulator of $GABA_A$ receptor trafficking (Cheung *et al.*, 2010). Taken together there is multiple evidence for TRIM3 being involved in receptor recycling/endosome trafficking. In *D. rerio,* TRIM3 was proven to function as an E3 ubiquitin ligase in autoubiquitination assays (Zhang *et al.*, 2012). Furthermore, TRIM3 regulates post-synaptic density proteins in cultured hippocampal neurons: TRIM3 was found to ubiquitinate the synaptic scaffolding protein GKAP (**g**uanylate **k**inase-**a**ssociated **p**rotein) and to be responsible for activity-dependent downregulation of GKAP at the post-synapse (Hung *et al.*, 2010).

#### 1.4.5.3 TRIM32

TRIM32 was identified in a yeast-two-hybrid screen as a **h**uman immunodeficiency virus **t**ransactivator of transcription interacting protein **2A** (therefore initially termed HT2A). In contrast to TRIM2 and TRIM3, TRIM32 is ubiquitously expressed: it is present in spleen, thymus, prostate, testis, ovary, intestine, colon, brain and muscle (Fridell *et al.*, 1995; Kudryashova *et al.*, 2009; 2005). The 72 kDa protein consists of an N-terminal RING, B box and short coiled coil domain (20 aa), it lacks the filamin domain and contains only five C-terminal NHL repeats, thereby rendering it the smallest TRIM-NHL protein (Fridell *et al.*, 1995).

*Trim32* knockout mice are viable and show mild myopathic changes in skeletal muscle caused by reduced motor axon diameter (Kudryashova *et al.*, 2009). TRIM32 was found to functions as an E3 ubiquitin ligase and to interact with MYOSIN II via its coiled-coil domain (Kudryashova *et al.*, 2005). The D487N mutation in the TRIM32 NHL domain is causative for Limb-Girdle Muscular Dystrophy type 2H (LGMD2H), a rare and mild autosomal-recessive myopathy (Frosk *et al.*, 2002) and sarcotubular myopathy (STM), a mild to moderate proximal muscle weakness (Schoser *et al.*, 2005). More *TRIM32* mutations have since been discovered in the NHL domain in patients with LGMD and STM (Borg *et al.*, 2009; Saccone *et al.*, 2008; Schoser *et al.*, 2005). Most of these

NHL-mutations were shown to abrogated homodimerization of TRIM32 and interaction with the E2 enzyme E2N. Furthermore, structural predictions showed that the mutated NHL domains fold differently and potentially mask the coiled-coil domain, preventing other protein-protein interactions (Saccone *et al.*, 2008). Two mutations found in patients, R394H and D489N, have been introduced into the analogous positions in mouse. Both mutations abrogated TRIM32 E3 ligase activity towards dysbindin – a skeletal muscle protein (Locke *et al.*, 2009). TRIM32 was also suspected to target ACTIN, TOPOMYOSIN and MYOSIN light chain for degradative ubiquitination, as their levels were upregulated upon TRIM32 loss (Cohen *et al.*, 2009; Kudryashova *et al.*, 2005). TRIM32 was also reported to be expressed in satellite cells – the resident, adult stem cells of skeletal muscle – and to be upregulated upon muscle injury or reloading. *Trim32* knockout mice show delayed muscle regeneration, probably due to impaired differentiation of *Trim32*$^{-/-}$ satellite cells, which show signs of premature senescence (Kudryashova *et al.*, 2012; Nicklas *et al.*, 2012). Taken together TRIM32 plays a critical role in muscle protein turnover and muscle function.

*Trim32* mRNA is much more abundant in brain compared to muscle, therefore it does not come as a surprise that the *Trim32* knockout phenotype has a neurogenic component: the mice show reduced motor axon diameter. The levels of neurofilament light, medium and heavy polypeptides are reduced in knockout mouse brains (Kudryashova *et al.*, 2005). And *Trim32* D489N knock in resulted in a 25% loss of neurofilament light and heavy polypeptides in brain (Kudryashova *et al.*, 2011). P130S missense mutation in the coiled-coil domain of *Trim32* causes to Bardet-Biedl syndrome, an autosomal recessive disease that displays, among other symptoms, a cognitive impairment phenotype (Chiang *et al.*, 2006). Finally, a screen for copy number variant overlaps between **a**ttention **d**eficit **h**yperactivity **d**isorder (ADHD) and **a**utism **s**pectrum **d**isorder (ASD) patients revealed duplications and deletions of the *Trim32* locus (Lionel *et al.*, 2011).

On a molecular level, recent studies shed more light on TRIM32 function in neurodifferentiation and neurodevelopment. In cultured cerebral cortex cells

established from E13.5 mice (when division of neural progenitor cells switches from symmetric to asymmetric), *Trim32* mRNA was asymmetrically inherited by the differentiation-prone daughter cell (Kusek *et al.*, 2012). Accordingly, after cell division *in vivo* at E14.5, about 80% of the TRIM32 protein is localized in the cells exiting the subventricular zone (compared to the progenitor cells that remain). Moreover, *Trim32* RNA interference applied by *in utero* electroporation abrogated neuronal migration and maturation (Schwamborn *et al.*, 2009). The **r**etinoic **a**cid **r**eceptor α (RARα), a driver of neural differentiation, was also reported to be a target of TRIM32 ubiquitination activity (Clagett-Dame *et al.*, 2006; Sato *et al.*, 2011). In this case, RARα was stabilized by ubiquitination and acted as positive transcriptional regulator of neural differentiation in P19 embryocarcinoma and Neuro2A cells (Sato *et al.*, 2011). TRIM32 might promote differentiation by more than one mechanism: Schwamborn and colleagues reported E3 ubiquitin ligase activity towards c-MYC, a major stem cell transcription factor. In addition, they found that TRIM32 enhanced the activity of the microRNA let-7, which is known to promote neural differentiation (Schwamborn *et al.*, 2009, see section 1.3.2).

## 1.5 Aims of this thesis

As demonstrated in the previous sections, the TRIM-NHL protein LIN41 is essential in early neurogenesis, although the detailed mode of action has yet to be elucidated. Therefore, the major aim of this thesis was to characterize novel LIN41 functions in stem cell differentiation and embryonic neurogenesis. For further mechanistic clarification, the following questions were addressed.

1. In stem cells, LIN41 localizes to processing bodies and ubiquitinates ARGONAUTE2 for proteasomal degradation. The question if LIN41 is able to influence other proteins of the microRNA biogenesis cascade was addressed using small hairpin RNAs that repress Lin41 mRNA translation and their stable integration into the P19 embryocarcinoma cell genome.
2. The reciprocal expression of LIN41 and let-7 and their mutual regulation in stem cell differentiation led to the hypothesis that LIN41

may also be critical for pluripotency maintenance. This issue was targeted with the above mentioned LIN41 knockdown model.

3. Common interaction partners of the mammalian TRIM-NHL proteins raised the question if LIN41 shares functions of the TRIM-NHL proteins that are expressed in adult CNS (association with MYOSINs and endosomes).
4. Along the same line of argument, TRIM2, TRIM3 and TRIM32 were hypothesized to mimic LIN41 repression of microRNA activity. To this end, their function in microRNA sensor assays was monitored.
5. Due to known multimerization of TRIM proteins, an interaction of mammalian TRIM-NHL proteins was hypothesized. To characterize potential co-localization and interaction, exogenous LIN41 was co-expressed with TRIM2, TRIM3 and TRIM32.
6. To target the problem of physiological relevance of the TRIM-NHL interactions, endogenous proteins were detected by immunostaining in early neurodevelopmental stages and analyzed for spatiotemporal co-expression of the TRIM-NHL proteins. Moreover TRIM2, TRIM3 and TRIM32 were precipitated from early neurogenic stages to test for co-purification of LIN41.
7. A possible interplay among the TRIM-NHL proteins in early neurogenesis was addressed in two *in vitro* stem cell differentiation models and with the induction of LIN41 expression in proliferative stem cells.
8. To generalize from the findings, TRIM-NHL protein levels were analyzed in different stem and committed cell lines.

# 2 MATERIAL AND METHODS

## 2.1 Material

### 2.1.1 Reagents

| Name | Cat. Number | Company | Use |
|---|---|---|---|
| Agarose SeaKem® LE | 50004 | Lonza | Agarose gel electroph. |
| SERVA DNA Stain G | 39803 | SERVA | Agarose gel electroph. |
| 100 bp-DNA-Ladder extended | T835.1 | Roth | Agarose gel electroph. |
| 1 kbp DNA-Ladder | Y014.1 | Roth | Agarose gel electroph. |
| 2,2,2-Tribromoethanol | T48402 | SIGMA | Avertin - sedative |
| tert-Amyl Alcohol | A730-1 | Fisher | Avertin - sedative |
| Oligo(dT) primer | SO132 | Thermo Sci. | cDNA synthesis |
| RiboLock RNase Inhibitor | EO0381 | Thermo Sci. | cDNA synthesis |
| RevertAid™ Reverse Transcriptase | EP0733 | Thermo Sci. | cDNA synthesis |
| dNTP Mix, 10 mM | R0192 | Thermo Sci. | cDNA synthesis |
| 0.05% Trypsin-EDTA (1x) | 25300-054 | Gibco | Cell culture |
| 2-Mercaptoethanol 50mM | 31350-010 | Gibco | Cell culture |
| DMEM (1x) | 21969-035 | Gibco | Cell culture |
| DMEM (1x) | 41966 | Gibco | Cell culture |
| DMEM/F12 | 10565 | Gibco | Cell culture |
| Neurobasal medium | 21103 | Gibco | Cell culture |
| EGTA | E-4378 | Sigma | Cell culture |
| GlutaMAX 100x | 35050-038 | Gibco | Cell culture |
| HEPES, 1 M | 15630-114 | Gibco | Cell culture |
| Penicillin-Streptomycin, Liquid | 15140-122 | Gibco | Cell culture |
| Sodium Pyruvate, 100 mM | 11360-039 | Gibco | Cell culture |
| Fetal Bovine Serum GOLD | A15-151 | PAA | Cell culture |
| N-2 Supplement | 17502-048 | Gibco | Cell culture - ESC diff. |
| B27 Supplement | 17504 | Gibco | Cell culture - ESC diff. |
| KnockOut™ Serum Replacement | 10828010 | Ambion | Cell culture - ESC diff. |
| Retinoic acid | R2526 | SIGMA | Cell culture - ESC diff. |
| ESGRO® (LIF) | ESG1106 | Millipore | Cell culture - ESCs |
| Gelatin 2% | G1393 | Sigma | Cell culture - ESCs |
| MEM NEAA | 11140-035 | Gibco | Cell culture - ESCs |
| Bovine Albumin Fraction V Sol (7.5%) | 15260-037 | Gibco | Cell culture - ESCs |

| | | | |
|---|---|---|---|
| Glycerol | 1040921000 | Merk | Cryoprotection |
| TOPO TA Cloning® kit | K4510-20 | Life Techn. | DNA cloning |
| QuikChange® II site-directed mutagenesis kit | 200523 | Agilent Techn. | DNA cloning |
| QIAquick Gel Extraction Kit | 28704 | QIAGEN | DNA extraction |
| T4 DNA Ligase | M0202L | NEB | DNA ligation |
| T4 DNA Polymerase | M0203 | NEB | DNA ligation |
| NucleoBond® Xtra Midi | 740410100 | Macherey Nagel | DNA preparation |
| Paraformaldehyde | P6148 | Sigma | Fixation |
| Goat serum | G9023-10ML | Sigma | IF Blocking |
| DAPI | 6335.1 | Roth | IF DNA staining |
| FluorSave™Reagent | 345789 | Calbiochem | IF mounting |
| ImmEdge™ pen | H-4000 | Vector | IF on sections |
| Phusion™ Hot Start DNA Polymerase | F-540L | NEB | PCR |
| dATP 100 mM | 272-050 | Pharm. Biotech | PCR |
| dCTP 100 mM | 272-060 | Pharm. Biotech | PCR |
| dTTP 100 mM | 272-080 | Pharm. Biotech | PCR |
| dGTP 100 mM | 272-070 | Pharm. Biotech | PCR |
| Protease Inhibitor Cocktail Set I | 539131-10VL | Calbiochem | Protein lysis buffer |
| Bio-Rad Protein Assay Dye Reagent | 500-0006 | BIO-RAD | Protein measure |
| Standard Cuvettes (PS) and (PMMA) | 67740 | Sarstedt | Protein measure |
| BSA Standard | 23209 | Pierce | Protein measure |
| TRIzol Reagent | 15596026 | Ambion | RNA isolation |
| 30% Acrylamide/Bis Solution 29:1 | 161-0156 | BIO-RAD | SDS-PAGE |
| TEMED | T-8133 | SIGMA | SDS-PAGE |
| Dimethyl sulfoxide | A994.2 | Roth | Solvent |
| OCT COMPOUND | 3808610E | Leica | Tissue embedding |
| Lipofectamine® 2000 | 11668-019 | Invitrogen | Transfection |
| Opti-MEM® I 1x | 31985-047 | Gibco | Transfection |
| Whatman 3MM Chr sheets, 46 x 57 cm | 3030-917 | Whatman | Western blot |
| PageRulerTM Protein Ladder Plus | SM1811 | Fermentas | Western blot |
| Immobilon-P Transfer Membrane | IPVH00010 | Millipore | Western blot |
| Ponceau S solution | P7170 | Sigma | Western blot |
| Albumin Fraction V | 8076.2 | Roth | Western blot |

| | | | |
|---|---|---|---|
| Milk powder | T145.2 | Roth | Western blot |
| Amersham Hyperfilm ECL | 521572 | GE Healthcare | Western blot |
| Clarity Western ECL Substrate | 170-5060 | BIO-RAD | Western blot |

### 2.1.2 Vectors

| Vector | Produced by |
|---|---|
| p3xFLAG-CMV™-7.1 | SIGMA |
| p3xFLAG-CMV™-10 | SIGMA |
| pDsRed2-N1 | Clontech |
| peGFP-C1 | Clontech |
| pCR2.1 TOPO | Invitrogen |

### 2.1.3 Constructs

| Vector | cDNA | Produced by |
|---|---|---|
| pCAGEN | | Takahiko Matsuda, Cepko lab |
| pXho | based on peGFP-C1 | Heiko Fuchs, Wulczyn lab |
| pXho | 2x let-7a binding sites | Heiko Fuchs, Wulczyn lab |
| pXho | 2x miR124 binding sites | Heiko Fuchs, Wulczyn lab |
| pXho | 2x miR128 binding sites | Heiko Fuchs, Wulczyn lab |
| p3xFLAG-CMV™-10 | gMyoVa | Eickholt lab |
| peGFP | gMyoVa | Estéban lab |
| peGFP | gMyoVb | Estéban lab |
| peGFP | gMyoVI | Estéban lab |
| peGFP | hAgo2 | Addgene #11590 |
| pFRT/FLAG/HA-DEST | EIF2C2 (AGO2) | Addgene # 19888 |
| p3xFLAG-CMV™-7.1 | Lin41 | Agnieszka Rybak, Wulczyn lab |
| p3xFLAG-CMV™-7.1 | Lin41 C12LC15A mut | Agnieszka Rybak, Wulczyn lab |
| peGFP-C1 | Lin41 | Agnieszka Rybak, Wulczyn lab |
| peGFP-C1 | Lin41del #1 (Ring+BBox) | Agnieszka Rybak, Wulczyn lab |
| peGFP-C1 | Lin41del #2 (Ring+BBox+CC) | Agnieszka Rybak, Wulczyn lab |
| peGFP-C1 | Lin41del #3 (Ring+BBox+CC+FLM) | Agnieszka Rybak, Wulczyn lab |

| | | |
|---|---|---|
| peGFP-C1 | Lin41del #4 (BBox+CC+FLM+NHL) | Agnieszka Rybak, Wulczyn lab |
| peGFP-C1 | Lin41del #5 (CC+FLM+NHL) | Agnieszka Rybak, Wulczyn lab |
| peGFP-C1 | Lin41del #6 (FLM+NHL) | Agnieszka Rybak, Wulczyn lab |
| peGFP-C1 | Lin41del #7 (NHL) | Agnieszka Rybak, Wulczyn lab |
| peGFP | Rab5 | Haucke lab |
| peGFP | Rab7 | Haucke lab |
| pCS2-myc | Trim2 | Balastik lab |
| pGW1-FLAG | Trim3 | Sheng lab |
| pQBI-25-fA1 (GFP) | Trim32 | Spencer lab |

### 2.1.4 Primers

| Name | Sequence 5'-3' | $T_a$ | size |
|---|---|---|---|
| **shRNA primer:** | | | |
| shLin41 #1 for | GATCCCCCCAAAGGCCTTTGAATGTATTCAAGAGATACATTCAAAGGCCTTTGGTTTTTA | 95-4 °C | 64 bp |
| shLin41 #1 rev | AGCTTAAAAACCAAAGGCCTTTGAATGTATCTCTTGAATACATTCAAAGGCCTTTGGGGG | 95-4 °C | 64 bp |
| shLin41 #2 for | GATCCCCGACTCTAGGTTGAAAGTGTTTCAAGAGAACACTTTCAACCTAGAGTCTTTTTA | 95-4 °C | 64 bp |
| shLin41 #2 rev | AGCTTAAAAAGACTCTAGGTTGAAAGTGTTCTCTTGAAACACTTTCAACCTAGAGTCGGG | 95-4 °C | 64 bp |
| shLin41 #3 for | GATCCCCGAGCCTGTGAAGTGATAATTTCAAGAGAATTATCACTTCACAGGCTCTTTTTA | 95-4 °C | 64 bp |
| shLin41 #3 rev | AGCTTAAAAAGAGCCTGTGAAGTGATAATTCTCTTGAAATTATCACTTCACAGGCTCGGG | 95-4 °C | 64 bp |
| shLuci for | GATCCCCCATCACGTACGCGGAATACTTTCAAGAGAAGTATTCCGCGTACGTGATGTTTTTA | 95-4 °C | 64 bp |
| shLuci rev | AGCTTAAAAACATCACGTACGCGGAATACTTCTCTTGAAAGTATTCCGCGTACGTGATGGGG | 95-4 °C | 64 bp |
| **Site-directed mutagenesis:** | | | |
| mTrim2_C26A | CAAGCAGTTTCTGATCTGCAGTATAGCCCTGGAACGGTA | 60 °C | |
| mTrim2_C26A_as | GTACCGTTCCAGGGCTATACTGCAGATCAGAAACTGCTTG | 60 °C | |
| rTrim3_C25A | TCTGGTATGCAGTATCGCCCTGGATCGGTACCGG | 60 °C | |
| rTrim3_C25A_as | CCGGTACCGATCCAGGGCGATACTGCATACCAGA | 60 °C | |
| mTrim32_C24A | GTGCTAGAATGTCCCATCGCCATGGAGTCCTTCACTGA | 60 °C | |
| mTrim32_C24A_as | TCAGTGAAGGACTCCATGGCGATGGGACATTCTAGCAC | 60 °C | |
| **Recovery of Lin41 deletion constructs:** | | | |
| fwdL41_1 | TATAGTCGACATGGCTTCGTTCCCGGAG | 60 °C | |
| fwdL41_900 | TATAGTCGACTTCGCCTACCTCCAGGAT | 60 °C | |
| fwdL41_1340 | TATAGTCGACATTATGTTCACGCCCCCTGA | 60 °C | |
| revL41_900 | TATAGGATCCATCCTGGAGGTAGGCGAA | 60 °C | |
| revL41_2560 | TATAGGATCCGAAGATGAGGATTCGATTGTTG | 60 °C | |
| **Subcloning of Trim2:** | | | |
| mTrim2_fwd1<br>mTrim2_rev2235 | ATTGATATCTTTGGCCAGTGAGGGCGC<br>GGAGTCGACTTACTGTAAGTACCGGTAGAC | 50-60°C | 2235bp |

| **Quantitative Real-Time PCR:** | | | |
|---|---|---|---|
| β-actin qRT for | GGCTGTATTCCCCTCCATCG | 60 °C | 154 bp |
| β-actin qRT rev | CCAGTTGGTAACAATGCCATGT | 60 °C | |
| Trim2 qRT for | TCACGAACCTCATGGATGTGC | 60 °C | 152 bp |
| Trim2 qRT rev | ACAGGACTGGCAGTAAAATTCC | 60 °C | |
| Trim3 qRT for | GCGTCTCAGCCCTACAAAACA | 60 °C | 161 bp |
| Trim3 qRT rev | AAACTCCATTGTCTTGCCTTCA | 60 °C | |
| Trim32 qRT for | CCTCCGGGAAGTGCTAGAATG | 60 °C | 102 bp |
| Trim32 qRT rev | CACTGGCGGCAGATGGTATG | 60 °C | |
| Lin41 f | GACTCTCGGGCACTCACCAT | 60 °C | 132 bp |
| Lin41 r | CGCCTTCATCTCCACCTGTT | 60 °C | |

### 2.1.5 Restriction enzymes

| **Enzyme** | **Cat. Number** | **Buffer** | **Company** |
|---|---|---|---|
| ApaI | R0114 | NEBuffer 4 | NEB |
| BamHI | R0136 | NEBuffer 3 | NEB |
| BglII | R0144 | NEBuffer 3 | NEB |
| BspEI | R0540 | NEBuffer 3 | NEB |
| BssHI | R0199 | NEBuffer 4 | NEB |
| EcoRI | R0101 | NEBuffer 2 | NEB |
| EcoRV | R0195 | NEBuffer 3 | NEB |
| HincII | R0103 | NEBuffer 3 | NEB |
| HindIII | R0104 | NEBuffer 2 | NEB |
| NotI | R0189 | NEBuffer 3 | NEB |
| PspXI | R0656 | NEBuffer 4 | NEB |
| SalI | R0138 | NEBuffer 3 | NEB |
| SpeI | R0133 | NEBuffer 4 | NEB |
| XhoI | R0146 | NEBuffer 4 | NEB |
| BSA | 10 mg/ml (100x) | | NEB |

### 2.1.6 Bacterial strains

| ***E. coli*** | **Genotype** | **Source** |
|---|---|---|
| DH5α | F- φ80dlacZΔM15 Δ(lacZYA-argF)U169, deoR, recA1, endA1, hsdR17(rk-, mk+), phoA, supE44, λ-, thi-1, gyrA96, relA1 | Invitrogen |
| XL10Gold | endA1 glnV44 recA1 thi-1 gyrA96 relA1 lac Hte Δ(mcrA)183Δ(mcrCB-hsdSMR-mrr)173 tetR F'[proAB lacIqZΔM15 Tn10(TetR Amy CmR)] | Stratagene |
| TOP10 | F- mcrA Δ(mrr-hsdRMS-mcrBC) Φ80lacZΔM15 lacX74 recA1 deoR araD139 Δ(araleu)7697 galU galK rpsL (StrR) endA1 nupG | Invitrogen |

### 2.1.7 Antibiotics

| Antibiotic | Stock Concentration | Working Concentration | Use |
|---|---|---|---|
| Ampicillin | 100 mg/ml in $H_2O$ | 50-100 µg/ml | Prokaryotes |
| Kanamycin | 12,5 mg/ml in $H_2O$ | 25 µg/ml | Prokaryotes |
| Geneticin (G418) | 50 mg/ml in $H_2O$ | 1 µg/ml | Eukaryotes |

### 2.1.8 microRNA mimics and siRNAs

| microRNA mimic / siRNA | Type | Company |
|---|---|---|
| hsa-let-7e | Pre-miR | Ambion (life technologies) AM17100 ID: PM12304 |
| hsa-miR-124 | *mir*Vana® miRNA mimic | Ambion (life technologies) 4464066 ID: MC10691 |
| hsa-miR-128 | *mir*Vana® miRNA mimic | Ambion (life technologies) AM17100 ID: PM11746 |
| siMyoVa #5 (human) | ON Target Plus | Thermo Scientific, J-019321-05 |
| siMyoVa #7 (human) | ON Target Plus | Thermo Scientific, J-019321-05 |

### 2.1.9 Buffers and Solutions

### 2.1.10 Agarose gel electrophoresis

| Buffer | Ingredients |
|---|---|
| DNA 10x Loading buffer | 50 g Sucrose, 0.25 g Bromphenol blue, 100 ml in 1x TBE |
| TBE 10x (1L) | 0.45M Trisbase, 0.45 M Boric Acid, 10 mM EDTA 0.5M (pH 8.0) |

### 2.1.11 Immunofluorescence staining

| Buffer | Ingredients |
|---|---|
| Avertin Stock solution | 25 grams avertin (2, 2, 2-Tribromoethanol)<br>15. 5 ml tert-Amyl Alcohol (2-methyl-2-butanol) |
| Avertin working solution (20 mg/ml) | 0.5 ml Avertin stock 39.5 ml 0.9% saline (NaCl) |
| 0.2 M PB (5L) pH 7.3 | 137,6 g $Na_2HPO_4$, 35,26 g $NaH_2PO_4$ x $2H_2O$ |
| PBS 10x (1L) pH 7.4 | 80g NaCl, 0.2g KCl , 14.4g $Na_2HPO_4$ • 2 $H_2O$, 0.2g $KH_2PO_4$ |
| PFA 4% (w/v) in 0.2 M PB | |

### 2.1.12 Bacteria culture

| Buffer | Ingredients |
|---|---|
| LB medium | 10 g/L Peptone, 10 g/L NaCl, 5 g yeast extract, adjust pH 7.4 |
| LB agar | 10 g/L Peptone, 10 g/L NaCl, 5 g yeast extract, 15 g agar agar, adjust pH 7.4 |

### 2.1.13 Western blot

| 5% Stacking gel | ml/2ml | 6% Separating gel | ml/10 ml |
|---|---|---|---|
| $H_2O$ | 1.4 | $H_2O$ | 5.3 |
| 30% acrylamide mix (29:1) | 0.33 | 30% acrylamide mix (29:1) | 2.0 |
| 1.0 M Tris (pH 6.8) | 0.25 | 1.5 M Tris (pH 8.8) | 2.5 |
| 10% SDS | 0.02 | 10% SDS | 0.1 |
| 10% ammonium persulfate | 0.02 | 10% ammonium persulfate | 0.1 |
| TEMED | 0.002 | TEMED | 0.008 |

| 8% Separating gel | ml/10 ml | 10% Separating gel | ml/10 ml |
|---|---|---|---|
| $H_2O$ | 4.6 | $H_2O$ | 4.0 |
| 30% acrylamide mix (29:1) | 2.7 | 30% acrylamide mix (29:1) | 3.3 |
| 1.5 M Tris (pH 8.8) | 2.5 | 1.5 M Tris (pH 8.8) | 2.5 |
| 10% SDS | 0.1 | 10% SDS | 0.1 |
| 10% ammonium persulfate | 0.1 | 10% ammonium persulfate | 0.1 |
| TEMED | 0.006 | TEMED | 0.004 |

| Buffer | Ingredients |
|---|---|
| Protein lysis buffer TNN | 50mM Tris pH7.4, 150 mM NaCl , 0.5% NP-40 (Igepal), 5mM EDTA, Protease Inhibitor Cocktail Set I 1x |
| Protein lysis buffer CoIP | 2% TritonX-100 in PBST |
| Protein lysis buffer CoIP | 1 % NP-40 in 50 mM Tris-HCL pH 7.8 and 300 mM KCl |
| Protein lysis buffer CoIP | 1 % NP-40 in 1 M Tris-HCL pH 7.8 and 200 mM KCl |
| 4x Laemmli sample buffer | 200 mM DTT, 100 mM Tris-HCl pH6.8, 20% (v/v) glycerol, 4% SDS, 0.2% brom phenol blue |
| 10x Electrophoresis buffer | 25 mM Tris, 200 mM glycin, 1% SDS |
| 10x Blotting buffer 2 l | 25 mM Tris, 150 mM mM glycin (15% MeOH in 1x buffer) |
| Ponceau-S | 0.1 % Ponceau S , 5% acetic acid |
| PBST | PBS, 0.1% Tween 20 |
| Stripping buffer | 0,2M Glycin pH2.5, 0.05%Tween |

### 2.1.14 Cell culture media

#### 2.1.14.1 HeLa, HEK 293T and N2A cell culture medium

| Component | Catalog number | Volume |
|---|---|---|
| DMEM | Gibco, 41966 | 440 ml |
| FBS | PAN, P30-3306 | 50 ml |
| GlutaMax | Gibco, 35050 | 5 ml |
| Penicillin/streptomycin | Gibco 15140 | 5 ml |

#### 2.1.14.2 P19 embryocarcinoma cell culture medium

| Component | Catalog number | Volume |
|---|---|---|
| MEM, α-modification | Gibco, 41966 | 445 ml |
| FBS | PAN, P30-3306 | 50 ml |
| Penicillin/streptomycin | Gibco 15140 | 5 ml |

#### 2.1.14.3 W4 embryonic stem cell culture medium

| Component | Catalog number | Volume |
|---|---|---|
| DMEM | Gibco, 41965 | 395 ml |
| GlutaMax | Gibco, 35050 | 5 ml |
| MEM NEAA | Gibco, 11140 | 5 ml |
| ESC-qualified FBS | PANSera, 2602-P272405 | 75 ml |
| β-Mercaptoethanol, 10 mM | Gibco, 31350 | 5 ml |
| Penicillin/streptomycin | Gibco, 15140 | 5 ml |
| ESGRO (Lif) | Millipore, ESG1107 | 1 µl/2ml |

#### 2.1.14.4 iLin41 embryonic stem cell culture medium

| Component | Catalog number | Volume |
|---|---|---|
| DMEM | Gibco, 21969 | 395 ml |
| L-glutamine | Gibco, 25030 | 5 ml |
| HEPES, 1M | Gibco, 15630 | 10 ml |
| MEM NEAA | Gibco, 11140 | 5 ml |
| ESC-qualified FBS | PANSera, 2602-P272405 | 75 ml |
| β-Mercaptoethanol, 10 mM | Gibco, 31350 | 5 ml |
| Penicillin/streptomycin | Gibco 15140 | 5 ml |
| ESGRO (Lif) | Millipore, ESG1107 | 1 µl/2ml |

### 2.1.15 Antibodies

| Primary antibody | Company | Dilution for WB | Dilution for IF |
|---|---|---|---|
| rabbit anti-TRIM2 | Sigma, SAB4200206 | 1:2000 | 1:200 |
| mouse anti-TRIM3 | St. Cruz, sc-136363 | 1:1000 | 1:50 |
| rabbit anti-TRIM32 | Abcam, ab96612 | 1:1000 | 1:100 |
| rabbit anti-LIN41 (peptide) | Pineda | | 1:50 |
| rabbit anti-LIN41 (serum) | Pineda | 1:2000 | |
| mouse anti-N-Cadherin | BD Transd., 610920 | | 1:500 |
| mouse anti-DCP1a | Sigma, WH0055802M6 | | |
| mouse anti-FLAG | Sigma, F1804 | 1:2000 | 1:1000 |
| rabbit anti-GFP | Abcam, ab290 | 1:500-1000 | |
| mouse anti-Vinculin | Sigma, V9131 | 1:10000 | |
| **Secondary antibody** | **Company** | **Dilution for WB** | **Dilution for IF** |
| anti-mouse-IgG HRP | JacksonImmuno | 1:5000 | |
| anti-mouse-IgG lightchain spec. HRP | JacksonImmuno | 1:5000 | |
| anti-rabbit-IgG HRP | JacksonImmuno | 1:5000 | |
| anti-rabbit-IgG light chain spec. HRP | JacksonImmuno | 1:5000 | |
| anti-rat-IgG HRP | Dako | 1:2500 | |
| anti-rat-IgG light chain spec. HRP | JacksonImmuno | 1:5000 | |
| donkey anti-rabbit Cy3 | JacksonImmuno | | 1:1000 |
| goat anti-rabbit594 | JacksonImmuno | | 1:1000 |
| donkey anti-rabbit-Alexa 488 | Invitrogen | | 1:1000 |
| donkey anti-mouse 594 | JacksonImmuno | | 1:1000 |
| goat anti-mouse 488 | Invitrogen | | 1:1000 |

Both rabbit anti-LIN41 antibodies are in house antibodies, produced in cooperation with Pineda.

### 2.1.16 Equipment

| Name | Company | Use |
|---|---|---|
| Microscope Olympus BX51 with MagnaFire Image acquisition | Olympus | Microscopy |
| Confocal equipment TCS SL (Leica Microsystem) | Leica | Microscopy |
| Eppendorf Thermomixer® compact | Eppendorf | Equipment |
| Environmental Shaker-Incubator ES-20 | Grant-bio | Equipment |
| Centrifuge 5415 D | Eppendorf | Equipment |
| Centrifuge 5417 R | Eppendorf | Equipment |
| Owl* EasyCast* B1 and B2 Mini Gel Electrophoresis Systems | Thermo Scientific | agarose gel electrophoresis |
| ChemiDoc™ XRS+ System 170-8265 | BIO-RAD | Western blot development |
| Mini Trans-Blot® Cell 170-3930 | BIO-RAD | Western blot transfer |
| Nanophotometer 1374 | IMPLEN | Equipment |
| BD FACSCanto II flow cytometer | BD | FACS |
| PXE 0.2 Thermal Cycler | Thermo Scientific | PCR |
| StepOnePlus Real-Time PCR System | Applied Biosystems | qRT-PCR |
| Leica CM1900 Cryostat | Leica | Histology |

### 2.1.17 Software

Microsoft Office 2011 for Mac
Adobe Illustrator CS4
Adobe Photoshop CS4
Adobe Acrobat 8.3
Papers2 from Mekentosj
Fiji 1.0
Prism 5 for MacOS
e!*Ensembl* genome browser (http://www.ensembl.org/index.html)
BLAST (http://www.ncbi.nlm.nih.gov/BLAST/)
Leica Confocal Software v. 2.61 Build 1537
Magnafire
NCBI database (http://www.ncbi.nlm.nih.gov/)
Primer3 program (http://frodo.wi.mit.edu/)
TargetScan software (http://genes.mit.edu/targetscan)
Image Lab – BioRad
Flow Jo vX for Mac
DNA molar ratio calculator ((http://www.insilico.uni-duesseldorf.de/Lig_Input.html))
Primer Bank (http://pga.mgh.harvard.edu/primerbank/)
DKFZ e-RNAi (http://www.dkfz.de/signaling/e-rnai3//)
The RNAi Consortium (http://www.broadinstitute.org/rnai/trc)

## 2.2 Methods

### 2.2.1 Agarose gel electrophoresis

For size separation of DNA fragments, agarose gels were cast in Owl* EasyCast* B1 and B2 Mini Gel Electrophoresis Systems at a concentration of 1 to 2.5 %. The appropriate amount of agarose (Lonza, 50004) was melted in Tris/Borate/EDTA (TBE) buffer. To visualize DNA with UV light 2 µl Serva DNA Stain G solution/50 ml (SERVA, 39803) were added when the agarose solution had cooled to about 60 °C. The appropriate volume of 10x Loading buffer was diluted in the DNA prior to loading the agarose gel. For size comparison 10 µl of either 100 bp-DNA-Ladder extended or 1 kbp DNA-Ladder (Roth, T835.1 or Y014.1 respectively) was loaded in a separate well.

### 2.2.2 Polymerase chain reaction (PCR)

PCR was performed using the Phusion™ Hot Start DNA Polymerase (NEB, F-540L) and the corresponding reagents in 0.2 ml tubes in a PXE 0.2 Thermal Cycler (Thermo Scientific). Unless otherwise is specified, 20 µl reaction was prepared as follows:

| Reagent | Volume (µl) | Final concentration |
|---|---|---|
| $H_2O$ (MilliQ grade) | 12.3 | |
| 5x Phusion GC Buffer | 4 | 1x |
| 10mM dNTPs | 0.5 | 200 µM each |
| 10mM Primer A | 1 | 1 µM |
| 10mM Primer B | 1 | 1 µM |
| Template DNA (100ng/µl) | 1 | |
| Phusion Hot Start polymerase | 0.2 | 0.02 U/µl |

The PCR reaction was performed using the program displayed below. After step 4 the program cycles back to step 2 24 times.

| Step | Temperature | Time |
|---|---|---|
| 1 | 98 °C | 30 sec |
| 2 | 98 °C | 10 sec |
| 3 | 60 °C | 30 sec |
| 4 | 72 °C | 40 sec |
| 5 | 72 °C | 5 min |
| 6 | 4 °C | endpoint |

### 2.2.3 RNA isolation and cDNA synthesis

RNA was isolated from cells or tissue using TRIzol® reagent (Life Technologies, 15596026) according to manufacturer's instructions, and stored at -80°C. First strand cDNA synthesis was performed with the RevertAid Premium Reverse Transcriptase using OligodT primers to amplify from all transcribed mRNAs.

| Reagent | Volume |
|---|---|
| RNA (1 µg/µl) | 1 µl |
| OligodT | 1 µl |
| 10 mM dNTP | 1 µl |
| 5x RT buffer | 4 µl |
| dd$H_2O$ | 11.5 µl |
| Ribolock RNAse inhibitor | 0.5 µl |
| RevertAid Premium Reverse Transcriptase | 1 µl |

### 2.2.4 Quantitative Real-Time PCR (qRT-PCR)

For quantitative analysis of mRNA expression levels, qRT-PCR was performed using $RT^2$ SYBR® Green qPCR Mastermix (QIAGEN) according to the instructions. The cDNA was 3x diluted in water prior to using 1µl for the qRT-PCR in a total volume of 10 µl. The amplification step (step 2) is repeated 40 times. After each cycle fluorescein intensity is measured and compared to control dye intensity as a measure for the DNA content.

| Reagent | Volume | Step | Temperature | Time |
|---|---|---|---|---|
| RT2 Master Mix | 5 µl | 1 | 95 °C | 10 min |
| 3x diluted cDNA | 1 µl | 2 | 95 °C | 15 sec |
| 10 mM for primer | 0.2 µl | | 60 °C | 50 sec |
| 10 mM rev primer | 0.2 µl | 3 | 60-95 °C | melting curve |
| $ddH_2O$ | 3.6 µl | 4 | 4 °C | endpoint |

### 2.2.5 DNA restriction digestion

To digest DNA in specific fragments, restriction enzymes (NEB, section 2.1.5) were used with the corresponding buffers according to manufacturer's instructions. DNA was digested from 30 min to 1 h at 37 °C, and enzymes were thermally inactivated at 65 °C if required for subsequent procedures. If two enzymes did not employ the same optimal digestion buffer subsequent digestions with intermediate DNA purification were performed.

### 2.2.6 DNA isolation and precipitation

When two incompatible restriction enzymes were used for DNA digestion, the DNA was purified in an intermediate step, to allow buffer change. Also when the DNA fragments needed to be separated to proceed, the digested samples were run in an agarose gel electrophoresis and purified using the QIAquick Gel Extraction Kit (QIAGEN, 28704) according to manufacturer's instructions.

### 2.2.7 DNA ligation

Purified DNA fragments were ligated using T4 DNA ligase (NEB, M0202L) 1h at room temperature according to manufacturer's the instructions.

### 2.2.8 Transformation

50% of the ligation reaction was transformed into 50-100 µl chemically competent XL-10 Gold or TOP10 *E. coli* bacteria. First the mixture was incubated on ice for 5 min, then 45 sec at 42°C followed by 2 min on ice. 250 µl LB medium was added and the bacteria were incubated 30-60 min at 300 rpm and 37°C for recovery. 10% and 90 % of the sample were spread to separate agar plates containing the appropriate antibiotic.

### 2.2.9 Bacterial cultures

Separate LB medium samples (3 ml for Mini preparation) were inoculated with one bacteria colony each (after ligation) or with bacteria from the glycerol stock (100 ml for Midi preparation) and incubated over night at 37 °C, 140 rpm. The bacteria were pelleted by centrifugation (5000 rpm for 5 min) at 4 ° and either stored at -20 °C or directly used for DNA preparation.

### 2.2.10 DNA preparations

The NucleoBond® Xtra Midi kit buffers (Macherey Nagel, 740.410.100) were used for DNA Mini preparations. 2 ml of the bacteria culture were centrifuged at 5000 rpm, 4 °C for 5 min. The supernatant was removed and the pellet resuspendet in 200 µl RES (resuspension) buffer. 200 µl LYS (lysis) buffer were added and the tubes inverted 15 times. After 5 min incubation time at room temperature, 200 µl NEU (neutralisation) buffer were added and the tubes inverted 10 times. The precipitated proteins were pelleted by centrifugation at 14000 rpm, 4 °C for 20 min. The supernatant was transferred to a new tube and the pellet discarded. 1000 µl EtOH or 500 µl isopropanol were added for DNA precipitation. The tubes were inverted 15 times and centrifuged at 14000 rpm, 4 °C for 5 min. The dried (10-15 min) pellet was resuspended in 20-50 µl $H_2O$ (MilliQ grade). DNA Midi preparations performed with the NucleoBond® Xtra Midi (Macherey Nagel, 740.410.100) according to manufacturer's instructions. DNA concentration was measured with a nanophotometer (IMPLEN).

### 2.2.11 Sub-Cloning

#### 2.2.11.1 *Lin41* shRNA constructs

Three different shRNA constructs targeting the Lin41 3'UTR were designed with the help of algorithms from DKFZ e-RNAi and The RNAi Consortium. The 64 bp long forward and reverse oligomers (sequences in section 2.1.4) were annealed and digested with BglII and HindIII and ligated into p.Super.retro.neo+GFP vector digested with the same enzymes. The following steps were performed as described in section 2.2.7 - 2.2.10.

#### 2.2.11.2 TRIM2-GFP and TRIM2-FLAG

Mouse *Trim2* cDNA sequence was amplified by PCR from pCS2-myc plasmid (gift from M. Balastik) using Phusion polymerase (NEB) with primers including an EcoRV (5'site) and a SalI (3'site) restriction digestion site. After amplification, the PCR product and the recipient p3xFLAG-CMV vector were digested with EcoRV and SalI. peGFP-C1 was digested first with BspI in the 5' end, then incubated with T4 DNA polymerase 15 min at 12°C to create a blunt end (for inactivation EDTA was added in 10 mM final concentration and it was incubated at 75°C for 20 min) and subsequently digested with SalI in the 3'end. The fragments were run on a 1 % agarose gel and purified with the QIAquick gel extraction kit. Purified fragments were ligated using T4 DNA ligase (NEB) 1h at room temperature according to the instructions. 50% of the ligation reaction was transformed into 50-100 µl chemically competent XL-10 Gold E. coli bacteria. Colonies were grown agar plates containing the respective antibiotic.

#### 2.2.11.3 TRIM3-GFP

Rat TRIM3-FLAG was a gift from M. Sheng. The 5' end of rat *Trim3* was cut with BssHI, the one of peGFP-C1 with BspEI. Then both were treated with T4 DNA polymerase to create blunt ends. Afterwards both were digested with BglII in the 3' end. Fragments were run on a 1 % agarose gel and were purified, ligated and transformed into bacteria.

#### 2.2.11.4 TRIM32-FLAG

Mouse *Trim32* cDNA sequence was cut from the pQBI25-fA1 plasmid (gift from M. Spencer) in 5' end using ApaI followed by T4 DNA polymerase treatment to create a blunt end and digestion with EcoRI in the 3'end. The destination vector p3xFLAG-CMV7.1 (Sigma) was cut in 5' by NotI followed T4 DNA polymerase and EcoRI in the 3' end. The fragments were separated in a 1 % agarose gel, cut and purified using the QIAquick gel extraction kit (QIAGEN). The fragments were ligated and transformed into bacteria.

#### 2.2.11.5 LIN41 C12LC15A mut – GFP

The RING domain mutation C12LC15A was inserted into wildtype *Lin41* cDNA in peGFPC1 by restriction digestion and ligation using FLAG-LIN41 C12LC15A as template. peGFPC1 *Lin41* was cut with HindIII, treated with T4 DNA polymerase and digested with NotI (5': at ~bp700 in *Lin41* sequence). The mutated RING domain was amplified with the Lin41_fwd1 and Lin41_rev900 primer with the Phusion polymerase including 10 %betaine in the reaction because of the GC-rich region. The amplified fragment was digested with HincII and NotI. The fragments were purified, ligated and transformed into bacteria.

#### 2.2.11.6 Recovery of GFP-LIN41 depletion constructs

Agnieska Rybak cloned the original GFP-LIN41 depletion constructs (Agnieska Rybak, PhD thesis, 2009). Nonetheless, not the whole set could be recovered from the stock boxes. Depletion construct #1 (containing RING and B box 1), #5 (containing coiled-coil, filamin and NHL domain), #6 (containg the filamin and NHL domain) had to be recloned, using the primers designed by Agnieska Rybak. The sequences of the LIN41 domains were amplified with the Phusion™ Hot Start DNA Polymerase (NEB, F540L) with additional 10 % betaine in the polymerase reaction (because of the GC-rich region in the LIN41 N-terminus). The PCR products were ligated to the TOPO2.1 vector from the TOPO TA Cloning® kit (Life Technologies, K4510-20). From there they were excised using SalI and BamHI and ligated to the equally digested peGFP-C1. After ligation the DNA was transformed in to chemically competent *E. coli* bacteria.

### 2.2.12 Site-directed mutagenesis

The second cysteines in the C3HC4 RING finger domains of *Trim2*, *Trim3* and *Trim32* were mutated in the FLAG- and GFP-tagged constructs using primers that contain the *Trim2* C26A, *Trim3* C25A and respectively *Trim32* C24A mutation. Site-directed mutagenesis was performed by amplifying the whole vector with primers, which contained the desired mutation. Thereby the mutation was introduced with each amplification using the QuikChange® II site-directed mutagenesis kit (Agilent Technologies, 200523) according to the manufacturers instructions.

### 2.2.13 Cell culture

HeLa, HEK 293T and N2A cells were cultured in DMEM (41966) with 10% FBS 1% GlutaMax and 1% penicillin/streptomycin. Every 3-4 days the cells were subcultured in a 1:10 ratio. P19 neuroblastoma cells were cultured in MEM with alpha-modification, 10% FBS and 1% penicillin/streptomycin. They were subcultured at a ratio of 1:20-1:30 every 3-4 days. To generate a LIN41 downregulation model, P19 cells transfected with pSuper.retro.neo+gfp containing shRNAs targeting *Luciferase* or *Lin41* were grown in the same meduium supplemented with 1 µg/ml of the antibiotic G418. The surviving cells were pooled and kept under selective pressure. The GFP fluorescence was downregulated after about three days in selection, but the constructs remained integrated into the P19 cell genome as long as the selective pressure was maintained. Reduction to 10 % of the selection antibiotoic after the initial selection phase (common procedure) led to immediate loss of the integration. All cell lines were cultured for two month maximum, before thawing a new stock vial.

Doxycyclin-inducible FLAG-LIN41 KH2 ESCs (iLin41) were a kind gift of Dr. Richard I. Gregory. Doxycycline-inducible FLAG-tagged *Lin41* cDNA was stable inserted downstream of the ColA1 locus under control of tetracycline operator minimal CMV promoter (tetOP). Additionally a tetracycline controllable transactivator (rtTA) was introduced in the Rosa26 locus of KH2 ESCs (iLin41). Doxycycline treatment causes expression of the transactivator and therefore the

transcription of FLAG-LIN41 from the ColA1 locus and subsequent synthesis of FLAG-LIN41 protein (Chang *et al.*, 2012). iLin41 embryonic stem cells were cultured in DMEM (21969) supplied with Glutamax (GIBCO 35050), Hepes (GIBCO 15630), MEM NEAA (GIBCO 11140), penicillin/streptomycin (GIBCO 15140), β-mercaptoethanol (GIBCO, 31350-010), FBS for ESCs (PANSera, 2602-P272405PAN ) and LIF (ESGRO, Millipore, ESG1107). For subculture, they were split 1:10 every second or 1:20 every third day. Experiments were performed between passage number 10 and 30.

### 2.2.14 Transfection

For immunofluorescence assays adherent cells were transfected using Lipofectamine®2000 (Life Technologies, 11668-019) according to the instructions. For immunoprecipitation assay cells were transfected with calcium phosphate. The 25 µg total DNA is mixed with 62.5 µl 2 M $CaCl_2$, then double-destilled water is added up to 500 µl. This mixture is added dropwise to vortexed 500 µl 2x HBS to form calcium phosphate – DNA precipitates. The solution was incubated at room temperature for 30 min and then added to the medium. Unless other wise stated the samples were analysed 24 h after transfection.

### 2.2.15 FACS sensor assay

4 x $10^5$ HEK 293T cells were seeded in a 12-well-plate (4 x $10^5$/well) and reverse transfected with Lipofectamine®2000 according to the instructions. 100 ng pCAGEN pDR1 construct were introduced as transfection control together with 20 pmol microRNA mimic and 100 ng of the respective sensor construct (pXho backbone containing GFP cassed followed by an artificial 3'UTR with two respective microRNA binding sites) and 100 ng of the FLAG-tagged TRIM-NHL construct in question and or FLAG-AGO2 (EIF2C2) (see section 2.1.3). After 48h the cells were trypsinized briefly, centrifuged at 1500 rpm for 5 min and resuspended in 1ml PBS with 2% FBS. Subsequently, the cells were analysed by flow cytometry (FACS Canto II, BD Biosciences).

### 2.2.16 Animals

For different embryonic stages timed matings of C57Bl/6J were ordered from Charité's animal facility FEM (Forschungseinrichtung für experimentelle Medizin). Upon delivery, the pregnant mice were sedated and immediately sacrificed. The uterus horns containing the embryos were removed and transferred to 10 cm dishes with ice-cold PBS. Embryos were dissected from uterus and subjected to further analysis. All procedures involving animals were performed in accordance with the german federal animal welfare act, under project number T0102/11.

### 2.2.17 Embryo embedding and cryostat sectioning

For immunofluorescence on embryonic tissue, embryos at different stage were fixed with 4%PFA in 0.2 M PB over night at 4°C and subsequently washed with 0.2 M PB three times 20 min at room temperature. Excessive liquid was removed with a paper towel. The embryos were transferred to mildly shaking, 10% sucrose in 0.2 M PB buffer and were incubated until they sank to the bottom. Then they were transferred to 20% sucrose in 0.2 M PB buffer and allowed to sink again. The embryos were transferred to 20% sucrose / 7.5% gelatine in 0.2 M PB buffer and incubated for 1-2h before they were embedded in an embedding mold. The mold was prepared with a base of 20% sucrose / 7.5% gelatine in 0.2 M PB buffer that was allowed to harden at 4 °C. The embryo was placed inside and covered with the same buffer. Then the molds were cautiously held into isopentane pre-cooled with dry ice. Embedded embryos were stored at -80°C. Frozen blocks were mounted with OCT COMPUND (Leica, 3808610E) on a supporting plate to be clamped in the cryostat. For immunofluorescence stainings embryos were cut sagitally in 12 µm thick sections and transferred to glass slides by electrostatic force. The sections were either stored at -80°C again, or directly dried and used for immunofluorescence assays.

### 2.2.18 SDS-PAGE and western blot

Cells were washed twice with ice-cold PBS and scraped into 2x 500µl PBS. After pelleting the cells at 6000 rpm for 5 min, they were lysed in approximately

200 µl TNN Buffer (volume according to cell number) unless otherwise stated. After 20 minutes on ice, non-dissolved components like DNA, cytoskeletal proteins etc were pelleted at 14000 rpm for 20 min. The protein concentration of these crude lysates was determined with Protein Assay (BioRad) at 595nm wavelength in the photometer. Equal amounts of protein were adjusted and loaded on SDS-PAGEs. Gels were run for 15 min at 75V and approximately 1h at 135V until the running front reached the bottom. Subsequently, the proteins were transferred to PVDF membrane (Millipore) for 1h at 100V. The transfer was controlled by staining with Ponceau-S solution and the membrane was blocked in 5% milk in PBST before it was incubated with primary antibody over night at 4°C. Membranes were washed 4 times (5 sec, 1 min, 5 min, 10 min) with PBST before incubating for 1h at RT with secondary antibody. After that it was washed as described above and films were exposed and developed using ECL (Cell Signaling). For *in vivo* expression analysis head or brain tissue from different developmental stages were lysed with TNN buffer and processed as described above.

### 2.2.19 Immunostaining

Cells were washed with PBS prior to fixation with 4%PFA in PBS for 10 min at 4°C and then washed 3 times 5 min with PBS. Sagittal embryo sections were mounted on glass slides. The sections were circumscribed with a hydrophobic barrier pen (ImmEdge™ pen, Vector, H-4000) to prevent leakage. Cryo-preserved tissue was dried and directly fixed with 4%PFA in PBS for 10 min at 4°C washed twice shortly and twice 5min with PBS. Cells and slices were blocked and permeabilized simultaneously using 5% goat serum with 0.1% Triton-X100 for one hour at room temperature, before adding the primary antibody in blocking solution over night. After washing twice shortly and 2x 5 minutes with PBS, the secondary antibody is applied in blocking solution for 1h at ambient temperature. The cells and sections were washed again as described above but including DAPI with the last washing step. Then they were mounted with fluoro-protective mounting medium (FluorSave™Reagent, Calbiochem, 345789). Cells were washed and stained in 12-well-plates on coverslips. Glass slides with embryo slices were washed in cuvettes and stained in a wet chamber covered with parafilm to protect from drying.

### 2.2.20 Co-Immunoprecipitation

HeLa cells were transfected in 10 cm dishes with calcium phosphate as described above. After 16 h at the earliest, the cells were lysed in 200 µl nondenaturing lysis buffer (either 2 % TritonX-100 in PBS or 1 % NP-40 in 50 mM Tris-HCL pH 7.8 and 300 mM KCl). The basic procedure did not differ from regular protein lysates (see Western Blot section). 10 % of the lysates were analysed separately as input samples. The samples were treated with RNase A (and T1) for 1 h at 37°C to avoid false positive results due to RNA-binding. The immunoprecipitation was performed rotating headfirst over night at 4°C using either anti-FLAG conjugated agarose beads (Sigma) or 1 µg anti-GFP (abcam) with ProteinA/G coupled agarose beads (Sigma). The beads were washed 5x with lysis buffer, transferred to new tubes and washed 2x with PBS (centrifugation 10000 rpm for 10 s). After removing all supernatant, 30 µl 2x Laemmli sample buffer was added and the beads were boiled for 5 min at 95°C for protein recovery. Subsequently, the supernatants were analysed by SDS-PAGE and western Blot. Endogenous co-immunoprecipitation was performed on P19 lysates with 1 µg specific antibody and ProteinA/G coupled agarose beads (Sigma) as described above. For endogenous *in vivo* co-immunoprecipitation from embryonic stages the heads of E10.5 and E11.5 embryos were lysed in 2%Triton-X100, and 10% input sample was separated. The lysates were precleared with 15 µl ProteinA/G coupled agarose beads and 4,5 µg of the respective antibody was coupled to the beads during rotation at 4°C for 7 hours, before incubating the precleared lysates with antibody-bead conjugates over night rotating at 4°C. Washing and sample preparation was performed as described above.

### 2.2.21 Stem cell differentiation

Doxycyclin inducible FLAG-LIN41 KH2 ESC were differentiated using two different methods: simple serum deprivation and addition of retinoic acid induces general loss of pluripotency (Buckley *et al.*, 2012; Rybak *et al.*, 2009) and a transfer to N2B27 medium differentiates ESCs to neuroectodermal precursors (Liu *et al.*, 2005a; Sen and Blau, 2005; Ying *et al.*, 2003). Employing the protocol published by Buckley and colleagues, addition of 5 µM RA to stem

cell medium after splitting in a 1:6 ratio, induces differentiation to cells from all three germlayers. The medium was changed every 2d, to remove deattached cells and to have a constant supply of RA. Cells were harvested at day 0, 2, 4 and 6. For differentiation to neuroectodermal precursors, 1.5 – 4.5 x $10^4$ cells/$cm^2$ were seeded into N2B27 medium (1:1 mixture of DMEM/F12 (Gibco, 10565) containing N2 supplement (Gibco, 17502) and 50 µg/ml BSA fraction V (SIGMA, A9647) with Neurobasal medium (Gibco, 21103) with B27 (Gibco, 17504); supplemented with 0.5 mM Glutamax, 0.1 mM β-mercaptoethanol and 1% penicillin/streptomycin) containing LIF for proper cell attachment and avoidance of massive cell death due to serum deprivation. The next day the day 0 timepoint was harvested and for day 4, 8 and 12 medium was changed to N2B27 without Lif, to induce differentiation. During the differentiation process the medium was changed every other day.

# 3 RESULTS

The goal of this thesis was to study LIN41 function in different contexts: its role in regulation of microRNA biogenesis pathway proteins, maintenance of pluripotency, and its interplay with MYOSINs and endosomes, as well as other TRIM-NHL proteins.

## 3.1 LIN41 influence on microRNA biogenesis pathway proteins

Previous studies showed that endogenous and exogenous LIN41 protein co-localized with AGO2 in defined cytoplasmatic foci, known to be mRNA processing bodies (P bodies, Figure 3.1).

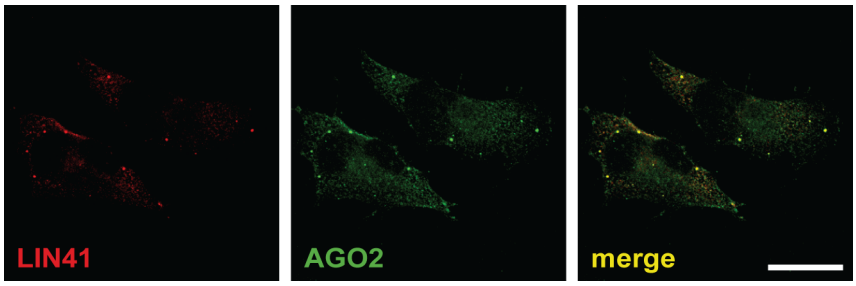


**Figure 3.1 Exogenous LIN41 co-localizes with AGO2-GFP in P bodies.**
Representative confocal image of HeLa cells, co-transfected with LIN41-FLAG and AGO2-GFP. Immunostaining with anti-FLAG antibody shows that LIN41 co-localizes with AGO2 in mRNA processing bodies. Scale bar: 20 µm. These pictures are a reproduction of previously published data (Rybak *et al.*, 2009).

The question if LIN41 influences other microRNA biogenesis and P body proteins, apart from AGO2, was studied using a LIN41 knockdown model. Such a model was inavailable at that time, but not dispensable for addressing the issue. Therefore several shRNAs targenting the *Lin41* 3'UTR were designed using the algorithms of from DKFZ e-RNAi and The RNAi Consortium and cloned into pSuper.retro.neo+GFP vector (*shLin41*; find the detailed procedure in section 2.2.11.1). The shRNA constructs were then separately transfected into P19 embryocarcinoma (P19) cells. One out of three Lin41 shRNAs successfully reduced endogenous LIN41 protein levels notably, compared to the Luciferase-targeting control shRNA. (Figure 3.2 A). The pSuper.retro.neo+GFP vector contains a geneticin (G418) resistance cassette.

To select for a stable integration of the shRNA into the P19 genome, the cells were treated with 1 µg/ml G418 for two weeks after transfection. Cells that did not integrate the construct died. The surviving cells were pooled to create one cell line per shRNA and kept under selective pressure.

These transient and stable *shLin41* transfected P19 cells were then used to investigate the LIN41 influence on the levels of microRNA biogenesis and P body proteins by western blot analysis (Figure 3.2).

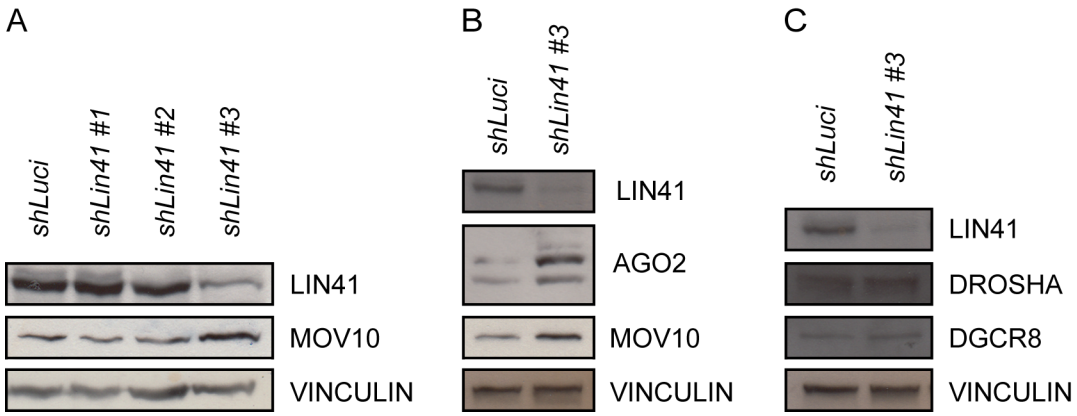


**Figure 3.2 LIN41 knockdown enhances expression of RISC proteins.**
P19 cells were transfected with shRNA targeting the 3'UTR of *Lin41* or *Luciferase* (control) and with 1µg/ml G418. Cells with stable integration of the shRNA construct were pooled and kept under selective conditions (see section 2.2.11.1 and 2.2.13). Crude cell lysates from three different harvesting time points were analysed by SDS-Page and western blot, representative blots are shown. The commercially available and in house antibodies (see section 2.1.15) used for protein detection are indicated on the right side of the blots. (A) Transfection of *shLin41 #3* reduced LIN41 protein levels. Transient knockdown of LIN41 increased MOV10 levels. (B) Stable LIN41 knockdown correlated with upregulation of MOV10 and the major RISC effector protein AGO2. (C) Reduction of LIN41 levels did not influence the levels of nuclear microprocessor proteins DROSHA and DGCR8.

Apart from microRNA biogenesis proteins, the levels of the **R**NA-**i**nduced **s**ilencing **c**omplex (RISC) proteins MOV10 and (LIN41 substrate) AGO2 were investigated in response to LIN41 knockdown. MOV10 expression was increased in transient as well as stable LIN41 knockdown (Figure 3.2 A and B). Also AGO2 was slightly increased upon stable LIN41 protein reduction (Figure 3.2 B). The levels of the nuclear microprocessor proteins DROSHA and DGCR8, however, seemed to be unaffected by LIN41 depletion (Figure 3.2 C). The mechanism underlying the observed level changes of the potential RNA helicase MOV10 is currently not known.

## 3.2 LIN41 affects pluripotency marker expression

To test the hypothesis of LIN41 being critical for pluripotency maintenance, crude cell lysates of P19 cells with stable LIN41 knockdown (see section 3.1) were used to analyze pluripotency marker expression. Depletion of LIN41 in P19 cells, led to downregulation of the pluripotency markers OCT4 and LIN28, while SOX2 (**s**ex determining region Y – B**ox 2**) seemed to be unaffected (Figure 3.3). This indicates a role for LIN41 in stemness maintenance.

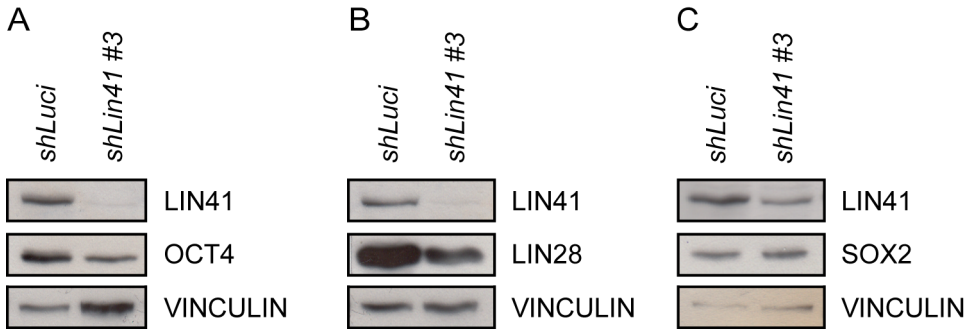


**Figure 3.3 LIN41 knockdown decreases pluripotency marker levels.**
P19 cells were transfected with shRNA targeting the 3'UTR of *Lin41* or *Luciferase* (control) and with 1µg/ml G418. Cells with stable integration of the shRNA construct were pooled and kept under selective conditions (see section 2.2.11.1 and 2.2.13). Crude cell lysates from three different harvesting time points were analysed by SDS-Page and western blot, representative blots are shown. The antibodies used for protein detection are indicated on the right side of the blots. (A) OCT4 and (B) LIN28 expression were reduced, while (C) SOX2 expression were unchanged in comparison to the house-keeping protein VINCULIN. The experiments were repeated three times.

## 3.3 Association of LIN41 with endosomes and MYOSIN V

Described interactions of other mammalian TRIM-NHL proteins with class V MYOSINs and their influence on endosomes led to the hypothesis that LIN41 may share this function and interact with endosomes and MYOSINs.

### 3.3.1 Co-localization of LIN41 and endosomes

As a test for LIN41 association with endosomes, similar to that described for TRIM3 (see section 1.4.5.2), LIN41-FLAG was transfected into HeLa cells. Constructs encoding GFP-tagged versions of either the early endosomal marker protein RAB5 or the late endosomal marker protein RAB7 were co-transfected.

Anti-FLAG antibody immunostaining was used to visualize the LIN41 expression pattern allowing analysis of a potential co-localization.

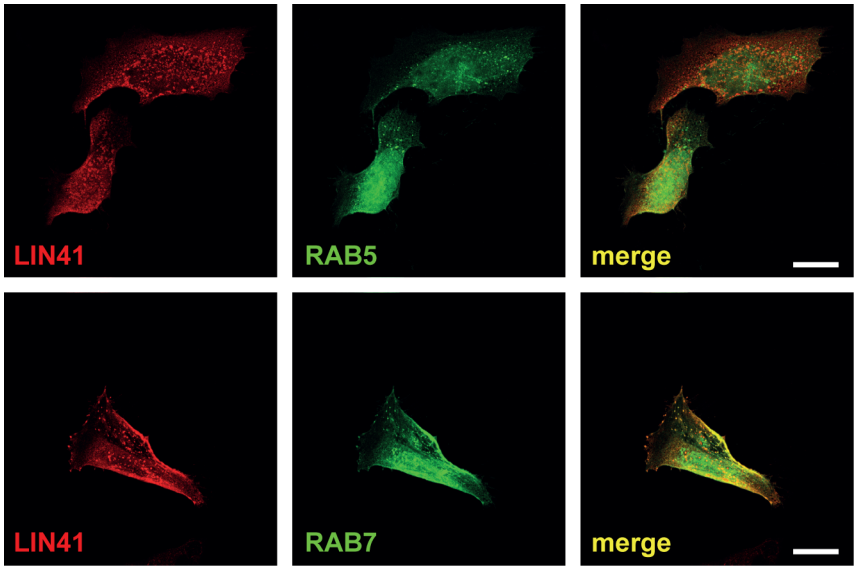


**Figure 3.4 Co-localization of LIN41 with endosomal markers.**
Representative confocal images of three independent experiments show HeLa cells, transfected with LIN41-FLAG and RAB5 or RAB7-GFP. Immunofluorescence staining with anti-FLAG antibody shows LIN41 co-localization with some but not all endosome-like structures positive for RAB5 and RAB7-GFP. Scale bar: 20 µm.

FLAG-LIN41 co-localized with both endosomal markers in a co-transfection assay (Figure 3.4). Co-localization with the early endosomal marker RAB5 was observed to a low extent, while the localization of the LIN41 and (late endosomal marker) RAB7 signals showed substantial overlap in particular in bright stained foci in the cell periphery.

### 3.3.2 Association of LIN41 and MYOSIN V

TRIM2 and TRIM3 have been shown to bind the globular domain of class V MYOSINs (see section 1.4.5). To elucidate the issue of shared functions among TRIM-NHL family members, a potential interaction of LIN41 with MYOSIN Va, Vb and VI was investigated. The GFP-tagged globular (cargo-binding) domains of the aforementioned MYOSINs (gMYO Va, gMYO Vb, gMYO VI) were either transfected alone (Figure 3.5) or co-transfected with FLAG-LIN41 (Figure 3.6) in

HeLa cells. Immunofluorescence staining with anti-FLAG antibody was used to visualized LIN41 by confocal microscopy images.

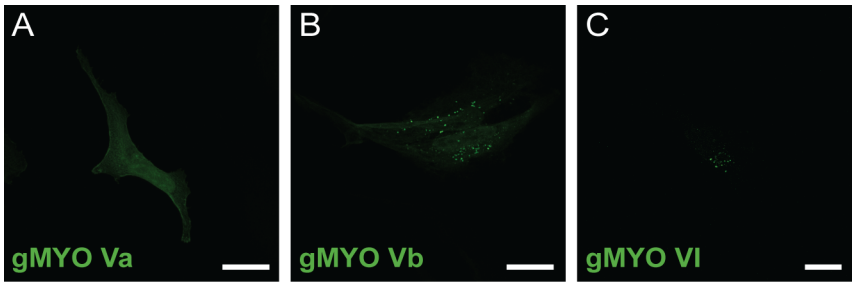


**Figure 3.5 Subcellular localization of GFP-gMYO Va, -gMYO Vb, -gMYO VI.**
HeLa cells were transfected with GFP-gMyoVa, -gMyoVb and -gMyoVI and analyzed with confocal microscopy. The experiment was repeated three times, representative images are depicted. (A) gMYO Va showed a diffuse localization with some accumulation at cell borders and filaments that resemble actin, while (B) gMYO Vb was enriched in foci observed throughout the cytoplasm and (C) gMYO VI in less disperse foci. Scale bar: 20 µm.

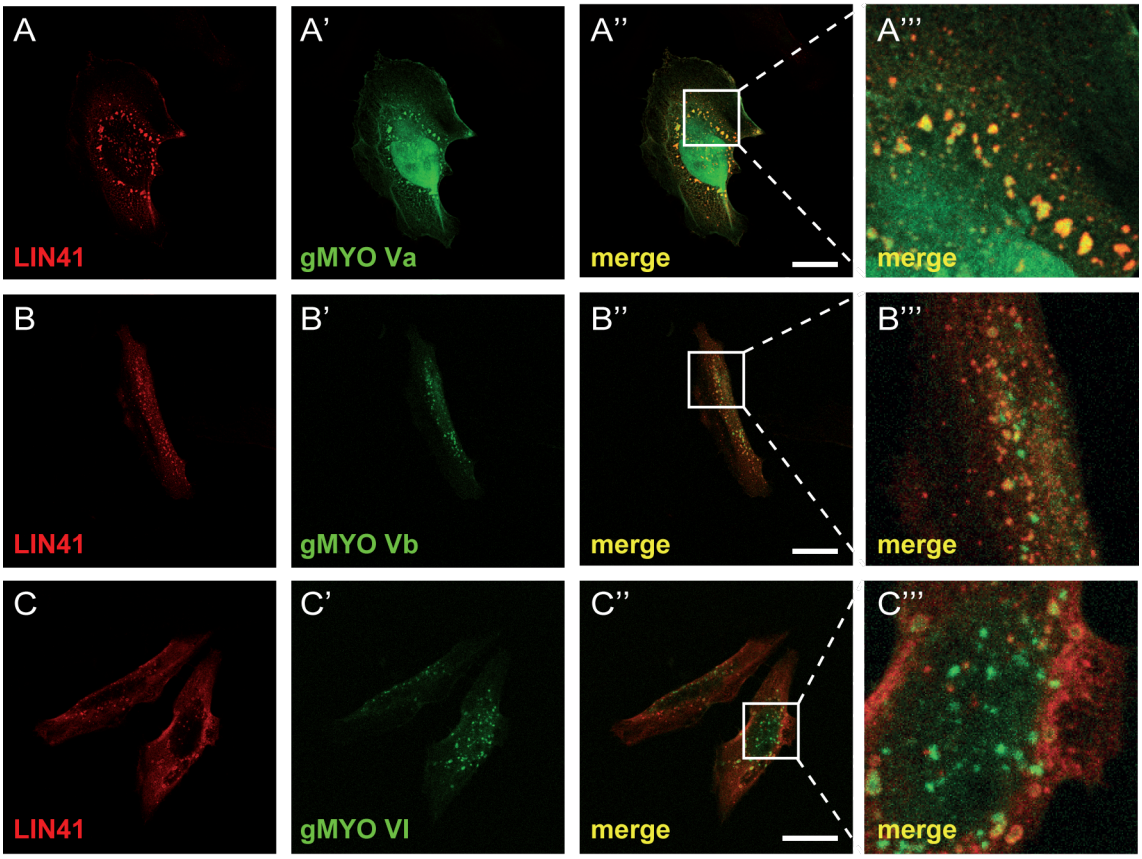


**Figure 3.6 LIN41 co-localizes with gMYO Va, Vb and VI.**
FLAG-LIN41 was co-transfected with GFP-tagged gMYO Va, Vb and VI into HeLa cells in three independent experiments. LIN41 was visualized by immunostaining with anti-FLAG antibody and is depicted in red. Representative confocal images were taken. (A) LIN41 and gMYO Va localize to foci arranged around the nucleus, while LIN41 co-localizes with (B) gMYO Vb and (C) gMYO VI in more distributed foci. Scale bar: 20 µm.

In HeLa cells, FLAG-tagged LIN41 displayed various degrees of co-localization with gMyoVa, gMyoVb, and gMyoVI to cytoplasmatic foci that resembled P bodies (see Figure 3.6). Similar results were obtained in P19 cells (data not shown). Interestingly, the intracellular distribution of the stained foci appeared to be different for each co-transfected MYOSIN. When co-transfected with LIN41, gMYO Va positive foci were localized almost exclusively around the nucleus (Figure 3.6A), quite different to the diffuse distribution when transfected alone (Figure 3.5 A). gMYO Vb and gMYO VI localized to specified foci (Figure 3.5 B and C). When co-expressed with LIN41, the localization of gMYO Vb positive foci did not change (Figure 3.6 B), while gMYO VI positive foci were more dispersed compared to the single transfection (Figure 3.6 C).

To analyze if a potential physical interaction of LIN41 and gMYO Va underlies the observed co-localization, co-immunoprecipitation assays with FLAG-tagged gMYO Va as bait and GFP-tagged TRIM-NHL proteins as prey were performed (Figure 3.7). The upper three panels depict protein expression after transfection (input control), the lower three panels depict precipitated protein (IP: FLAG). Expression of the GFP-tagged TRIM-NHL prey proteins (as seen in Figure 3.7, first panel, lane 2, 3, 4 and 5) and the GFP control (Figure 3.7, second panel, lane 1) were readily detected in the input samples. Note that the anti-GFP antibody detects a non-specific signal with similar mobility than GFP. Unfortunately, detection of the FLAG-tagged gMYO Va protein at 95 kDa was obscured in this experiment due to insufficient stripping of the membrane after using anti-GFP as the first detection antibody (Figure 3.7, third panel, all lanes). Nonetheless, FLAG-gMYO Va was sufficiently expressed as demonstrated by probing the eluates obtained after immunoprecipitation with anti-FLAG antibody as control (Figure 3.7, sixth panel, all lanes).

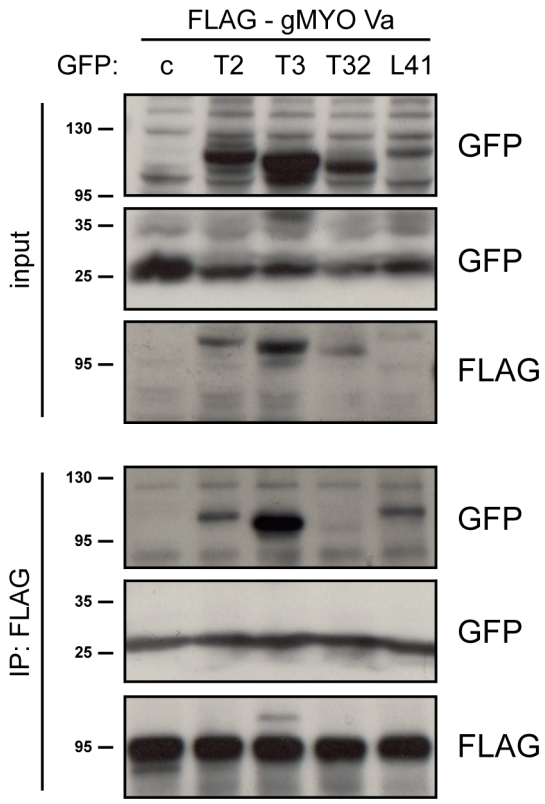


**Figure 3.7 Exogenous TRIM-NHL proteins physically interact with gMYO Va.**
GFP control (c, lane 1) or GFP-tagged TRIM2 (T2, lane 2), TRIM3 (T3, lane 3), TRIM32 (T32, lane 4) and LIN41 (L41, lane 5) constructs were co-transfected with FLAG-gMYO Va in Hela cells and lysates were subjected to immunoprecipitation with anti-FLAG agarose beads. The upper panels show immunoblots of the input control of the transfected constructs, the lower panels show immunoblots after FLAG-gMYO Va immunoprecipitation. Antibodies used in western blot are indicated on the right side.

Probing the eluates with anti-GFP to detect TRIM2 and TRIM3 (as positive control) revealed a clear co-precipitation (Figure 3.7, fourth panel, lane 2 and 3). But this analysis of the complete mammalian TRIM-NHL family showed that also LIN41 and (to a small extent) TRIM32 interact with the globular domain of MYOSIN Va under these conditions (fourth panel, lane 4 and 5). The GFP control was not co-precipitated, as only the non-specific band common to all lanes was observed in the appropriate size range (Figure 3.7, fifth panel, lane 1).

LIN41 was shown to co-localize with gMYO Va, gMYO Vb and gMYO VI (Figure 3.6) and to co-purify with gMYO Va (Figure 3.7). Knowing that Lin41 localizes to P bodies (Figure 3.1), MYOSIN Va (MYO Va) was hypothesized to influence LIN41 localization, P body localization, P body assembly and thereby maybe also microRNA activity. To look for changes in LIN41 and P body localization,

FLAG-Lin41 was transfected together with siRNAs targeting *MYO Va* in HeLa cells. Subsequent immunofluorescence staining with anti-DCP1a antibody was used to visualize a key P body component: mRNA decapping enzyme 1a (DCP1A).

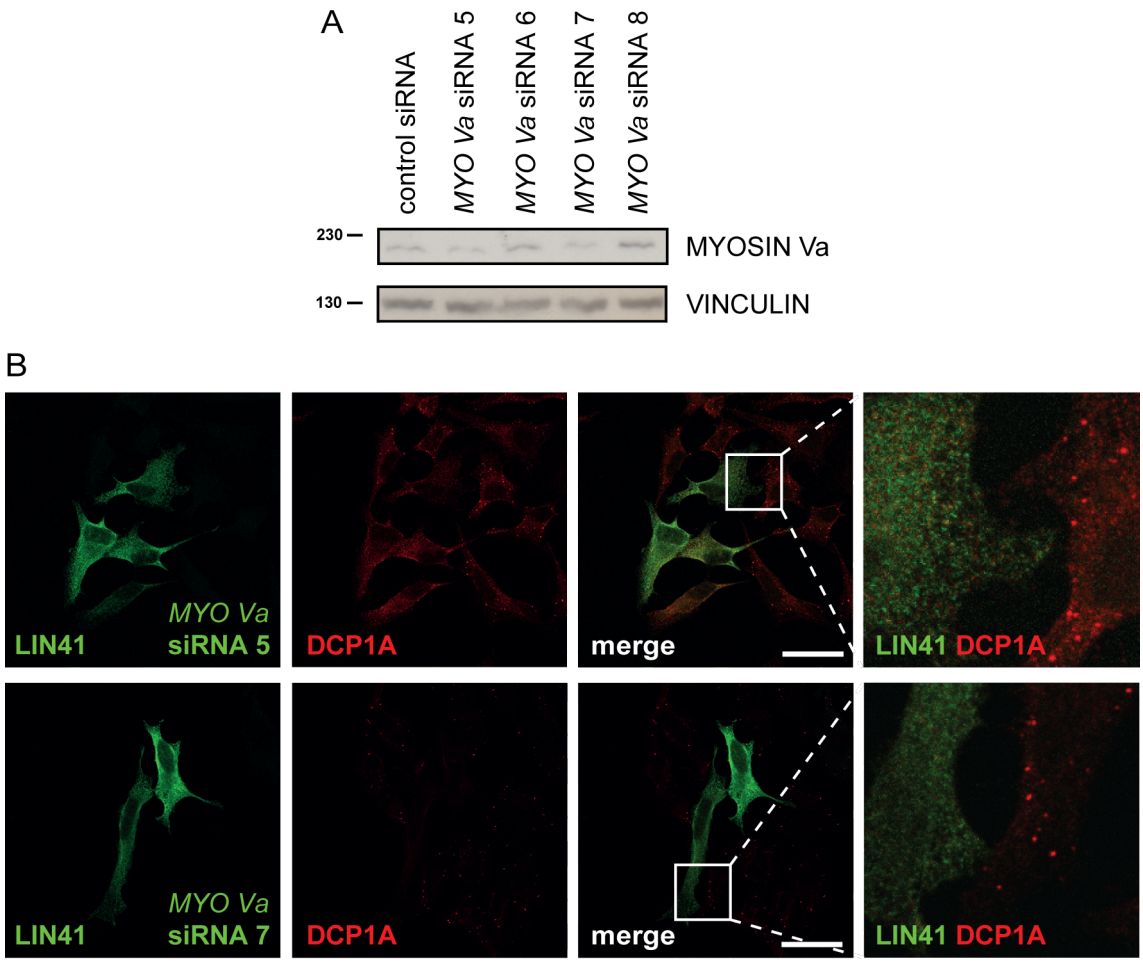


**Figure 3.8 *MYO Va* siRNA disrupts P body structures in HeLa cells.**
*MYO Va* siRNA was co-transfected with FLAG-LIN41 in HeLa cells. (A) Immunoblotting showed knockdown of MYOSIN Va was obtained with *MYO Va* siRNA 5 and 7 (upper panel, lane 2 and 4) compared to non-targeting control siRNA (upper panel, lane 1) and VINCULIN levels (lower panel). Protein size is indicated in kDa on the left side, antibodies used for protein detection on the right side of the western blot. (B) Transfected HeLa cells were immunostained with anti-FLAG antibody to depict FLAG-LIN41 and *MYO Va* siRNA co-transfected cells in green. Immunostaining with anti-DCP1a antibody visualized P bodies in red. Representative confocal microscopy pictures show dispersed LIN41 and DCP1a staining in cells transfected with *MYO Va* siRNA 5 and 7, while non-transfected cells showed the expected P body characteristics. This is indicative of disassembly of the overall P bodies population. Scale bar: 20 µm. The experiments were repeated three times.

In fact, HeLa cells transfected with *MYO Va* siRNA did not show the characteristic DCP1a localization to P body foci. Instead the staining was

dispersed throughout the cytoplasm (Figure 3.8, DCP1a visualized in red). Co-transfected FLAG-LIN41 showed the same irregular staining pattern in presence of *MYO Va* siRNA (Figure 3.8, depicted in green, compare with Figure 3.1). Non-transfected cells, however, still show DCP1a localization in P bodies, leading to the conclusion that MYOSIN Va seems to be crucial for P body maintenance.

## 3.4 TRIM32 mimics LIN41 repression of microRNA activity

To test the idea if all mammalian TRIM-NHL proteins influence microRNA activity, several neurogenic microRNA (see section 1.3.2) were studied in response to exogenous TRIM-NHL proteins. MicroRNA activity was monitored using a cell-based FACS assay. In this assay, a sensor construct containing a eGFP cassette followed by an artificial 3'UTR with two binding sites for a certain microRNA was co-transfected with the respective synthetic microRNA. This assay can detect either microRNA-mediated translational inhibition or target slicing, depending on the degree of complementarity between the sensor binding sites and the tested microRNA. The application of imperfect matching microRNAs (e.g. let-b with a let-7a sensor construct) reduces the GFP fluorescence by AGO proteins blocking GFP translation. Perfect sequence matches, as in the miR-124 and miR-128 experiments, are primarily silenced by the more efficient AGO2 slicing activity. This post-transcriptional block serves as baseline condition (Figure 3.9, control or 0 ng columns) and proteins influencing this process may increase (lower GFP fluorescence intensity) or decrease (leading to higher GFP fluorescence intensity, e.g. LIN41, (Rybak *et al.*, 2009) microRNA function.

Ectopic expression of TRIM2 and TRIM3 gain-of-function in HEK 293T cells did not influence microRNA activity, when monitored with this sensor assay (data not shown). Ectopic expression of wild type TRIM32, however, led to reduced microRNA activity (higher fluorescence intensity of the GFP sensor) in sensor systems for let-7, miR-124 and miR-128 (Figure 3.9, A-C second column). To test if this reduction of microRNA activity is dependent on the E3 ligase function of TRIM32, a mutation was introduced in the RING domain (cysteine to alanine in amino acid position 24). This mutation in the TRIM32 zinc fingers leads to a

conformation change and loss of E3 ligase activity (Schwamborn *et al.*, 2009). This E3-deficient TRIM32 RING Zn-finger point mutant (TRIM32 C24A) did not have any effect on microRNA activity, implying the TRIM32-mediated decrease of microRNA function is dependent on E3 ligase activity (Figure 3.9, A-C third column).

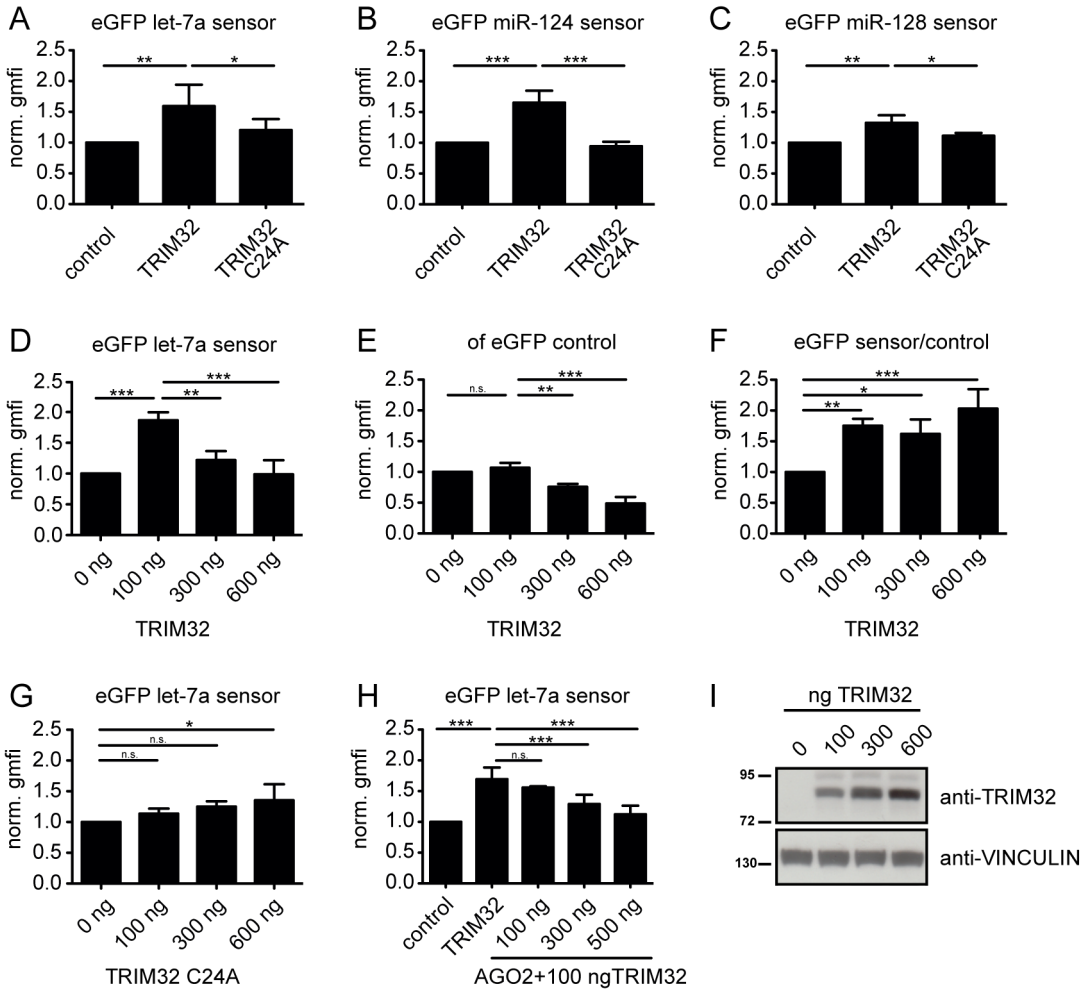


**Figure 3.9 TRIM32 overexpression decreases microRNA activity.**
(A-H) FACS sensor assays: HEK 293T cells were transfected with the indicated eGFP sensor constructs. Geometric means of fluorescence intensity (gmfi) were monitored; repression of the eGFP sensor mRNA by the respective synthetic microRNA was set as baseline (control (A-D,H) or 0 ng (D-G, I). (A-C) The presence of wild type (but not C24A mutant) TRIM32 reduces the ability of let-7, miR-124 and miR-128 to inhibit their respective eGFP sensor mRNAs. (D) The decrease of let-7 activity is dose-dependent. (E) High TRIM32 levels decrease fluorescence of GFP control construct in a non-specific fashion. (F) Division of sensor by control fluorescence intensities shows that TRIM32 inhibits let-7 activity and yields higher sensor mRNA levels in a dose-dependent fashion. (G) The TRIM32 C24A mutant reduces microRNA activity construct only mildly even at the highest dosage. (H) Increasing AGO2 levels led to more sensor repression. (I) Immunoblot showing increased TRIM32 expression after transfection of increased DNA amounts. The experiments were repeated at least three times. Error bars indicate standard deviation, One-way Anova with Bonferroni analysis was performed using GraphPad Prism, * denotes P-value < 0.05, ** denotes P-value < 0.01, *** denotes P-value < 0.001.

This result contradicts the one of Schwamborn and colleagues, who found that TRIM32 increased microRNA activity in similar a luciferase-based sensor assay (Schwamborn *et al.*, 2009). To explain this discrepancy, the let-7 sensor assay was repeated with increasing amounts of transfected *Trim32* construct. A dose-dependent effect of TRIM32 became apparent: higher doses of expression construct, leading to higher protein expression (Figure 3.9 I), led to loss of the previously observed TRIM32 function (Figure 3.9 D). Although this result approximates that of Schwamborn and colleagues, these higher TRIM32 levels also led to cell detachment and subsequent death (Figure 3.9 I, Figure 3.10). To control for this adverse effect, the same *Trim32* DNA amounts were co-transfected with a control eGFP plasmid lacking the artificial 3'UTR. Surprisingly, GFP expression also decreased as TRIM32 levels increased, under these micro-RNA irresponsive conditions (Figure 3.9, E). This shows that high levels of TRIM32 suppressed GFP expression non-specifically, most likely due to cell toxicity. To correct for these non-specific effects, the ratio of geometric mean fluorescence intensity of the eGFP sensor with and without the 3'UTR was calculated for each *Trim32* concentration (dividing the eGFP sensor by the eGFP control data). The results showed a TRIM32 dose-dependent decrease in let-7 activity, indicated by an increase of eGFP fluorescence (Figure 3.9, F). Transfecting increasing amounts of the *Trim32* C24A RING mutant construct did not result in cell death and did not significantly affectlet-7 activity (Figure 3.9 G, Figure 3.10).

The LIN41 ubiquitination substrate AGO2 is known to be limiting for microRNA activity in sensor assays (Winter and Diederichs, 2011). Co-transfection of *Ago2* to the lowest amounts of *Trim32* leads to a dose-dependent increase of microRNA activity, indicated by a reduction of sensor fluorescence (Figure 3.9 H). The ability of exogenous AGO2 to compensate for Trim32-mediated loss of microRNA activity suggests that TRIM32 acts via AGO2. In support of this interpretation, cell viability is increased when high amounts of *Trim32* are co-expressed together with *Ago2* (Figure 3.10). Taken together, these results indicate that Trim32 has a similar E3 ligase-dependent inhibitory effect on microRNA activity like LIN41.

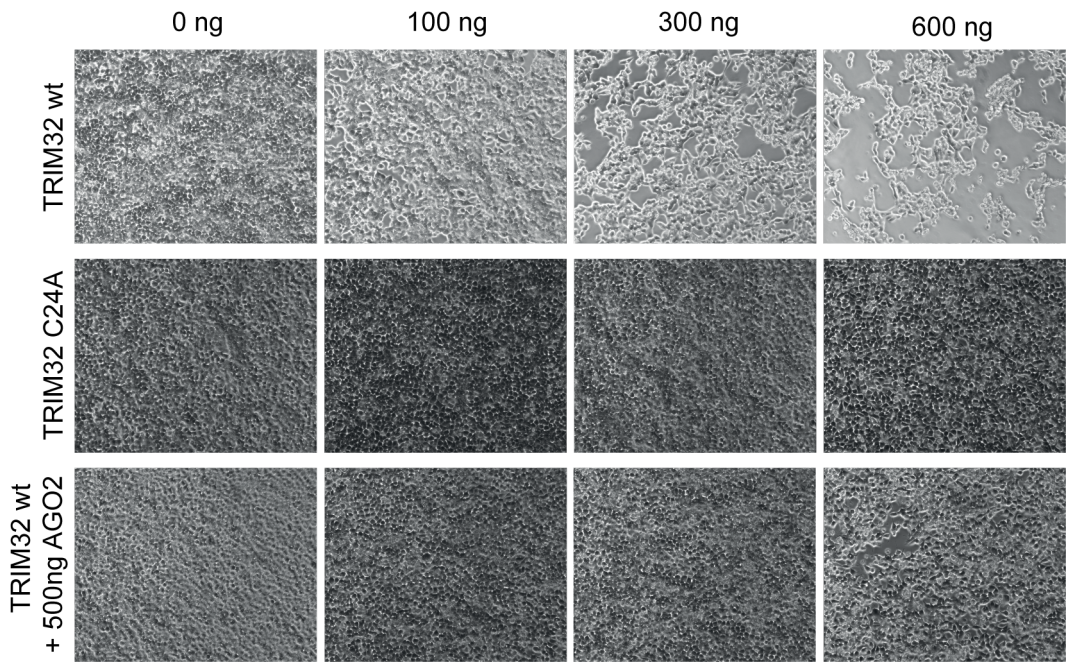


**Figure 3.10 Influence of TRIM32 and AGO2 on cell viability.**
HEK 293T cells were transfected with the indicated amount of TRIM32 wt, TRIM32 C24A mutant or 500 ng AGO2 and the indicated amount of TRIM32 wt. The experiment was repeated three times. Representative 100x magnification bright field pictures show high levels of TRIM32 wild type but not C24A mutant led to cell death. Co-expression of AGO2 with TRIM32 wt increases cell viability.

## 3.5 *In vitro* characterization of TRIM-NHL protein interactions

To address the issue of potential heteromerization of TRIM-NHL proteins, ectopic LIN41, TRIM2, TRIM3 and TRIM32 were analyzed for co-localization and co-immunoprecipitation.

### 3.5.1 LIN41 co-localizes with TRIM2, TRIM3 and TRIM32

To directly compare the subcellular localization of LIN41 with the other mammalian TRIM-NHL proteins, HeLa cells were transfected with TRIM2-eGFP and LIN41–FLAG (Figure 3.11 A), TRIM3-FLAG and LIN41-eGFP (Figure 3.11 B) or TRIM32-eGFP and LIN41–FLAG (Figure 3.11 C) and fixed after 24 hours for immunofluorescence staining. FLAG-tagged proteins were immunostained with anti-FLAG and are depicted in red (Figure 3.11).

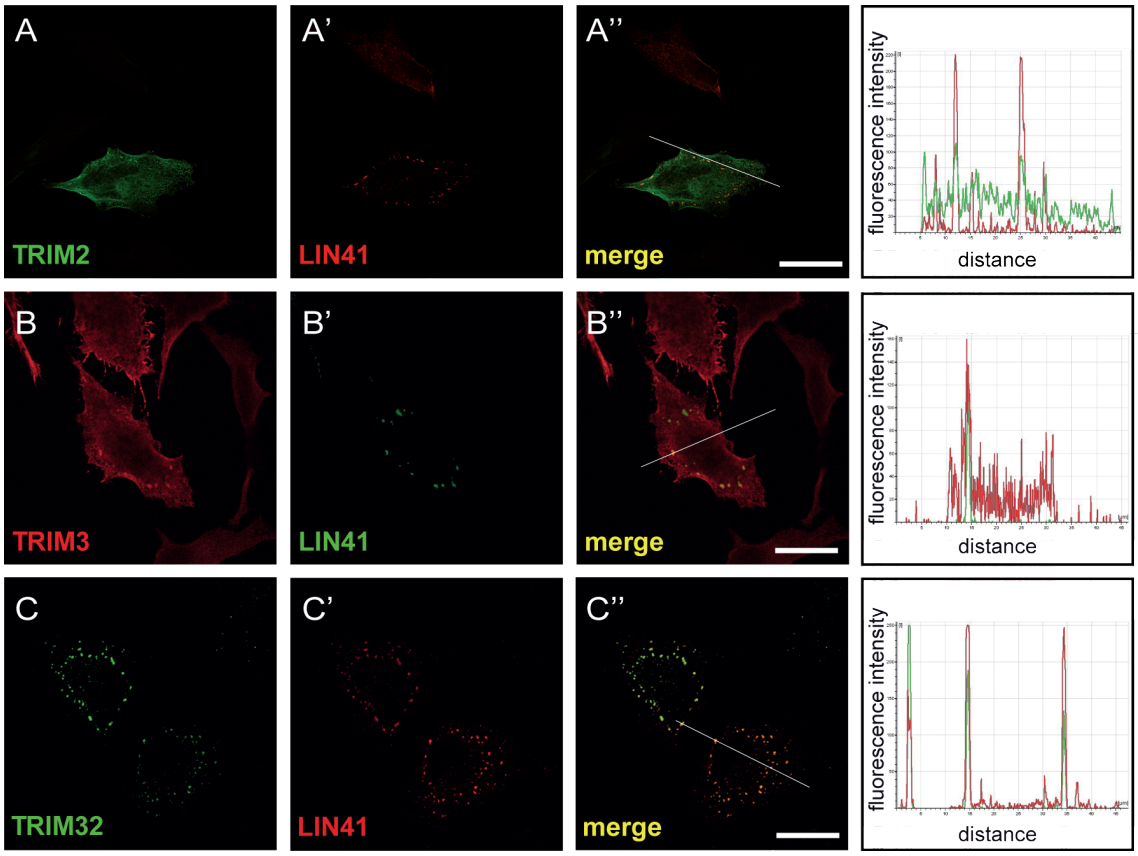


**Figure 3.11: Co-localization of exogenous TRIM-NHL proteins in HeLa cells.**
HeLa cells were transfected with (A) TRIM2-eGFP and Lin41–FLAG, (B) TRIM3-FLAG and LIN41-GFP or (C) TRIM32-eGFP and LIN41–FLAG. Immunofluorescence staining using anti-FLAG antibody shows FLAG-tagged proteins in red. The experiment was repeated three times, representative pictures show z-projections of confocal stacks. Fluorescence intensity was measured along the indicated lines (in a single layer of the stack). LIN41 co-localizes with TRIM2 and TRIM3 in some, and with TRIM32 in almost all foci. Scale bar correlates to 20µm.

In all transfections, LIN41 localizes to distinct cytoplasmatic foci, similar to those seen upon co-transfection with AGO2 (Figure 3.1). TRIM32 also localizes to this kind of distinct foci, while TRIM2 and TRIM3 are primarily evenly distributed and concentrate in fewer specific foci per cell. Localization of LIN41 and TRIM32 show an almost complete overlap, while TRIM2 and TRIM3 localization to distinct foci seemed to be increased upon co-expression with LIN41, resulting in a partial co-localization of the proteins (Figure 3.11).

### 3.5.2 LIN41 interacts with TRIM2, TRIM3 and TRIM32

The observed co-localization raised the question of an underlying physical interaction. To test this hypothesis, LIN41-eGFP and FLAG-tagged TRIM2,

TRIM3 and TRIM32 were expressed in HeLa cells for immunoprecipitation using anti-FLAG conjugated agarose beads.

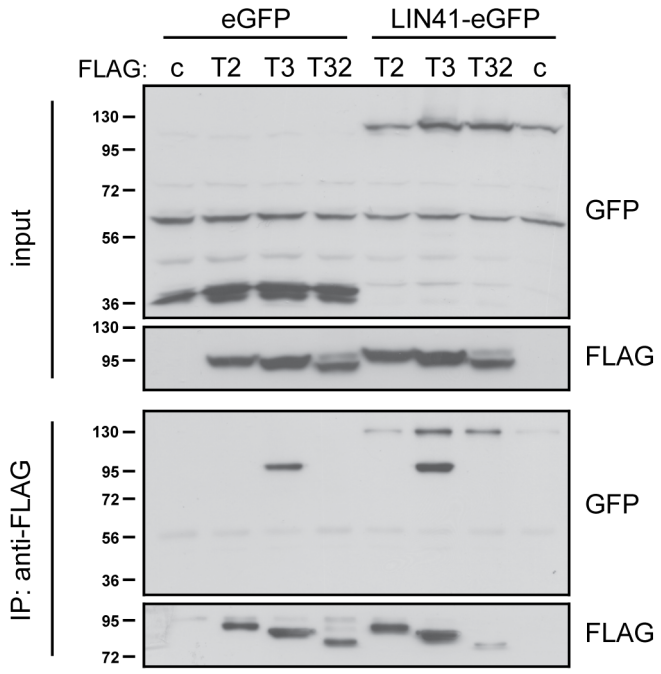


**Figure 3.12 Exogenous LIN41 interacts with the other TRIM-NHL proteins.**
eGFP control (lane 1-4) or LIN41-eGFP (lane 5-8) were overexpressed with FLAG control (c, lane 1 and 8), TRIM2-FLAG (lane 2 and 5), TRIM3-FLAG (lane 3 and 6) and TRIM32-FLAG (lane 4 and 7) in HeLa cells. Protein extracts were treated 30 min with RNaseA before immunoprecipitation with anti-FLAG conjugated agarose beads and subsequent SDS-PAGE and western blot analysis. The molecular mass in kDa is indicated on the left, while the antibodies used are indicated on the right hand side. The experiment was repeated three times. Upper panels show western blots of the input control, while the lower panels depict western blots of purified proteins. LIN41-eGFP but not eGFP alone is co-purified with TRIM2, TRIM3 and TRIM32.

Western blot analysis of the input lysates show sufficient and equal expression of TRIM2-, TRIM3- and TRIM32- FLAG (Figure 3.12, second panel, lane 2+5, lane 3+6 and lane 4+7 respectively) as well as the eGFP control (Figure 3.12, first panel, lane 1-4) and LIN41-eGFP (Figure 3.12, first panel, lane 5-8). After immunoprecipitation with anti-FLAG antibody conjugated agarose beads, precipitation of FLAG-TRIM2, -TRIM3 and -TRIM32 was confirmed in the eluates (Figure 3.12, fourth panel, lane 2+5, lane 3+6 and lane 4+7 respectively). Probing the blot with anti-GFP antibody revealed that LIN41-eGFP, but not the eGFP control, copurified with each of the TRIM-NHL proteins (Figure 3.12, third panel, lane 5-8 and lane 1-4). LIN41-eGFP recovery under

these conditions was dependent on the respective TRIM-NHL protein, as it was below detection limit when transfected alone (Figure 3.12, third panel, lane 8).

### 3.5.3 LIN41 interacts with other TRIM-NHL proteins via several domains

LIN41 protein contains several domains able to mediate protein-protein interaction (see section 1.4.2). To identify the LIN41 domain responsible for the interaction with other TRIM-NHL proteins, LIN41 deletion constructs were co-transfected with the indicated TRIM-NHL protein for expression in HeLa cells. The deletion constructs are presented in Figure 3.13 A. Deletion Construct 1 contains only the N-terminal RING and B box domains, Construct 2 in addition the coiled-coil and Construct 3 the RING, B box, coiled-coil and the filamin domain. Deletion Construct 6 contains the filamin (FLM) domain and the six C-terminal NHL repeats and Construct 7 only the NHL-repeats. The LIN41-eGFP deletion series contains additional constructs that were not used in this experiment (Construct 4: B box 2, CC, FLM and NHL and Construct 5: CC, FLM and NHL).

The lysates were pretreated with RNaseA to prevent interference by RNA-protein interactions. Western blot analysis did not show a clear preference of any LIN41 domain for binding other TRIM-NHLs with standard stringency buffer (2% Triton-X100 in PBS). Usually higher stringency can yield information on relative affinities for individual domains. Increasing the stringency with the addition of 300 mM NaCl to the lysis and washing buffers did not affect the result: interaction of each of the deletion constructs with the respective TRIM-NHL protein was maintained (data not shown). Employing high molarity lysis buffer containing 1 M Tris-HCl revealed a preference for all constructs that contained the filamin domain of LIN41 (see Figure 3.13). Taking the known structure of isolated RING domain dimers and the ability of B boxes to dimerize as a starting point, these results suggest TRIM-NHL proteins form dimers in parallel with homophilic contacts between each domain. Contacts between the filamin domains may anchor the structure.

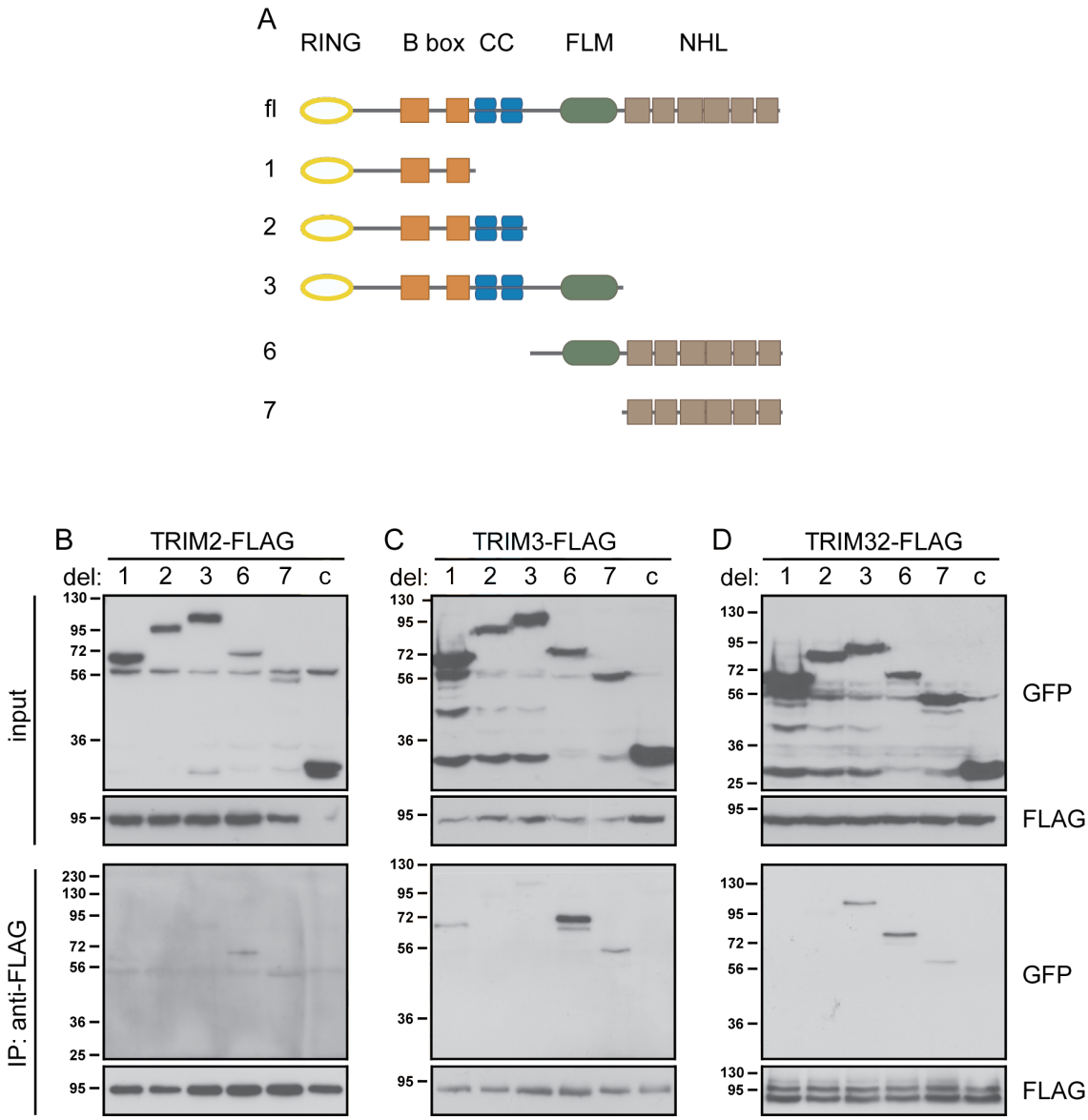


**Figure 3.13 The LIN41 FLM domain mediates the TRIM-NHL interaction.**
(A) The indicated LIN41 deletion constructs (CC coiled-coil domain; FLM filamin domain) and a eGFP control (c) were co-expressed with (B) TRIM2-FLAG, (C) TRIM3-FLAG, or (D) TRIM32-FLAG in HeLa cells for immunoprecipitation performed with anti-FLAG conjugated agarose. (B-D) The upper panels show western blots using 10% of the input samples while the lower panels show blots of the immunoprecipitated samples. Molecular mass is indicated on the left side of each blot (in kDa), the detection antibodies are depicted on the right side. The experiments were performed three times; representative images are shown. Immunoprecipitation with LIN41 deletion constructs did not reveal one specific interaction domain, when performed under physiological conditions. High molarity precipitation buffer revealed that the LIN41 N-terminus containing the filamin and NHL domain shows the highest affinity for the other TRIM-NHL proteins.

## 3.6 The TRIM-NHL proteins interact during early neurogenesis

The TRIM-NHL co-localization and co-precipitation data obtained so far were intriguing even though they were predicated on exogenous protein overexpression. To attend to the problem of physiological relevance, the mammalian TRIM-NHL protein expression and interaction were analyzed in neurodevelopment.

### 3.6.1 TRIM-NHL antibody specificity

To address the question of endogenous protein expression and localization, control experiments to confirm that the available antibodies are sufficiently specific and do not cross react were performed. Various commercially available and in house antibodies against the mammalian TRIM-NHL proteins were tested for cross-reactivity toward the other TRIM-NHL family members. For this purpose each of the FLAG-tagged TRIM-NHL constructs was overexpressed in HeLa cells and antibody specificity was analyzed by western blot (Figure 3.14).

LIN41 is specifically recognized by an antibody raised against the amino acids 584-855, encoding the six NHL repeats in the LIN41 C-terminus (Rybak *et al.*, 2009). Antibodies were identified for each of the family members that firstly faithfully detected the expected protein and secondly did not cross-react with the other family members (for TRIM2 SAB4200206 from Sigma-Aldrich, for TRIM3 sc-136363 from Santa Cruz Biotechnology and for TRIM32 ab96612 from Abcam). However, all selected TRIM-NHL antibodies recognized a second signal in addition to the one at the expected mobility. The C-terminal LIN41 antibody specifically recognizes FLAG-LIN41; but a non-specific signal of higher molecular weight was also observed (Figure 3.14 A, second panel, lane 1). TRIM2 and TRIM3 did not seem to be expressed in HeLa cells, immunoblotting showed two major signals for each exogenous protein (Figure 3.14 A, third panel, lane 2 and fourth panel lane 3 respectively). TRIM32 showed two signals presumably from endogenous protein in addition to the two signals of the exogenous protein (Figure 3.14 A, fifth panel, lane 4).

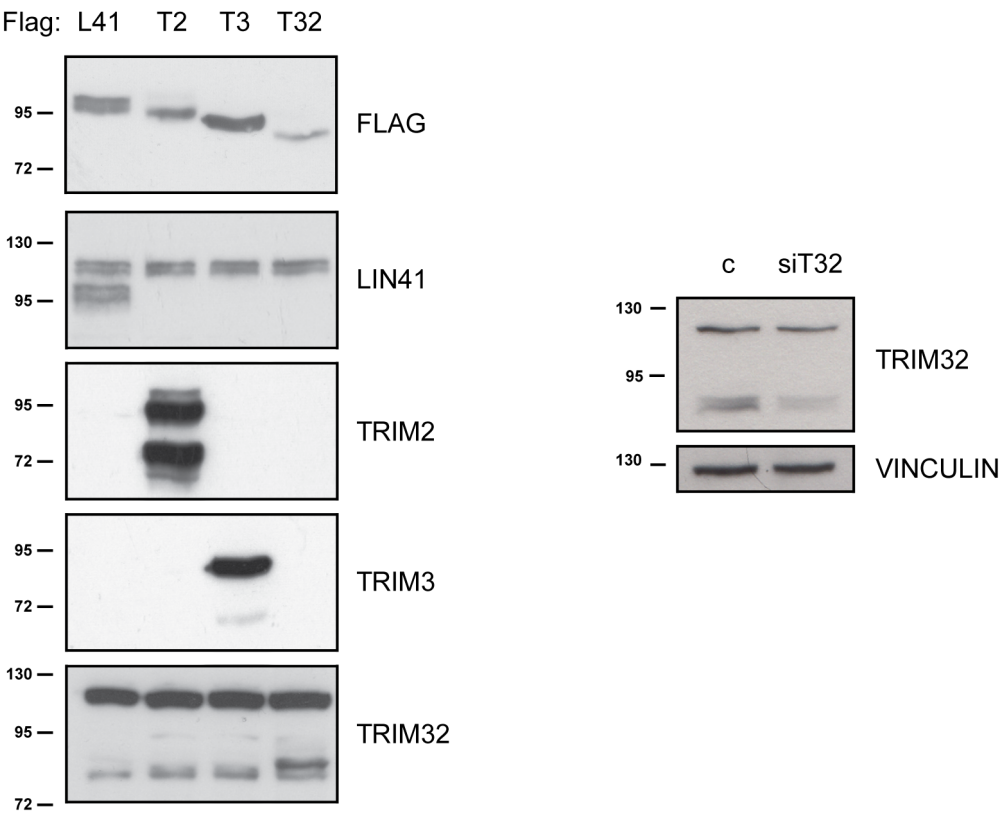


**Figure 3.14 TRIM-NHL antibody specificity test.**
(A) FLAG-tagged expression constructs of LIN41 (L41, lane 1), TRIM2 (T2, lane 2), TRIM3 (T3, lane 3) and TRIM32 (T32, lane 4) were expressed in HeLa cells. In western blot analysis anti-LIN41 serum specifically recognized exogenous LIN41 and an endogenous non-specific band. TRIM2 and TRIM3 antibody specifically recognized the FLAG-tagged exogenous protein and a band of higher molecular weight present only in the respective transfected sample. Anti-TRIM32 recognized FLAG-tagged TRIM32 in addition to two endogenous bands. (B) N2A cells were transfected with non-targeting siRNA control (c, lane 1) or siRNA targeting *Trim32* (siT32, lane 2) for SDS-PAGE and western blot analysis. Transfection of *Trim32* siRNA hardly reduced the intensity of the higher molecular weight band, but considerably reduced intensity of the lower, compared to the VINCULIN control. Molecular mass in kDa is indicated on the left, the antibodies used on the right hand side of each blot. The experiment was performed three times; representative immunoblots are shown.

To test if the upper signal observed in untransfected cells corresponds to TRIM32, N2A cells were employed. This mouse neuroblastoma cell line expressed endogenous TRIM32 (Figure 3.14 B). N2A cells were transfected with siRNA targeting *Trim32* mRNA or scrambled control; TRIM32 protein levels were analyzed by western blot. SiRNA treatment had little effect on the upper, approximately 110 kDa signal, but considerably reduced the intensity of the 72 kDa signal compared to the control (Figure 3.14 B). Hereafter, the 72 kDa band will be regarded as the specific TRIM32 signal.

### 3.6.2 Expression of TRIM-NHL proteins in CNS development

After observing co-localization and co-precipitation of TRIM-NHL members *in vitro,* it was interesting to see if this interaction has biological relevance. Therefore, it was of major interest to see if the TRIM-NHL interplay might occur *in vivo*. The question if TRIM-NHL proteins are expressed at the same time and space in mouse development still remained to be answered. To study TRIM-NHL expression during development of the rodent CNS, RNA and protein extracts were prepared from mouse embryonic head (E9.5-E13.5) or from dissected brains (E12.5-P4). Reverse transcription of E9.5 head mRNA, as well as E13.5 and E18.5 brain mRNA with subsequent quantitative RT-PCR showed that each of the *Trim-NHL* mRNAs was present during CNS development. The levels of *Trim2* and *Trim3* mRNA increased between E9.5 and E13.5, while *Trim32* mRNA expression showed its strongest increase only later in brain development between E13.5 and E18.5. *Lin41* mRNA was present in early neurodevelopment at E9.5 and was at or below detection limit thereafter (Figure 3.15).

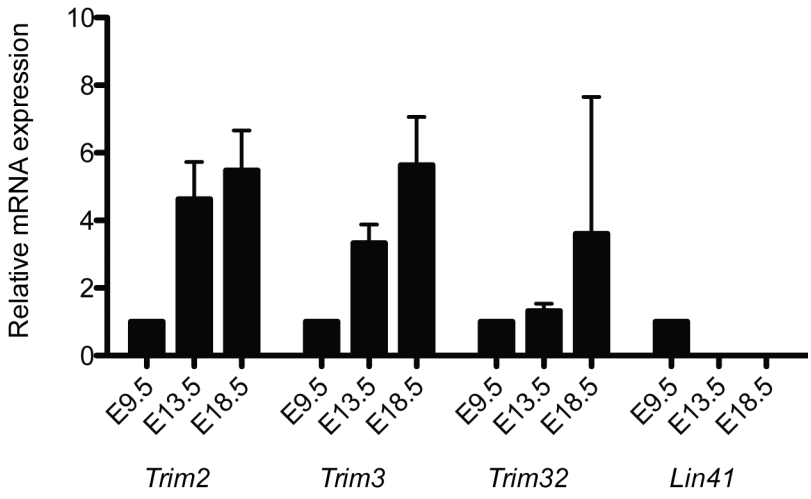


**Figure 3.15 *Trim-NHL* mRNA expression in neurodevelopment.**
Whole RNA was extracted from embryonic head (E9.5) and brain (E13.5 and E18.5) using TRIzol® reagent for cDNA synthesis and qRT-PCR. $C_t$ values of each gene and timepoint were normalized to β-actin ($\Delta C_t$). Subsequently, these relative values were normalized to the E9.5 timepoint ($\Delta\Delta C_t$). $Log_2(-\Delta\Delta C_t)$ then yielded the fold change values in relation to E9.5. The experiment was repeated at three times. Average values are shown and the error bars indicate standard deviation among the experiments.

Western blot analysis performed on protein samples prepared in parallel supported the results obtained by qRT-PCR. The full length 95 kDa LIN41 protein was only expressed at early developmental stages (E10.5 and E11.5) as expected. After E11.5, head and brain samples only showed non-specific bands of different molecular weights, but full length LIN41 was not detected (Figure 3.16, upper panels). TRIM2 and TRIM3 showed the inverse pattern, both were expressed at very low levels at E10.5 and gradually increased with developmental time (Figure 3.16, second and third panels). TRIM32 showed a distinct expression dynamic, without clear up or down regulation of the specific 72 kDa band as a function of developmental time. However, the higher molecular weight band, believed to be non-specific, did display an increase in intensity (Figure 3.16, fourth panels). Anti-VINCULIN immunoblotting was used as loading control (Figure 3.16, lowest panels).

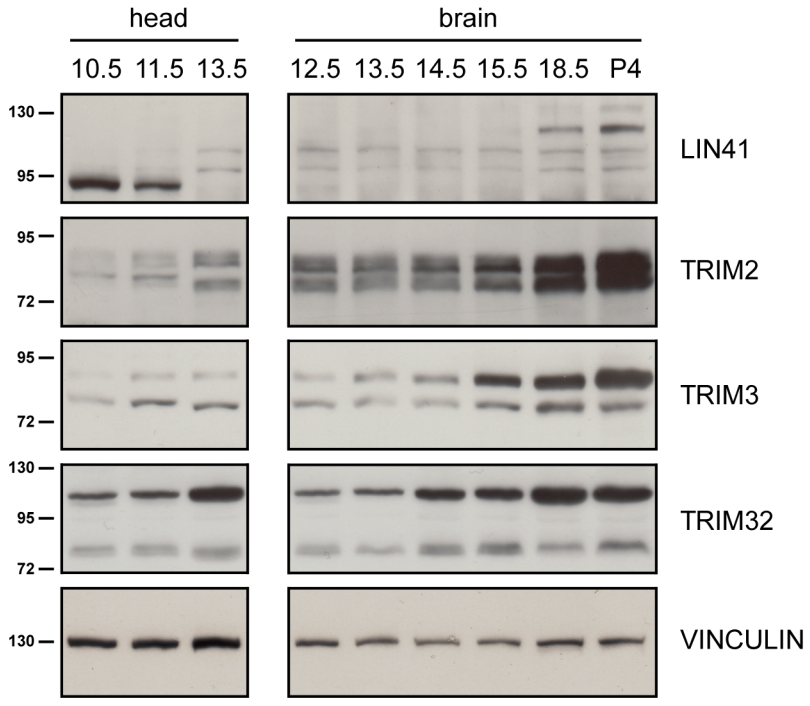


**Figure 3.16 TRIM-NHL protein expression in neurodevelopment.**
Crude protein extracts were collected from the indicated stages in development either from mouse head or brain for SDS-PAGE and western blot analysis. The molecular mass in kDa is indicated on the left, while the antibodies used for western blot analysis are indicated on the right hand side of each panel. LIN41 is expressed exclusively at E10.5 and E11.5 (lane 1 and 2). Levels of TRIM2 and TRIM3 increase over the course of the experiment, while TRIM32 does not show a clear trend.

### 3.6.3 LIN41 co-localizes with the other TRIM-NHL proteins *in vivo*

Expression of LIN41 and the other mammalian TRIM-NHL proteins overlapped at E10.5 and E11.5 (Figure 3.16). To determine the spatial localization of each protein at E11.5, immunofluorescence staining was performed on sagittal sections (described in section 2.2.17 and 2.2.19). Even though the TRIM-NHL proteins were outside their respective expression maxima, specific staining with each antibody was readily obtained in the neuroepithelium at E11.5 (Figure 3.17). LIN41 staining was more restricted to neuroepithelium (compared to the underlying mesoderm or surface ectoderm) than the other TRIM-NHL proteins. Staining for all TRIM-NHL proteins was also observed in the dorsal root ganglia and in the liver, though the latter is known for giving false positive results.

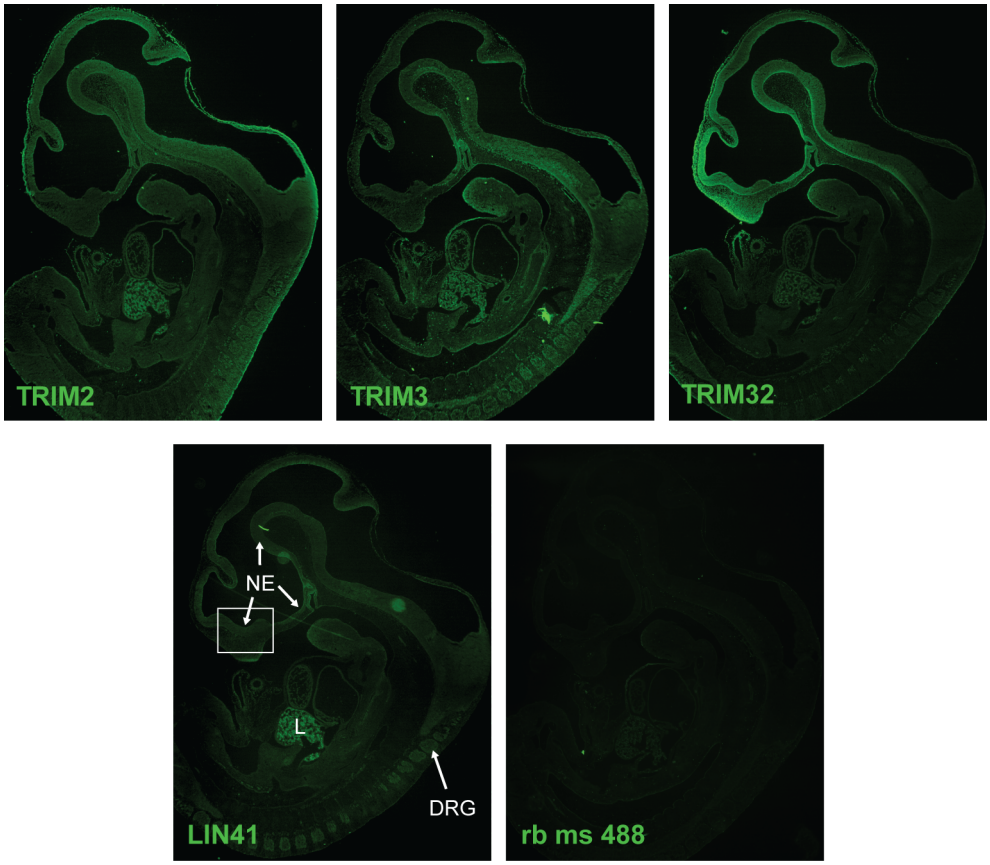


**Figure 3.17 TRIM-NHL proteins are expressed in mouse embryo at E11.5.**
Sagittal cryo-sections of fixed E11.5 embryos were immunostained for the TRIM-NHL protein indicated on each panel. Representative fluorescence microscopy images of the anterior and posterior median plane of the embryo were taken with 50x magnification, pseudocolored and photomerged. Due to low magnification the background signal was rather high and was reduced with Adobe Photoshop software. The TRIM-NHL proteins are expressed in neuroepithelium (NE), dorsal root ganglia (DRG) and liver (L). The square indicates the region of which pictures with higher magnification were taken (depicted in Figure 3.18).

N-CADHERIN, an adherens junction protein, was employed for co-stainings as a specific marker for neuroepithelial cells. TRIM2, TRIM32 and LIN41 are co-expressed with N-CADHERIN in radially aligned cells, as depicted in higher magnification in Figure 3.18. Co-staining for TRIM3 and N-CADHERIN could not be performed as both antibodies were raised in mouse. TRIM3 and LIN41 however, show a clear co-expression in neuroepithelium at E11.5 (Figure 3.18).

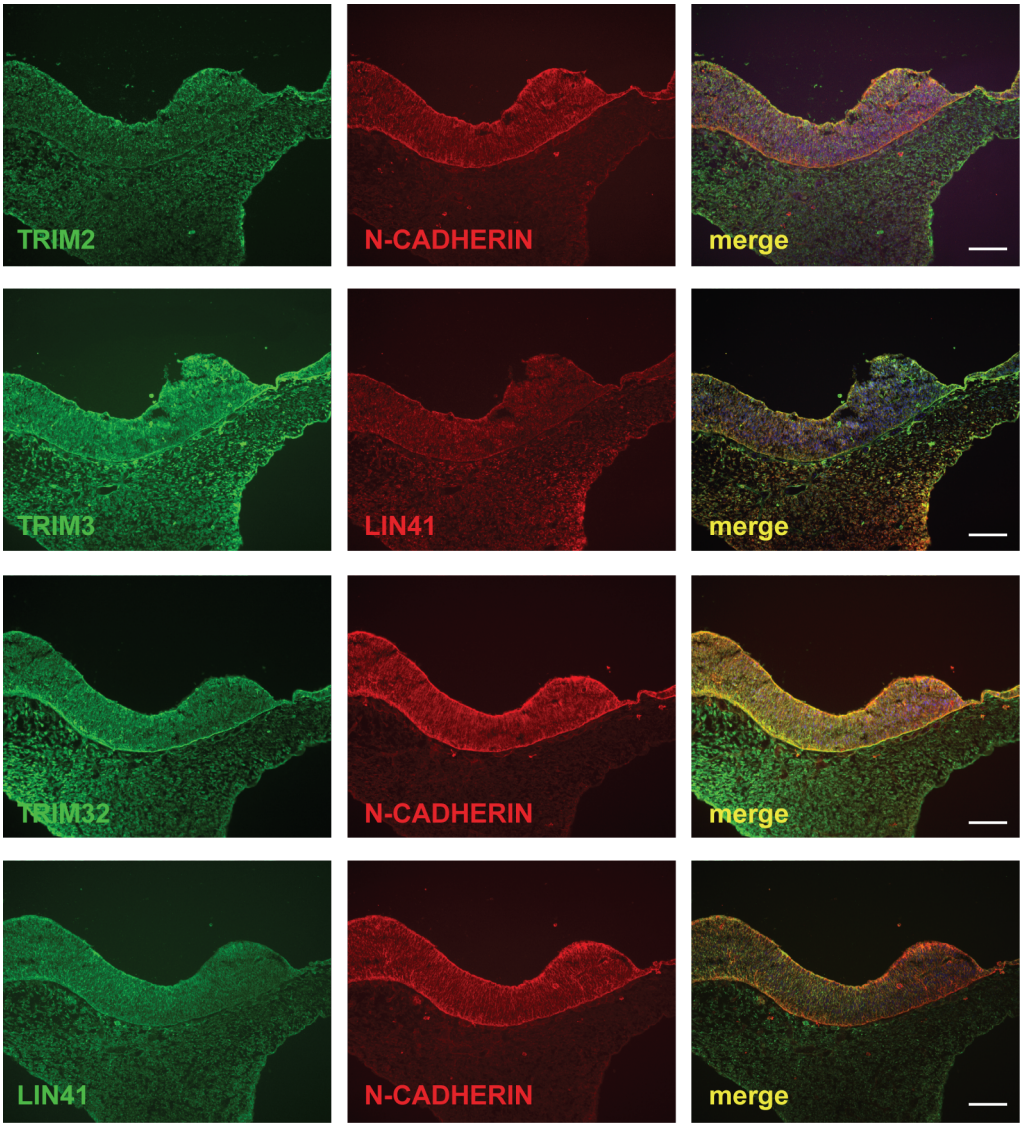


**Figure 3.18 TRIM-NHL proteins are expressed in the neuroepithelium.**
Sagittal cryo-sections of E11.5 mouse embryos were immunostained for the proteins indicated on each panel. The TRIM-NHL proteins are depicted in green. Co-staining with anti-N-CADHERIN antibody, a neuroepithelial cell marker, is depicted in red. Co-staining of TRIM3 with N-CADHERIN was replaced by co-staining with LIN41 (in red) due to antibody species compatibility. The experiment was repeated three times; representative images are shown. All TRIM-NHL proteins were expressed in radially aligned cells of the forebrain neuroepithelium at E11.5. Background was subtracted with Adobe Photoshop software only in the merged pictures, where DAPI in addition stains the nuclei. Scale bars correspond to 100 µm.

### 3.6.4 LIN41 interacts with TRIM2, TRIM3 and TRIM32 *in vivo*

After observing spatiotemporal congruence of TRIM-NHL family member expression, it was of major interest if a physical interaction between them also exists *in vivo*. Therefore, protein extracts of E11.5 embryo heads were analyzed for potential interaction of TRIM-NHL proteins. TRIM2, TRIM3 and TRIM32 were immunoprecipitated with specific antibodies or the respective control IgG. LIN41 co-precipitation was analyzed by SDS-Page and western blot using anti-LIN41 in house antibody. Approximately, one mouse litter was used per TRIM-NHL immunoprecipitation – six E11.5 embryonic heads were lysed and this lysate was equally distributed to the TRIM and IgG control immunoprecipitations. Each precipitation was repeated three times.

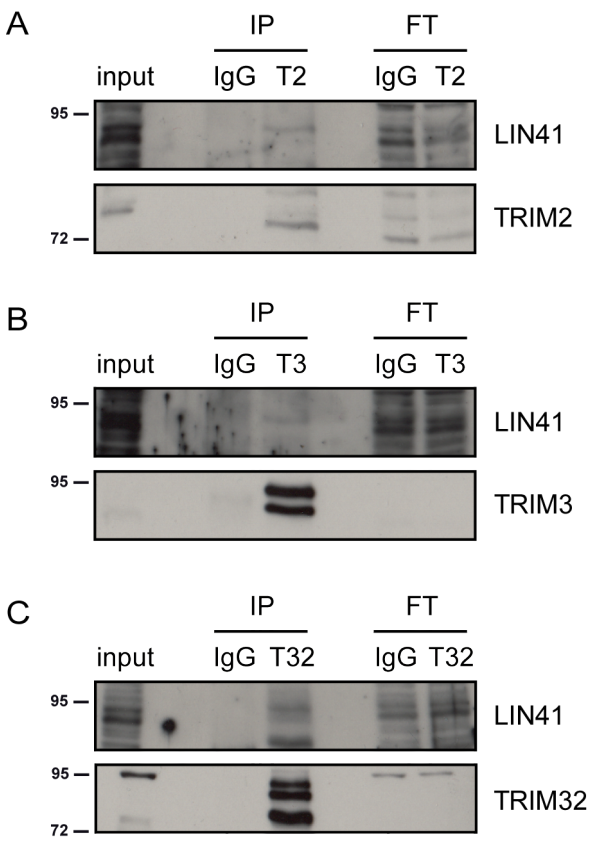


**Figure 3.19 TRIM2, TRIM3 and TRIM32 interact with LIN41 *in vivo* at E11.5.**
Crude lysates from six E11.5 mouse heads were split into two. One half was subjected to immunoprecipitation (IP) with IgG control antibody (lane 3), while the other half was immunoprecipitated with the indicated specific TRIM-NHL antibody (lane 4). 5% input (lane 1) was loaded next to the IP (lane 3 and 4) and flow through (FT, lane 6 and 7) samples. The molecular mass in kDa is indicated on the left, while the antibodies used for western blot analysis are indicated on the right hand side of the panels. The immunoprecipitation was repeated three times; representative immunoblots are depicted. LIN41 was copurified with (A) TRIM2, (B) TRIM3 and (C) TRIM32 but not the respective control IgGs (upper panels, lane 4).

Western blot analysis confirmed successful immunopurification of endogenous TRIM2, TRIM3 and TRIM32 (lower panels, lane 4 in Figure 3.19 A, B and C, respectively) and co-precipitation of endogenous LIN41 (upper panels, lane 4 in Figure 3.19 A, B and C, respectively). The species-specific IgG control purification did not precipitate the respective TRIM-NHL protein and did not co-precipitate LIN41 (upper panels, lane 3 in Figure 3.19 A, B and C), suggesting that the observed co-precipitation is specific and that TRIM-NHL proteins physically interact at E11.5. Further experiments are required to determine if TRIM-NHL proteins heterodimerize or co-purify from higher order complexes and what the functional consequences of these interactions are.

## 3.7 The TRIM-NHL family interplay in stem cell differentiation

Analysis of TRIM-NHL expression patterns in mouse CNS development showed a reciprocal expression pattern of LIN41 compared to the other TRIM-NHL proteins (Figure 3.16). This supports the idea of LIN41 regulating the other TRIM-NHL proteins. These observed expression changes coincide with the onset of neurogenesis *in vivo* and led to the hypothesis of a similar behavior in stem cell differentiation as a model for neurogenesis. To investigate this theory, doxycycline-inducible FLAG-LIN41 embryonic KH2 stem cells (iLin41 ES cells) were obtained from Richard I. Gregory's lab (see section 2.2.13). This LIN41 induction system is useful to rapidly increase LIN41 levels in the pluripotent state or to artificially maintain expression during differentiation, as the transgene is insensitive to microRNA regulation.

### 3.7.1 Differentiation of LIN41-inducible stem cells

To investigate if the inverse expression patterns of the TRIM-NHL proteins that were observed in *in vivo* CNS development (see Figure 3.16) are recapitulated during neurodifferentiation of ES cells, two different approaches to differentiate iLin41 ES cells were employed. In a protocol used by Buckley and colleagues, differentiation is based on the withdrawal of **L**eukemia **i**nhibitory **f**actor (LIF, a differentiation inhibitor) and retinoic acid supplementation. This protocol yields cells differentiated into lineages derived from all three germlayers (Buckley *et al.*,

2012). A protocol introduced by Austin Smith's lab employs LIF deprivation and N2B27 medium to drive differentiating cells specifically into neuronal lineages (Ying *et al.*, 2003). The differentiation kinetics observed with this protocol is considerably slower than with retinoic acid treatment. Applying the Buckley protocol, KH2 cells were deprived of LIF and feeders, seeded in growth medium and subjected to 5 µM retinoic acid. Cell death was high - about 70% - consistent with published results. The surviving cells were lysed at day 0, 2, 4 and 6 of differentiation. Cell lysates were subjected to SDS-PAGE and western blot analysis.

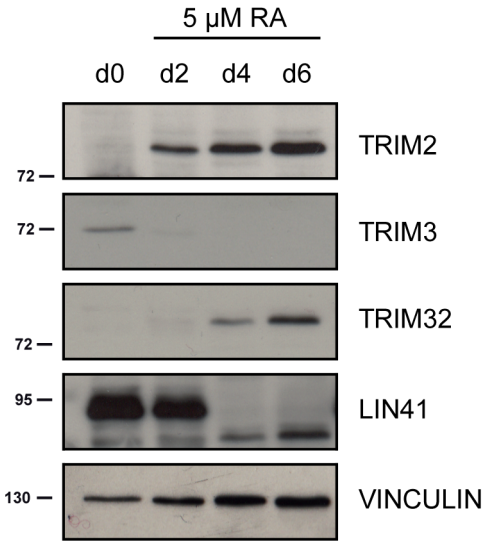


**Figure 3.20 Differentiation of iLin41 ES cells using retinoic acid application.**
iLin41 cells were deprived of feeder cells and LIF. 5 µM retinoic acid was supplemented to the growth medium. To obtain day 0 condition, iLin41 cells were maintained under proliferative conditions. Differentiated cells were harvested at day 2, 4 and 6, the expressed proteins were separated in SDS-PAGE and analyzed with western blot. The molecular mass in kDa is indicated on the left, while the antibodies for detection are specified on the right. TRIM2 and TRIM32 are upregulated while TRIM3 and LIN41 are downregulated upon differentiation stimulus. The experiment was repeated three times; representative immunoblots are shown here.

TRIM2 protein expression was hardly detectable in proliferating cells (day 0), but was highly upregulated (already from day 2 on) upon differentiation (Figure 3.20, first panel). TRIM3 was expressed at low levels in the pluripotent state and surprisingly immediately downregulated with differentiation stimulus at day 2 (Figure 3.20, second panel). TRIM32 was not detectable in proliferative conditions but was later upregulated and detectable from day 4 on (Figure 3.20,

third panel). LIN41 is abundant in proliferative conditions and at day 2, and was strongly downregulated later in differentiation (Figure 3.20, fouth panel). TRIM2 and TRIM3 as well as LIN41 and TRIM32 show exact mutually exclusive expression patterns using retinoic acid as differentiation stimulus.

To obtain neuroectodermal differentiation without artificial morphogen treatment, iLin41 stem cells were maintained in proliferative state on gelatine-coated culture dishes and differentiated using LIF deprivation and N2B27 medium (a 1:1 mixture of DMEM/F12 and Neurobasal medium supplemented with N2 and B27 supplements) to generate neuroectodermal cells (Ying *et al.*, 2003). Cell morphology was monitored by brightfield microscopy at day 0, 4, 8 and 12, before the cells were harvested for lysis.

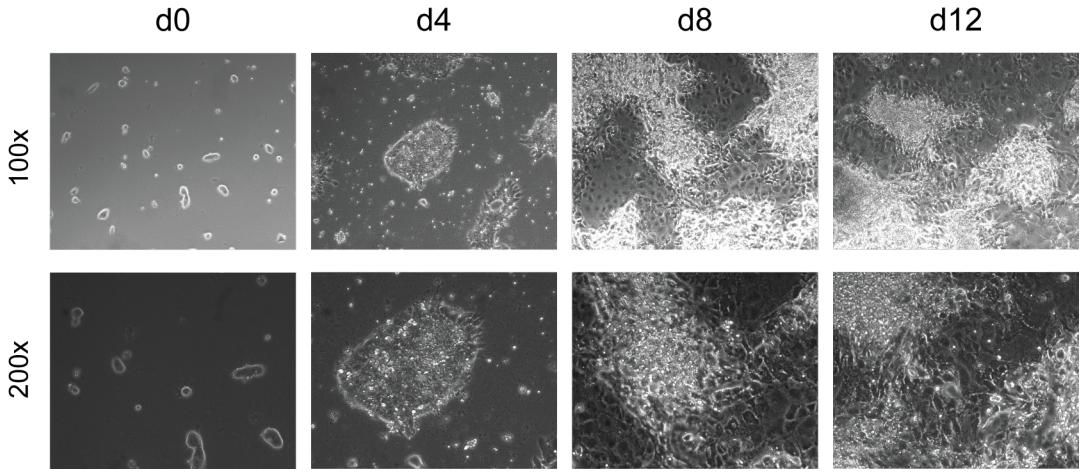


**Figure 3.21 Morphology of iLin41 ES cells during differentiation with N2B27.**
Inducible iLin41 stem cells were seeded in N2B27 medium and deprived of Lif. Brightfield microscopy pictures were taken with 100x and 200x magnification at the indicated timepoints during differentiation. iLin41 stem cells attached in small colonies to the surface. With time the colonies grow and show less defined contours – the cells grew lamellipodia that extended outward (day 4) until the whole vessel surface was covered with flattened cells (day 8). Three independent experiments were performed and representative images are shown here.

At day 0 cell colonies were small and round, with characteristic compact, defined and refringent contours. At day 4 the colonies were larger and had already lost the defined, refingent borders typical for the pluripotent state. In addition, larger and more flattened cells that extended lamellipodia outwards were observed. By day 8 the flattened cells had expanded to near confluence, although the core of the original colonies was still discernible. Proliferation in

three dimensions of the central cells led to cell masses more luminescent in brightfield microscopy. These cells were smaller than the initial stem cells and appeared undergo programmed cell death (apoptosis) with apoptotic vesicles. Many were dislodged with medium change. By day 12 three-dimensional growth was reduced probably due to a more differentiated state, but still the colony cores persisted (see Figure 3.21).

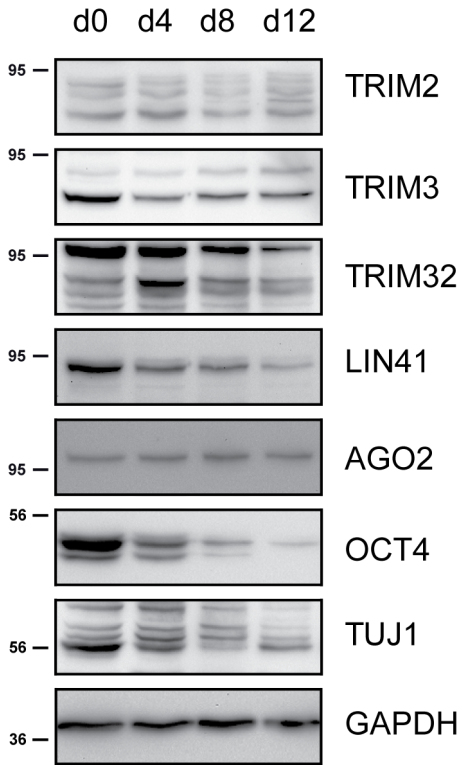


**Figure 3.22 TRIM-NHL levels during iLin41 ESC differentiation using N2B27.**
iLin41 cells were differentiated by LIF withdrawal and N2B27 medium for 12 days. Cells were harvested and protein expression was analyzed at day 0, 4, 8 and 12 by western blot. The molecular mass in kDa is indicated on the left, while the antibodies used are indicated on the right hand side of the panels. TRIM2 and TRIM32 levels did not change with differentiation while TRIM2 and LIN41 are downregulated. AGO2 levels are up, OCT4 levels downregulated during differentiation. Surprisingly, beta-III tubulin levels (depicted by staining with the monoclonal antibody Tuj1) are downregulated. GAPDH serves as loading control. The experiment was repeated three times; blots of a representative experiment are shown here.

To monitor loss of pluripotency during differentiation, protein levels of OCT4 (the major transcription factor in the pluripotency network) were examined. Expression of OCT4 was reduced over time but not lost after 12 days, indicating gradual loss of pluripotency under these conditions (Figure 3.22, OCT4 panel). LIN41 expression was also reduced during differentiation, albeit not completely

lost (Figure 3.22, fourth panel). Expression of the LIN41 target AGO2 was slightly upregulated in differentiation, consistent with a role for LIN41 in AGO2 turnover (Figure 3.22, fifth panel). Compared to differentiation with retinoic acid, there were no clear trends in expression levels of TRIM2, TRIM3 and TRIM32 over the course of the experiment (Figure 3.22, top three panels). Expression of TRIM2 was unchanged in differentiation, while TRIM3 and TRIM32 expression was slightly reduced. The increase in TRIM32 at day 4 is not representative, as it was not observed in other experiments. The efficiency of neuronal differentiation was estimated by probing for neuron-specific β-III TUBULIN using the monoclonal antibody Tuj1. β-III TUBULIN levels did not increase with time and in fact decreased slightly from the basal levels observed at day 0 (Figure 3.22, second lowest panel). This indicates that the majority of cells did not attain neuronal identity over the course of the experiment. The slow loss of OCT4 and LIN41 and the lack of induction of the other TRIM-NHL proteins therefore appear to correlate with a low efficiency of neuronal differentiation using this protocol.

Taken together, TRIM-NHL levels changed upon differentiation with either protocol, with TRIM3 and LIN41 consistently being reduced across all experiments. Treatment with retinoic acid more closely recapitulated the reciprocal expression of LIN41 *versus* TRIM2 and TRIM32 seen *in vivo* neurodevelopment. In contrast TRIM3 expression decreased upon neurodifferentiation of ES cells with either protocol, exactly opposite to *in vivo* neurodevelopment.

### 3.7.2 Induction of LIN41 in proliferative embryonic stem cells

All TRIM-NHL proteins localized and interacted with LIN41 *in vitro* as well as *in vivo* and showed a reciprocal expression pattern in neuronal development. Therefore, a functional interplay among the family members at specific time points in cell differentiation and early cortical development was hypothesized. To address this question, overexpression of exogenous LIN41 should have given a first impression if the observed interaction leads to changes either in target specificity or in mutual degradative ubiquitination. But expression of

LIN41 in N2A cells and analysis of TRIM2, TRIM3, and TRIM32 protein levels showed ambiguous results (data not shown). This was probably due to the artificial conditions, as the stem cell protein LIN41 was expressed in committed N2A neuroblastoma cells. To overcome these hurdles, doxycycline-inducible FLAG-LIN41 embryonic stem cells (for information on iLin41 ESC generation see section 2.2.13) were employed. The goal was to test if exogenous LIN41 influences other TRIM-NHLs, for example by targeting them for degradative ubiquitination. To determine optimal conditions for LIN41 induction, doxycycline was titrated as medium supplement under proliferative conditions and the resulting FLAG-LIN41 expression was monitored by western blotting (Figure 3.23).

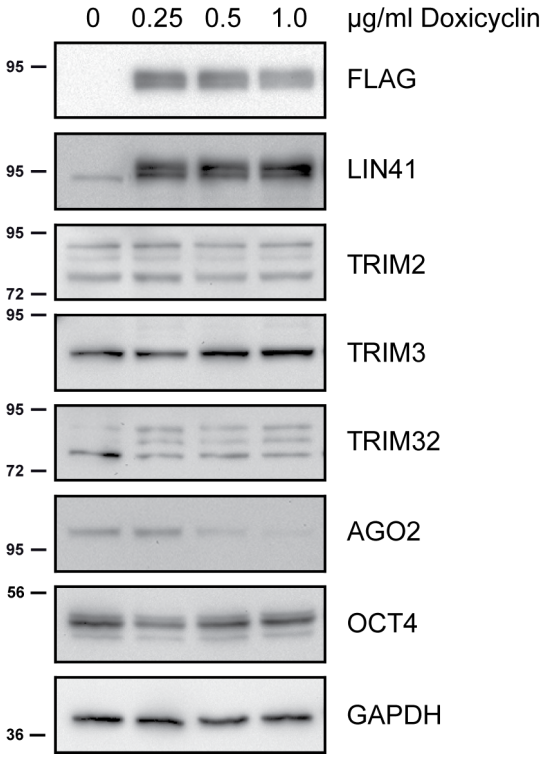


**Figure 3.23 FLAG-LIN41 induction reduces TRIM32 expression in stem cells.**
Inducible FLAG-LIN41 stem cells were induced with the indicated concentrations of doxycycline (0 µg/ml being the DMSO control) for SDS-PAGE and western blot analysis. The molecular mass in kDa is indicated on the left and the antibodies used on the right hand side of the panels. The experiment was repeated three times; representative blots are shown. LIN41 is induced about 8-fold, independent of the amount of doxycycline used (analyzed with Fiji 1.0). TRIM2 and TRIM3 levels did not respond to the upregulation of LIN41, while the 72 kDa signal of TRIM32 was reduced upon FLAG-LIN41 induction. Anti-GAPDH was used as loading control.

Doxycycline dissolved in DMSO was supplemented to the medium of proliferating iLin41 cells for 24 h. Concentrations ranging between 0 µg/ml (DMSO control) and 1 µg/ml (used in the original publication Chang *et al.*, 2012) were applied and assayed by SDS-PAGE and western blot analysis. Doxycycline induced FLAG-LIN41 expression in a non-dose-dependent manner (Figure 3.23, FLAG panel). LIN41 expression was enhanced about eight fold, compared to endogenous levels (Figure 3.23, LIN41 panel). Compared to DMSO control, the increase in LIN41 levels did not affect TRIM2 and TRIM3 expression levels (Figure 3.23, TRIM2 and TRIM3 panels). Interestingly, the expression of the 72 kDa TRIM32 band was reduced (Figure 3.23, TRIM32 panel). The expression levels of AGO2, a previously described LIN41 ubiquitination target, were also reduced with increasing LIN41 levels (Figure 3.23, AGO2 panel). Levels of OCT4, the central regulator of pluripotency, were unchanged in comparison to the housekeeping protein GAPDH (Figure 3.23, OCT4 and GAPDH panel). The reciprocal expression of LIN41 and TRIM32 indicates a regulatory relationship between these two TRIM-NHL proteins.

## 3.8 Mammalian TRIM-NHL expression in various stem cell lines

To see if the inverse correlation of TRIM32 and LIN41 expression can be recapitulated in other stem cell models, different stem cell lines for TRIM-NHL protein expression were analyzed. Crude extracts of the different cell lines in TNN lysis buffer were tested for TRIM-NHL protein expression by western blot analysis. Among them were stem cell lines with a gene trap cassette in the *Lin41* locus. The stem cell lines were isolated in collaboration with Dr. Geert Michels group at the FEM (Forschungseinrichtung für experimentelle Medizin, Charite Berlin) from a *Lin41* gene trap mouse model generated in our group. The *Lin41* gene is disrupted after the second exon by insertion of a gene trap cassette with a splice acceptor site. Therefore, the resulting mRNA encodes the LIN41 N-terminus (RING domain, the B boxes, and a part of the coiled-coil domain) fused to the inserted LacZ/Neo (βGeo) sequence. The 3$^{rd}$ and 4$^{th}$ *Lin41* exon, encoding the C-terminus (second part of the coiled-coil, filamin and NHL domain) and the 3'UTR are no longer transcribed. The truncation of LIN41 protein leads to a loss-of-function (Maller Schulman *et al.*, 2008). Replacement

of one *Lin41* wild type allele leads to heterozygous cells (*Lin41*$^{+/-}$), replacement of both to homozygous knockout cells (*Lin41*$^{-/-}$). To complement the *Lin41* knockout cells, a FLAG-LIN41 overexpression model is available (iLin41, see section 3.7.2). Doxycycline treatment induces the transcription of *Flag-Lin41* and therefore synthesis of FLAG-LIN41 protein (see Figure 3.23). Also wild type W4 embryonic stem cells, P19 embryocarcinoma cells (as pluripotent but not embryonic stem cell line) and N2A neuroblastoma cells (a cell line derived from a CNS tumor) were analyzed for TRIM-NHL expression by western blot.

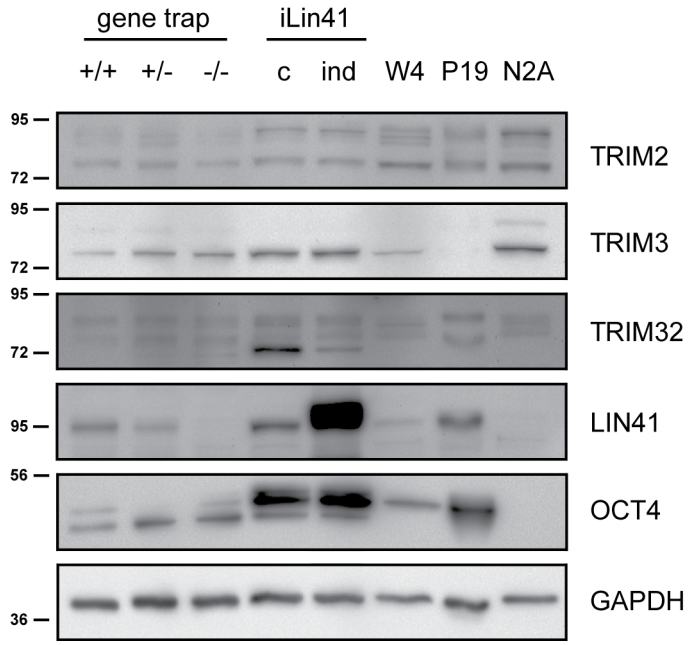


**Figure 3.24 TRIM-NHL expression in ES cell lines, P19 and N2A cells.**
Crude lysates of *Lin41*$^{wt, +/-, -/-}$, iLin41 control and doxycycline-induced as well as W4 embryonic stem cells, P19 embryocarcinoma and N2A neuroblastoma cells were subjected to SDS-PAGE and western blot analysis. The molecular mass in kDa is indicated on the left, while the antibodies used are indicated on the right hand side of the blots. Anti-GAPDH is used as loading control. All TRIM-NHL proteins are expressed in embryonic stem cells.

To date, with the exception of LIN41, it was not known that the other TRIM-NHL family members are expressed in embryonic stem cells. In terms of developmental expression, TRIM3 and TRIM32 were only shown to be expressed from E14.5 on (E15.5, respectively), while TRIM2 protein expression in development has not yet been reported (Hung *et al.*, 2010; Schwamborn *et al.*, 2009). However the results in Figure 3.24 clearly demonstrate for the first time expression of all four TRIM-NHL proteins in stem cells. Still, the TRIM2,

TRIM3 and TRIM32 levels were close to the detection limit. Their protein levels were very similar among *Lin41*$^{wt}$, *Lin41*$^{+/-}$ and *Lin41*$^{-/-}$ stem cells (Figure 3.24, lane 1-3), compared to GAPDH expression as loading control (Figure 3.24, lowest panel, lane 1-3). Induction of FLAG-LIN41 in iLin41 ES cells did not alter TRIM2 and TRIM3 levels, while it reduced TRIM32 (Figure 3.24, lane 4 and 5), reproducing the results shown in Figure 3.23. W4 cells express TRIM2 and 3, while TRIM32 and LIN41 on the other hand are hardly detectable compared to the other stem cell lines (Figure 3.24, lane 6). P19 embryocarcinoma cells express TRIM2, TRIM32 and LIN41 but lacked TRIM3 expression (Figure 3.24, lane 7). N2A neuroblastoma cells were used as example for more neuronally committed cells. They express higher levels of TRIM2 and TRIM3, lower levels of TRIM32 and lack LIN41 (Figure 3.24, lane 8). Different stem cell lines express rather different OCT4 levels. iLin41 KH2 ES cells express higher OCT4 levels than the gene trap embryonic stem cell lines. P19 cells express more OCT4 than W4, while N2A cells express none (Figure 3.24, OCT4 panel).

Comparing the different stem cell lines, high LIN41 levels did not correlate with low TRIM32 levels and *vice versa* in general. Most importantly, the inverse expression of LIN41 and TRIM32 was not recapitulated in *Lin41* knockout cell lines. It was a result only observable upon acute upregulation of LIN41 in iLin41 cells.

# 4 DISCUSSION

The E3 ubiquitin ligase LIN41 is expressed in pluripotent cells and co-localizes with ARGONAUTE 2 (AGO2) in processing bodies (P bodies, Rybak *et al.*, 2009, Figure 3.1), the foci of mRNA repression and decay in the cytoplasm (Liu *et al.*, 2005b). To date, AGO2 is the only known LIN41 ubiquitination target that is degraded by the proteasome. This AGO2 degradation resulted in a reduction of microRNA activity (Rybak *et al.*, 2009). In general, E3 ubiquitin ligases are known to have more than one target; therefore the aim of the presented thesis was to characterize additional functions of LIN41 in microRNA biogenesis, pluripotency, endosome and P body trafficking, as well as in neurodevelopment.

## 4.1 Characterization of various novel LIN41 functions

The question of additional LIN41 functions in microRNA biogenesis and pluripotency was addressed employing a LIN41 knockdown cell line and the issue of shared functions with the other TRIM-NHL proteins with immunostaining and co-immunoprecipitation of exogenous proteins.

### 4.1.1 LIN41 affects microRNA biogenesis proteins

Cytoplasmic AGO proteins are the major effectors in the RNA-induced silencing complex (RISC). To a small extent ARGONAUTE proteins were also found in the nucleus (Rüdel *et al.*, 2008; Tan *et al.*, 2009) and to interact with DICER (Tahbaz *et al.*, 2004). AGO2-DICER interaction is dependent on heat shock protein 90 activity and inhibited DICER processing (Tahbaz *et al.*, 2004). Therefore, a potential influence of LIN41 on other cytoplasmic and nuclear microRNA biogenesis components was hypothesized. To answer this question, a P19 embryocarcinoma cell line, which constitutively represses LIN41 expression, was established as an important tool for investigating LIN41 function. This LIN41 knockdown did not change the levels of the nuclear microprocessor proteins DROSHA and its cofactor DGCR8 (Figure 3.2). These results indicate that the E3 ligase activity of LIN41 does not affect nuclear microRNA biogenesis proteins under the conditions used. The lack of suitable antibodies for DICER and TRBP impeded analyzing its effect on the precursor

processing complex proteins. However, apart from AGO2, LIN41 might target other RISC proteins. In favor of this hypothesis, transient and stable LIN41 knockdown increased MOV10 levels in P19 cells (Figure 3.2). This leads to the conclusion that LIN41 is most likely not a general inhibitor of the entire microRNA pathway, but is more likely to be involved in the regulation of AGO-associated proteins in the RISC. By also targeting MOV10 for degradation (in addition to AGO), LIN41 would ensure low microRNA activity in pluripotent and multipotent stem cells. The investigation of MOV10 as a bona fide ubiquitination target of LIN41 requires specific experiments like ubiquitination assays.[1]

### 4.1.2 LIN41 influences the pluripotency network

Stable LIN41 knockdown in P19 cells is a versatile tool to study LIN41 function in pluripotent cells. After the initial selection phase, selective pressure by G418 could not be lowered without increasing LIN41 levels. This immediate response indicates that there may be selection pressure for LIN41 expression in the pluripotent P19 cell line. To test if LIN41 might influence core determinants of the pluripotent state, crude lysates of stable LIN41 knockdown P19 cells were analyzed for pluripotency marker expression. On the one hand, LIN41 loss in P19 cells triggered a reduction of OCT4 and LIN28 protein levels, two major pluripotency factors (Figure 3.3). On the other hand, LIN41 is unlikely to be essential for the pluripotent state *per se*, as the *Lin41* gene trap mouse (lacking any functional protein) is viable until embryonic day 9.5-11.5 (Maller Schulman *et al.*, 2008, Elisa Cuevas García PhD thesis) and Worringer and colleagues found LIN41 only important for initial events in reprogramming (Worringer *et al.*, 2014). These published data indicate a role for LIN41 in the course of de-/differentiation rather than in pluripotency. Moreover, the effect of LIN41 depletion on LIN28 is probably microRNA-mediated. LIN41 was reported to be a negative regulator of let-7 activity (Rybak *et al.*, 2009), so that let-7 activity is likely to be enhanced in the LIN41 knockdown cells. let-7, in turn, was reported to target *Lin28* mRNA in pluripotent cells, which would explain the reduction of LIN28 protein levels in LIN41 knockdown cells (Guo *et al.*, 2006; Moss and Tang, 2003; Rybak *et al.*, 2008). The mechanism of OCT4 decrease might be

[1] The investigaton of MOV10 as LIN41 ubiquitination substrate is part of a colleague's research project and was therefore not pursued further in this thesis.

similar. The microRNA miR-145 was shown to be expressed at very low levels in stem cells and to be upregulated in differentiation. It targets complementary sites in the *Oct4* 3'UTR resulting in OCT4 protein downregulation (Xu *et al.*, 2009). The effect of LIN41 is AGO-mediated and not microRNA specific, so that low levels of miR-145 constitutively expressed in P19 cells might be activated. However, if the reduction in OCT4 is mediated by miR-145, SOX2 levels should be affected too, as miR-145 also targets the *Sox2* 3'UTR (Xu *et al.*, 2009). This suggests that miR-145 activity in P19 cells is insufficient to account for the deregulation and that other mechanisms must be responsible. Furthermore, it remains unclear if the reduction in pluripotency markers influenced the ability of LIN41 knockdown cells to differentiate. Pilot experiments comparing the differentiation kinetics of these cells in response to retinoic acid were inconclusive (data not shown).

### 4.1.3 LIN41 influence on endosome localization

Potentially shared function among mammalian TRIM-NHL proteins led to the question if LIN41 influences endosome localization. When overexpressed in HeLa cells, LIN41 displayed partial co-localization with RAB5 and to a higher extent with RAB7 (Figure 3.4). One difficulty in interpreting this result, however, is the fact that the localization pattern of the RAB proteins appears to be affected by LIN41. RAB5-positive early endosomes were reported to localize in the cell periphery and RAB7-positve late endosomes to concentrate more centrally (Spang). This pattern was not entirely reproduced and there is also a high background of diffuse cytoplasmic staining (Figure 3.4). From these results, it appears possible that LIN41 is associated with late endosomes, as has been reported for TRIM3 (Yan *et al.*, 2005), and to affect localization of late endosomes. However, after consulting with Volker Haucke, an expert on vesicular trafficking and the source of the RAB expression plasmids used, it was concluded that these results are not convincing enough to warrant additional investigation.

### 4.1.4 LIN41, MYOSIN and P body trafficking

Previously, TRIM2 and TRIM3 were reported to interact with the globular domain of MYOSIN Va and TRIM3 was shown to influence endosome recycling (El-Husseini and Vincent, 1999; Ohkawa *et al.*, 2001; Yan *et al.*, 2005). Structural similarity of the TRIM-NHL proteins suggested that these functions might be shared among family members and that LIN41 might also interact with MYOSIN V. Indeed, Figure 3.6 showed co-localization of LIN41 with the globular domains of MYOSIN Va, MYOSIN Vb and MYOSIN VI (Figure 3.6), proteins that are known to mediate the outward and inward transport of organelles along actin filaments (Buss and Kendrick-Jones, 2008; Trybus, 2008). An interaction between LIN41 and the globular head domain of MYOSIN Va (gMYO Va) was confirmed using a co-transfection assay (Figure 3.7). Interestingly, the localization of LIN41 changed when co-transfected with gMYO Va (compare Figure 3.1 to Figure 3.6A), indicating a potential influence of MYOSIN Va on LIN41 localization and function.

The observed localization around the nucleus might be due to a dominant negative effect of the truncated motor protein. Uncoupling the globular (cargo-binding) domain from the MYOSIN Va motor domains was reported to lead to a collapse of transported organelles toward the minus end of actin filaments close to the nucleus (Correia *et al.*, 2008). Therefore it was tested if MYOSIN Va transports LIN41 to P bodies. MYOSIN Va levels were reduced by RNA interference and it was stained for co-transfected LIN41 and the endogenous P body marker protein DCP1a. Instead of a change in localization of LIN41 and DCP1a positive foci, their dispersion was observed (Figure 3.8). The results presented in this thesis led to the conclusion that MYOSIN Va is important for P body integrity and motility, which was confirmed by an independent study published after these experiments were completed (Lindsay and McCaffrey, 2011). In fact, an influence of LIN41 on P body localization could not be found, but MYOSIN Va was regulating LIN41 localization and P body maintenance. Most likely, it is the globular domain of MYOSIN Va that is important for the latter, as transfection of the truncated protein still allowed P body assembly and but changed their intracellular distribution (Figure 3.6). This leads to the speculation, that MYOSIN Va globular domain bound proteins – proteins like the

TRIM-NHL family members - might serve as scaffolds for P body proteins to maintain integrity.

Taken together, these experiments indicate a new function for Lin41 in affecting RISC protein levels that indirectly might contribute to pluripotency maintenance. By the interaction with MYOSIN Va, LIN41 is transported to P bodies to regulate RISC protein stability.

## 4.2 TRIM32 mimics LIN41 effect on microRNA activity

In order to look for shared functions among the TRIM-NHL proteins, their influence on microRNA activity in a GFP-fluorescence-based sensor assay was analyzed. TRIM2 and TRIM3 were found not to have an effect on microRNA function (data not shown). Unlike LIN41 and Tirm32, TRIM2 and TRIM3 are not specifically enriched in P bodies; although they do appear to enter them when complexed with LIN41 (Figure 3.11). Despite the evidence for interaction between both proteins and MYOSIN V, the lack of conspicuous localization to P bodies argues against a primary role for either protein in the microRNA pathway.

Using a similar sensor assay with luciferase as reporter, Schwamborn and colleagues found that TRIM32 enhanced activity of let-7. The results of the here presented thesis show that TRIM32 had the opposite effect and reduced let-7 activity, reflected in enhanced GFP fluorescence of the sensor (Figure 3.9). TRIM32 is known to bind ARGONAUTE proteins (Schwamborn *et al.*, 2009), suggesting that it might repress microRNA activity by ubiquitinating ARGONAUTE in the same manner as LIN41 does (Rybak *et al.*, 2009). To reconcile the contradiction between the results of this thesis and those of Schwamborn *et al.* it is helpful to compare the respective results in more detail. Schwamborn and colleagues profiled the microRNA content of immunoprecipitates of AGO1 and TRIM32-ARGONAUTE complexes. They claim to find let-7a and other microRNAs enriched with TRIM32 containing complexes. One issue with this approach is the difficulty in controlling for equivalent immunoprecipitation efficiency of two different antibodies as the

basis for quantification. A second is that Schwamborn and colleagues did not determine the identity of the ARGONAUTE proteins bound to TRIM32 in their co-precipitation. Because TRIM32 was shown to bind other AGO proteins (Loedige *et al.*, 2012), the differences in the bound microRNA landscape between AGO1 precipitation and TRIM32 precipitation might simply reflect different microRNA binding preferences of the four AGO proteins. A third issue is the lack of mechanistic insight into how TRIM32 might influence microRNA retention by AGO proteins, since specific sequences in the microRNA are predicted to be largely inaccessible within the RNA-binding pocket of AGO. In any case, specific association of AGO-TRIM32 with let-7 would in principle be compatible with either enhanced or reduced activity.

Another difference to the results presented here, is the assignment of the domain in TRIM32 responsible for the effect on silencing activity: The NHL domain was required for enhanced let-7 activity (Schwamborn *et al.*, 2009), while the repression observed here was RING-dependent (Figure 3.9 A-C). This discrepancy suggests that the two assays are detecting mechanistically unrelated activities. In this regard, the TRIM32 NHL domain has recently been implicated in microRNA-independent mRNA binding and repression (Loedige *et al.*, 2012), which may account for the enhanced mRNA-sensor repression (thereby mimicking enhanced microRNA activity) observed by Schwamborn and colleagues. On the other hand, the RING dependence found in the here presented experiments (Figure 3.9) is consistent with the published investigations of RING-dependent modification of AGO2 by LIN41 (Rybak *et al.*, 2009). Support for this view comes from an independent report that TRIM32 is able to ubiquitinate AGO2 in a cell-based assay (Loedige *et al.*, 2012). One further observation might be relevant, Figure 3.9 F shows a dose-response experiment which confirms that increased TRIM32 expression led to increased inhibition of microRNA activity (Figure 3.9 F). TRIM32 overexpression led to progressive loss of cell viability that correlated with a reduction in the apparent transfection efficiency (highly transfected cells would be the first to die) (Figure 3.9 E, Figure 3.10). This effect can be corrected for in the cell-based flow cytometry assay (Figure 3.9 D and I), but might have escaped notice in the lysate-based luciferase assay used by Schwamborn and colleagues.

## 4.3 The LIN41 - TRIM-NHL interplay in early neurogenesis

Due to known multimerization of TRIM proteins, the issue of potential TRIM-NHL heteromerization was raised. To address this question, exogenous as well as endogenous *in vivo* protein localization and interaction were analyzed.

### 4.3.1 The mode of TRIM-NHL heteromerization

LIN41 expression was reported to be restricted to stem cells (Rybak *et al.*, 2009), while TRIM2 TRIM3 and TRIM32 have only been studied in somatic cells thus far (El-Husseini and Vincent, 1999; Kudryashova *et al.*, 2005; Ohkawa *et al.*, 2001). In these publications, TRIM-NHL expression during mouse development was analyzed in heterogeneous datasets and expression of LIN41 and the other three TRIM-NHLs were thought to be mutual exclusive. Despite one study reporting that the deletion of the *Trim32* ortholog *nhl-2* rescued the phenotype of a hypomorphic *Lin-41* allele in *C. elegans* (Hammell *et al.*, 2009), so far no one has investigated the ability of TRIM-NHL proteins to directly interact. When LIN41 was co-expressed with TRIM2, TRIM3 or TRIM32 respectively, a partial, but significant overlap of LIN41 with TRIM2 and TRIM3 immunostaining was observed. In the case of TRIM32, the overlap was almost complete (Figure 3.11). In immunoprecipitation experiments using HeLa cells expressing epitope-tagged proteins, LIN41 co-purified with TRIM2, TRIM3 and TRIM32 (Figure 3.12). It was impossible to attribute the interaction of the TRIM-NHL proteins to one single LIN41 domain under physiological conditions. In high molarity buffer, however, TRIM2, TRIM3 and TRIM32 all preferentially bound the filamin domain of LIN41 (Figure 3.13). Based on the previously described structure of RING domain dimers and the ability of B boxes to homodimerize (reviewed in Knipscheer and Sixma, 2007), these results suggest that TRIM-NHL proteins form heterodimers in parallel with homophilic contacts between each domain. Contacts between the filamin domains may anchor the structure. In support of this view, Peng and colleagues reported that the entire tripartite motif acts as an integral structural unit, which mediates multimerization of TRIM proteins. Studying the interaction between two (non-NHL) TRIM proteins, they found that mutations in the tripartite motif, which destroy the functional integrity of any of the three domains, prevent binding to interaction

partners. Interestingly, independent RING, B box and coiled-coil domain swapping experiments (creating chimeric TRIM proteins) interfered with the wild type multimerization pattern. This points to a requirement for each of the individual domains (Peng *et al.*, 2000). Furthermore, Streich and colleagues recently reported that TRIM32 forms homodimers, tetramers and higher order oligomers. Dimerization was mediated by the RING domain and oligomerization by the coiled-coil domain. Moreover, oligomerization was a prerequisite for polyubiquitination in their assays. They reported the RING, B box and the coiled-coil but not the NHL domain to be essential for polyubiquitination (Streich *et al.*, 2013). These results indicate that multimerization of TRIM-NHL proteins requires the integrity of the whole tripartite motif rather than depending on one domain.

### 4.3.2 TRIM-NHL protein expression in early neurogenesis

Having shown that the mammalian TRIM-NHLs can physically interact, in co-expression assays, the next step was to investigate possible physiological relevance. Therefore, it was searched for evidence of co-expression in the developing embryo. In development, LIN41 was reciprocally expressed to TRIM2, TRIM3 and TRIM32 (at least to the higher molecular weight signal). LIN41 expression declined in early neurogenesis between E11.5 and E13.5, while the other three were upregulated with developmental time (Figure 3.16) leaving a brief period of coexpression. LIN41 is known to be subject to post-transcriptional silencing by increasing levels of the microRNAs let-7 and miR-125 during development. Less is known about the transcriptional control of *Lin41*. Chromatin-immunoprecipitation with subsequent high-throughput sequencing revealed that the mouse ES cell transcription factors n-Myc, Stat3, Klf4 and E2F1 bind to the *Lin41* promoter and were predicted to activate transcription of *Lin41* (Chen *et al.*, 2008). In luciferase assays for promoter activity, the stemness factor c-Myc was reported to bind an intronic enhancer in the 1$^{st}$ intron of *Lin41* to activate its transcription (Chen *et al.*, 2013). *In situ* hybridization showed that *Lin41* transcription was lost around E12.5 (Schulman *et al.*, 2005), which was confirmed by quantitative RT-PCR data (Figure 3.15). This loss of transcription is in good agreement with the western blot data

showing the loss of LIN41 protein by E13.5. In later stages, however, signals of higher molecular weight were observed (Figure 3.16). These may be unspecific, but could also originate from post-transcriptional modification of residual LIN41. In this scenario, ubiquitination is the least likely modification, as the tissue was not treated with proteasome and deubiquitinase inhibitors prior to harvesting. Ubiquitinated proteins are known to be rapidly degraded or deubiquitinated in the absence of these inhibitors (Thrower *et al.*, 2000). However, other modifications, like SUMOylation, NEDDylation or ISGylation, may account for these LIN41 antibody signals in late brain development.

The upregulation of TRIM2, TRIM3 and TRIM32 expression is most likely due to enhanced transcriptional activity (Figure 3.15). A transcriptional activator for *Trim2* has not been identified yet, but *Trim3* was reported to be a transcriptional target of p53 (**p**rotein of **53** kDa; a major tumor suppressor) in cancer cells (Cheung *et al.*, 2010). p53 is known to be upregulated in the telencephalon during development (Schmid *et al.*, 1991), which may account for the increasing *Trim3* mRNA and protein levels observed over time (Figure 3.15 and Figure 3.16). Another member of the p53 family, Tap73 (also referred to as Trp73, Tp73 or p73), was reported to transcriptionally activate *Trim32* when transfected into neuroprogenitor cell (Gonzalez-Cano *et al.*, 2013). It was reported to act as major survival factor in postmitotic neurons: Tap73 deficient mice displayed nervous system abnormalities including hippocampal dysgenesis, olfactory neuron defects and sympathetic neuron loss (Pozniak *et al.*, 2000; Yang *et al.*, 2000). So Tap73 might be responsible for increasing *Trim32* mRNA levels in brain development, that are in agreement with the increasing TRIM32 protein levels observed in developmental western blots (Figure 3.16). In addition to transcriptional regulation, the loss of potential downregulation by LIN41 may account for upregulation of TRIM2, TRIM3 and TRIM32 during CNS development.

Figure 3.16 shows co-expression of all four TRIM-NHL proteins at E10.5 and E11.5 in embryonic head lysates. Immunofluorescence staining of E11.5 embryos confirmed co-localization of all four TRIM-NHL proteins in the neuroepithelium and dorsal root ganglia (Figure 3.16, Figure 3.17 and Figure

3.18). To date, this is the first analysis showing early neurodevelopmental expression of TRIM2, TRIM3 and TRIM32. TRIM2 expression was not analyzed in neurodevelopment so far and the earliest reports of TRIM3 and TRIM32 expression are from E14.5 and E15.5 respectively (Hung *et al.*, 2010; Schwamborn *et al.*, 2009). Moreover, to date this is the first study reporting endogenous, spatiotemporal co-expression of TRIM-NHL proteins.

Based on these results, the physical interaction between LIN41 and the other three TRIM-NHL proteins was further investigated. In co-immunoprecipitation experiments, LIN41 could be co-purified with all other TRIM-NHL proteins from E11.5 head lysates (Figure 3.19). Therefore, it is indeed possible that the four E3 ubiquitin ligases influence each other directly. Moreover, TRIM32 was reported to interact with and ubiquitinate the retinoic acid receptor α (RARα). This ubiquitination had a stabilizing effect and TRIM32 binding enhanced RARα signaling (in contrast to TRIM2 and TRIM3). Cooperation between TRIM32 and RARα promoted neural differentiation of P19 and N2A cells (Sato *et al.*, 2011). Expression of retinoic acid and retinoic acid receptors are upregulated during brain development and in *in vitro* differentiation of neuroblastoma cells (Lovat *et al.*, 1993; Ruberte *et al.*, 1991; 1990). Furthermore, retinoic acid signaling was reported to be critical around E13.5 for cortical neuron generation (Siegenthaler *et al.*, 2009). In this respect, LIN41 might be a direct counter player of TRIM32-driven neurodifferentiation.

### 4.3.3 TRIM-NHL protein expression in ES cell differentiation

As a prerequisite for studying a potential regulation among TRIM-NHL proteins, embryonic stem cell differentiation models were tested for their ability to faithfully recapitulate the reciprocal expression pattern observed in early neurodevelopment (Figure 3.16). Employing KH2 ES cells (iLin41; described in more detail in section 2.2.13), two differentiation protocols were established. The first one, published by Buckley and colleagues, uses LIF deprivation and retinoic acid as differentiation stimulus, a treatment that induces the loss of pluripotency (Buckley *et al.*, 2012). This protocol is of particular interest because it was used to study global ubiquitination profiles in differentiation. The

second one, published by the Austin Smith lab, uses LIF deprivation and N2B27 medium to drive the differentiating cells specifically to neural lineage cell fates (Ying *et al.*, 2003). Applying retinoic acid as differentiation stimulus, a strong downregulation of LIN41 and a reciprocal upregulation of TRIM2 and TRIM32 were observed (Figure 3.20), similar to the observation in the embryonic neuroepithelium between E10.5 and E14.5 (Figure 3.16). The response of TRIM3 did not match the embryonic pattern, as TRIM3 was expressed at low levels without prior induction and declined rather than increased after retinoic acid treatment (Figure 3.20). Therefore, the stimulation with retinoic acid largely modeled aspects of TRIM-NHL protein regulation, but the use of such a potent extrinsic morphogen may obscure more complex and local signal transduction networks that may act on these proteins *in vivo*.

Using the milder differentiation stimulus N2B27 resulted in incomplete differentiation characterized by a slow decline in, but not a complete loss of, OCT4 and LIN41 expression over the course of 12 days (Figure 3.22). The levels of TRIM2, TRIM3 and TRIM32 were unchanged during the experiment (Figure 3.22), which does not resemble the reciprocal patterns observed in *in vivo* development (Figure 3.16). In contrast to the retinoic acid driven differentiation (Figure 3.20), TRIM2 and TRIM32 were expressed under proliferative conditions at day 0 in the N2B27 driven differentiation (Figure 3.22). In the time between experiments, the culture conditions for iLin41 cells were modified. Instead of culturing them on a feeder cell layer, iLin41 ES cells were kept on gelatin-coated plates for routine passages. This change may account for the differential TRIM-NHL expression on day 0 in the differentiation assays. Therefore culture conditions should be carefully chosen in the future. Moreover, proper neurodifferentiation and resemblance to the *in vivo* situation have to be ensured before a potential regulation among the TRIM-NHL proteins by manipulating LIN41 levels during differentiation can be investigated.

Analyzing brain lysates from E10.5 to P4 represents a change from multipotent to terminally differentiated cell states (Figure 3.16). In contrast, the neuroectodermal differentiation of mouse ES cells occurring in N2B27 medium recapitulates differentiation from pluripotent to more committed fates, yet

undifferentiated progenitors (Figure 3.22). Although this protocol has been successfully used to model let-7 induction during neural differentiation (Smirnova *et al.*, 2005), it does not seem to replicate the *in vivo* pattern of TRIM-NHL regulation. For the future, recent advances in embryonic stem cell protocols show more promise in recapitulating bona fide cortical neurogenesis. Cortical organoid culture systems developed by the Sasai and Knoblich labs rely on free floating aggregate culture to better model the three dimensional cell-cell interactions of the neural tube (Eiraku and Sasai, 2011; Lancaster *et al.*, 2013). Either protocol models many aspects of the temporal progression of neural stem cell differentiation, but TRIM-NHL regulation has not yet been reported. Alternatively, the Vanderhaeghen lab has used a similar approach to the N2B27-based Austin Smith protocol (Ying *et al.*, 2003) to achieve temporally accurate generation of cortical neurons *in vitro* (Gaspard *et al.*, 2009). Although this protocol is based on adherent culture and therefore cannot model migration or lamination as well as aggregate cultures, it is better suited for larger scale cell production. In addition, microarray analysis has been performed and *Trim2*, *Trim3* and *Trim32* mRNAs are all strongly upregulated during differentiation (Pierre Vanderhaeghen, personal communication).

### 4.3.4 Potential consequences of LIN41 - TRIM-NHL interaction

The interaction of TRIM-NHL proteins during neurodevelopment may have various functions. Napolitano and Meroni reviewed known interactions of TRIM E3 ligases and define different outcomes: homo- and heterodimers that use the same E2 enzyme may synergize functionally, while those using different E2s more frequently engage in cross-regulation (Napolitano and Meroni, 2011). In a large scale interaction study employing a two-hybrid strategy, TRIM proteins were tested for E2 interaction (Napolitano *et al.*, 2011). Unfortunately, only C3HC4-type RING containing TRIM proteins were included in the study, so that LIN41 with its C3H2C3-type RING domain was omitted. TRIM2 was shown to exclusively bind UBCH5a (Napolitano *et al.*, 2011). Auto-ubiquitination assays testing different E2 enzymes reported the UBCH5a-TRIM2 interaction to be functional (Balastik *et al.*, 2008). TRIM3 and TRIM32 interacted with UBCH5a-c, UBCH6a-c and UBC13; TRIM32 additionally interacted with UBE2v1 and

UBE2v2 (Napolitano *et al.*, 2011). TRIM32 self-ubiquitinated in conjunction with UBCH5a-c, and UBCH6 (Kudryashova *et al.*, 2005; Streich *et al.*, 2013), while LIN41 was reported to self-ubiquitinate in the presence of UBCH5a but not five other tested E2 enzymes (Rybak *et al.*, 2009). Taken together, all four TRIM-NHL proteins were reported to functionally interact with the E2 conjugating enzyme UBCH5a. As noted, this opens the possibility that heterodimers of these proteins may have enhanced activity in conjunction with UBCH5a. Nonetheless, TRIM3 and TRIM32 were also reported to employ additional E2 enzymes, rendering cross-regulation when interacting with LIN41 in early neurogenesis possible.

Moreover, the four TRIM-NHL proteins could target each other for ubiquitination after binding. It was hypothesized that the reciprocal expression patterns of these proteins seen in development is due to direct interaction. LIN41 might target the other TRIM-NHL proteins in pluripotent cells and early neurogenesis. Any of them might, in turn, target LIN41 during neural differentiation. Therefore, potential cross-targeting by transfecting N2A cells with LIN41 was investigated and changes in endogenous TRIM2, TRIM3 and TRIM32 levels were analyzed. Conversely, P19 cells were transfected with TRIM2, TRIM3 and TRIM32 to see if endogenous LIN41 levels changed. The results were not conclusive, and clear evidence for or against this hypothesis could not be obtained (data not shown). One caveat is that these experiments may lack critical signals required for ubiquitination activity during differentiation. One of the most famous examples of signal-induced ubiquitination is the activation of the transcription factor NF-κB. The inhibitor protein IκB binds NF-κB and prevents its access to the nucleus, rendering the transcription factor inactive. Various extracellular stimuli induce signal transduction pathways that ultimately phosphorylate IκB. Phosphorylated IκB is rapidly and efficiently ubiquitinated and degraded by the proteasome. Upon phosphorylation, IκB releases NF-κB, which translocates to the nucleus and activates transcription (Alkalay *et al.*, 1995; Chen *et al.*, 1995; Traenckner *et al.*, 1995). As for the TRIM-NHL proteins, one was already reported to require phosphorylation of the target for ubiquitination: TRIM2 only recognizes phosphorylated BIM2 (**B**cl-2 **i**nteracting **m**ediator of cell death) and ubiquitinates it for proteasomal degradation. Unphosphorylated BIM2 is not bound and

consequently not degraded (Thompson *et al.*, 2011). On the other hand, phosphorylation of the TRIM-NHL proteins themselves may influence their targeting capacity. For example, the phosphorylation of TRIM32 interferes with its targeting: TRIM32 overexpression was shown to lead to ubiquitination and degradation of ABI2 (**A**belson **i**nteractor **2**, acts in actin filament reorganization), resulting in enhanced tumorigenicity and cell migration (Kano *et al.*, 2008). 14-3-3σ, a protein known to interact with phospho-proteins, was shown to bind TRIM32 (Benzinger *et al.*, 2005). Upon phosphorylation of TRIM32 at serine 651 by phosphokinase A, 14-3-3σ binding is enhanced and TRIM32 is sequestered from its target, leading to abrogation of ABI2 ubiquitination (Ichimura *et al.*, 2013). In cancer cells, 14-3-3σ protein levels are frequently elevated (Urano *et al.*, 2002). This increase in 14-3-3σ may lead to enhanced TRIM32 sequestration and subsequently to higher ABI2 levels, therefore accounting for the enhanced tumorigenicity observed in the breast cancer model by Urano and colleagues. Based on these examples, it is possible that the interaction of TRIM-NHL proteins may require additional post-translational modifications to trigger either mutual ubiquitination or synergy. The establishment of an appropriate stem cell model would allow this possibility to be addressed.

### 4.3.5 The LIN41 - TRIM32 interplay in embryonic stem cells

To investigate a potential regulation of the other TRIM-NHL proteins by LIN41 under more physiological conditions, a transgenic mouse embryonic stem cell line engineered to permit a tetracycline-inducible FLAG-LIN41 expression (iLin41; details in section 2.2.13) was obtained. Using this system, LIN41 induction did not influence the expression levels of TRIM2 and TRIM3, but TRIM32 expression was reduced (Figure 3.23). Differential behavior of the three proteins may originate from their subcellular localization: TRIM32 staining showed the highest degree of overlap with LIN41 positive foci (Figure 3.11). It was also very interesting to see that the mobility of TRIM32 changed in response to LIN41 overexpression. The intensity of the specific 72 kDa band was reduced while bands of higher molecular weight were either increased or were unchanged (Figure 3.23). Although suggestive, it cannot yet be concluded

that these additional bands represent modified TRIM32 protein. Multiple commercially available antibodies for TRIM32 have been tested: specificity of the rabbit anti-TRIM32 (ab96612 from Abcam) used in this experiment was confirmed by transfection assays (Figure 3.14). In N2A cells this antibody recognizes a 72 kDa band matching the predicted size, as well as an additional band migrating at 110 kDa. Transfection of siRNA against TRIM32 in N2A cells led to a strong reduction of the 72 kDa TRIM32 band, while the upper band was only slightly reduced (Figure 3.14). During embryogenesis, the 72 kDa TRIM32 signal did not accumulate with developmental time, but the higher band did (Figure 3.16). These results may indicate that this signal is unspecific or the findings can be interpreted as the higher band being a modified TRIM32 form that is protected from degradative ubiquitination. Kudryashova and colleagues reported TRIM32 western blot signals of different size when analyzing lysates from different mouse tissues. In muscle samples they detected an approximately 72 kDa signal, while in brain lysates the signal (detected with the same antibody) was significantly higher (Kudryashova *et al.*, 2005). This indicates that TRIM32 might be differentially modified according to the tissue investigated. To investigate the nature of the additional TRIM32 signal, it is planned to test its sensitivity to phosphatase using iLin41 lysates. To determine if the signal might correspond to TRIM32 modified by NEDDylation, N2A cells will be transfected with a construct encoding a deNEDDylase and changes in the TRIM32 positive signals will be analyzed in western blot. To investigate a potential influence of these modifications on the interaction of TRIM32 with LIN41, changes in co-precipitation of the two proteins after phosphatase or deNEDDylase treatment will be analyzed.

The goal of this thesis was to functionally characterize LIN41 and in particular to identify new pathways and interaction partners for the E3 ubiquitin ligase activity of LIN41. These efforts have produced significant evidence for regulatory interactions between LIN41 and TRIM32. The reduction of TRIM32 protein seen upon LIN41 induction in iLin41 cells suggests that LIN41 may target TRIM32 for degradative ubiquitination. In parallel to the hypothesis driven approach in this thesis, a colleague has recently performed an unbiased screen for LIN41 targets. To analyse cellular ubiquitination, induced and uninduced iLin41 cell

lysates were sent to Cell Signalling for global ubiquitination profiling (UbiScan®, Cell Signalling). Trypsin digestion of ubiquitinated proteins yields peptides that contain a di-glycine mark at all ubiquitination sites. Immunoprecipitation with a specific anti-di-glycine antibody and subsequent mass spectrometry analysis gives information on the ubiquitination landscape in the cell. Only one TRIM32 peptide was retrieved in mass spectrometry meaning that TRIM32 was only modified at one site. LIN41 induction resulted in 2.5-fold more reads of this TRIM32 peptide. This indicates that LIN41 indeed post-transcriptionally modifies TRIM32, most likely by ubiquitination. However, an increase of NEDDylation and ISGylation is also possible, as both of these modifications also cause di-glycine motifs after trypsin digestion (reviewed in (Vertegaal, 2011). Therefore, it will be necessary to confirm these data by conventional ubiquitination assays.

As discussed in the introduction, multiple lines of evidence link LIN41 (and also TRIM32) to the microRNA pathway. LIN41 was shown to target AGO2 for degradation and thereby reduce microRNA activity in stem cells (Rybak *et al.*, 2009). Recently, LIN41 was reported to directly interact with the 3'UTR of certain mRNAs and to repress their translation (Kwon *et al.*, 2013; Loedige *et al.*, 2012). In addition to these recently published post-transcriptional effects, the results presented in this thesis show novel post-translational functions of LIN41. It could be demonstrated that LIN41 influences the stability of other RISC proteins, which may indirectly affect pluripotency marker expression, and is transported to P bodies by interaction with MYOSIN Va. Most importantly, it was shown that TRIM-NHL family members interact in early mammalian neurogenesis. The interaction between LIN41 and TRIM32 most likely leads to ubiquitination of TRIM32, as observed in stem cells. Thereby, in addition to previously described mechanisms (like repressing microRNA activity and mRNA translation) LIN41 may additionally prevent premature differentiation in neurogenesis by delaying TRIM32-enhanced retinoic acid signaling in pluripotent and multipotent cells.

# 5 BIBLIOGRAPHY

Alkalay, I., Yaron, A., Hatzubai, A., Orian, A., Ciechanover, A., and Ben-Neriah, Y. (1995). Stimulation-dependent I kappa B alpha phosphorylation marks the NF-kappa B inhibitor for degradation via the ubiquitin-proteasome pathway. Proc. Natl. Acad. Sci. U.S.a. *92*, 10599–10603.

Andersson, T., Rahman, S., Sansom, S.N., Alsiö, J.M., Kaneda, M., Smith, J., O'Carroll, D., Tarakhovsky, A., and Livesey, F.J. (2010). Reversible Block of Mouse Neural Stem Cell Differentiation in the Absence of Dicer and MicroRNAs. PLoS ONE *5*, e13453.

Bagga, S., Bracht, J., Hunter, S., Massirer, K., Holtz, J., Eachus, R., and Pasquinelli, A.E. (2005). Regulation by let-7 and lin-4 miRNAs results in target mRNA degradation. Cell *122*, 553–563.

Bain, G., Ray, W.J., Yao, M., and Gottlieb, D.I. (1994). From embryonal carcinoma cells to neurons: The P19 pathway. Bioessays *16*, 343–348.

Balastik, M., Ferraguti, F., Pires-da Silva, A., Lee, T.H., Alvarez-Bolado, G., Lu, K.P., and Gruss, P. (2008). Deficiency in ubiquitin ligase TRIM2 causes accumulation of neurofilament light chain and neurodegeneration. Proceedings of the National Academy of Sciences *105*, 12016–12021.

Barlow, P.N., Luisi, B., Milner, A., Elliott, M., and Everett, R. (1994). Structure of the C3HC4 domain by 1H-nuclear magnetic resonance spectroscopy. A new structural class of zinc-finger. Journal of Molecular Biology *237*, 201–211.

Bartel, D.P. (2004). MicroRNAs: genomics, biogenesis, mechanism, and function. Cell *116*, 281–297.

Bazzini, A.A., Lee, M.T., and Giraldez, A.J. (2012). Ribosome profiling shows that miR-430 reduces translation before causing mRNA decay in zebrafish. Science *336*, 233–237.

Benzinger, A., Muster, N., Koch, H.B., Yates, J.R., and Hermeking, H. (2005). Targeted proteomic analysis of 14-3-3 sigma, a p53 effector commonly silenced in cancer. Mol. Cell Proteomics *4*, 785–795.

Bernstein, E., Caudy, A.A., Hammond, S.M., and Hannon, G.J. (2001). Role for a bidentate ribonuclease in the initiation step of RNA interference. Nature *409*, 363–366.

Borchert, G.M., Lanier, W., and Davidson, B.L. (2006). RNA polymerase III transcribes human microRNAs. Nature Structural & Molecular Biology *13*, 1097–1101.

Borden, K.L., Boddy, M.N., Lally, J., O'Reilly, N.J., Martin, S., Howe, K., Solomon, E., and Freemont, P.S. (1995). The solution structure of the RING finger domain from the acute promyelocytic leukaemia proto-oncoprotein PML. The EMBO Journal *14*, 1532–1541.

Borden, K.L., Martin, S.R., O'Reilly, N.J., Lally, J.M., Reddy, B.A., Etkin, L.D., and Freemont, P.S. (1993). Characterisation of a novel cysteine/histidine-rich metal binding domain from Xenopus nuclear factor XNF7. FEBS Lett. *335*, 255–260.

Borg, K., Stucka, R., Locke, M., Melin, E., Ã hlberg, G., Klutzny, U., Hagen, M.V.D., Huebner, A., LochmÃ¼ller, H., Wrogemann, K., *et al.* (2009). Intragenic deletion of TRIM32in compound heterozygotes with sarcotubular myopathy/LGMD2H. Hum. Mutat. *30*, E831–E844.

Buckley, S.M., Aranda-Orgilles, B., Strikoudis, A., Apostolou, E., Loizou, E., Moran-Crusio, K., Farnsworth, C.L., Koller, A.A., Dasgupta, R., Silva, J.C., *et al.* (2012). Regulation of Pluripotency and Cellular Reprogramming by the Ubiquitin-Proteasome System. Stem Cell *11*,

783–798.

Buss, F., and Kendrick-Jones, J. (2008). How are the cellular functions of myosin VI regulated within the cell? Biochemical and Biophysical Research Communications *369*, 165–175.

Chang, H.-M., Martinez, N.J., Thornton, J.E., Hagan, J.P., Nguyen, K.D., and Gregory, R.I. (2012). Trim71 cooperates with microRNAs to repressCdkn1a expression and promote embryonicstem cell proliferation. Nature Communications *3*, 923–10.

Chen, J., Lai, F., and Niswander, L. (2012). The ubiquitin ligase mLin41 temporally promotes neural progenitor cell maintenance through FGF signaling. Genes & Development *26*, 803–815.

Chen, X., Xu, H., Yuan, P., Fang, F., Huss, M., Vega, V.B., Wong, E., Orlov, Y.L., Zhang, W., Jiang, J., *et al.* (2008). Integration of External Signaling Pathways with the Core Transcriptional Network in Embryonic Stem Cells. Cell *133*, 1106–1117.

Chen, Y.-L., Yuan, R.-H., Yang, W.-C., Hsu, H.-C., and Jeng, Y.-M. (2013). The stem cell E3-ligase Lin-41 promotes liver cancer progression through inhibition of microRNA-mediated gene silencing. J. Pathol *229*, 486–496.

Chen, Z., Hagler, J., Palombella, V.J., Melandri, F., Scherer, D., Ballard, D., and Maniatis, T. (1995). Signal-induced site-specific phosphorylation targets I kappa B alpha to the ubiquitin-proteasome pathway. Genes & Development *9*, 1586–1597.

Chendrimada, T.P., Gregory, R.I., Kumaraswamy, E., Norman, J., Cooch, N., Nishikura, K., and Shiekhattar, R. (2005). TRBP recruits the Dicer complex to Ago2 for microRNA processing and gene silencing. Nat Cell Biol *436*, 740–744.

Cheung, C.C., Yang, C., Berger, T., Zaugg, K., Reilly, P., Elia, A.J., Wakeham, A., You-Ten, A., Chang, N., Li, L., *et al.* (2010). Identification of BERP (brain-expressed RING finger protein) as a p53 target gene that modulates seizure susceptibility through interacting with GABA(A) receptors. Proceedings of the National Academy of Sciences *107*, 11883–11888.

Chiang, A.P., Beck, J.S., Yen, H.-J., Tayeh, M.K., Scheetz, T.E., Swiderski, R.E., Nishimura, D.Y., Braun, T.A., Kim, K.-Y.A., Huang, J., *et al.* (2006). Homozygosity mapping with SNP arrays identifies TRIM32, an E3 ubiquitin ligase, as a Bardet-Biedl syndrome gene (BBS11). Proc. Natl. Acad. Sci. U.S.a. *103*, 6287–6292.

Clagett-Dame, M., McNeill, E.M., and Muley, P.D. (2006). Role of all-trans retinoic acid in neurite outgrowth and axonal elongation. J. Neurobiol. *66*, 739–756.

Cohen, S., Brault, J.J., Gygi, S.P., Glass, D.J., Valenzuela, D.M., Gartner, C., Latres, E., and Goldberg, A.L. (2009). During muscle atrophy, thick, but not thin, filament components are degraded by MuRF1-dependent ubiquitylation. J. Cell Biol. *185*, 1083–1095.

Correia, S.S., Bassani, S., Brown, T.C., Lisé, M.-F., Backos, D.S., El-Husseini, A., Passafaro, M., and Esteban, J.A. (2008). Motor protein–dependent transport of AMPA receptors into spines during long-term potentiation. Nat Neurosci *11*, 457–466.

Cougot, N., Babajko, S., and Séraphin, B. (2004). Cytoplasmic foci are sites of mRNA decay in human cells. J. Cell Biol. *165*, 31–40.

Denli, A.M., Tops, B.B.J., Plasterk, R.H.A., Ketting, R.F., and Hannon, G.J. (2004). Processing of primary microRNAs by the Microprocessor complex. Nature *432*, 231–235.

DERRY, M.C., YANAGIYA, A., MARTINEAU, Y., and SONENBERG, N. (2006). Regulation of Poly(A)-binding Protein through PABP-interacting Proteins. Cold Spring Harbor Symposia on Quantitative Biology *71*, 537–543.

Diederichs, S., Jung, S., Rothenberg, S.M., Smolen, G.A., Mlody, B.G., and Haber, D.A. (2008).

Coexpression of Argonaute-2 enhances RNA interference toward perfect match binding sites. Proceedings of the National Academy of Sciences *105*, 9284–9289.

Ding, X.C., and Grosshans, H. (2009). Repression of C. elegans microRNA targets at the initiation level of translation requires GW182 proteins. The EMBO Journal *28*, 213–222.

Djuranovic, S., Nahvi, A., and Green, R. (2012). miRNA-Mediated Gene Silencing by Translational Repression Followed by mRNA Deadenylation and Decay. Science *336*, 237–240.

Domsch, K., Ezzeddine, N., and Nguyen, H.T. (2013). Abba is an essential TRIM/RBCC protein to maintain the integrity of sarcomeric cytoarchitecture. Journal of Cell Science *126*, 3314–3323.

Edwards, T.A. (2003). Model of the Brain Tumor-Pumilio translation repressor complex. Genes & Development *17*, 2508–2513.

Eiraku, M., and Sasai, Y. (2011). Mouse embryonic stem cell culture for generation of three-dimensional retinal and cortical tissues. Nat Protoc *7*, 69–79.

El-Husseini, A.E., and Vincent, S.R. (1999). Cloning and characterization of a novel RING finger protein that interacts with class V myosins. J. Biol. Chem. *274*, 19771–19777.

El-Husseini, A.E., Kwasnicka, D., Yamada, T., Hirohashi, S., and Vincent, S.R. (2000). BERP, a novel ring finger protein, binds to alpha-actinin-4. Biochemical and Biophysical Research Communications *267*, 906–911.

Frank, D.J., and Roth, M.B. (1998). ncl-1 is required for the regulation of cell size and ribosomal RNA synthesis in Caenorhabditis elegans. J. Cell Biol. *140*, 1321–1329.

Frank, D.J., Edgar, B.A., and Roth, M.B. (2002). The Drosophila melanogaster gene brain tumor negatively regulates cell growth and ribosomal RNA synthesis. Development *129*, 399–407.

Freemont, P.S. (1993). The RING finger. A novel protein sequence motif related to the zinc finger. Ann. N. Y. Acad. Sci. *684*, 174–192.

Freemont, P.S., Hanson, I.M., and Trowsdale, J. (1991). A novel cysteine-rich sequence motif. Cell *64*, 483–484.

Fridell, R.A., Harding, L.S., Bogerd, H.P., and Cullen, B.R. (1995). Identification of a novel human zinc finger protein that specifically interacts with the activation domain of lentiviral Tat proteins. Virology *209*, 347–357.

Frosk, P., Weiler, T., Nylen, E., Sudha, T., Greenberg, C.R., Morgan, K., Fujiwara, T.M., and Wrogemann, K. (2002). Limb-girdle muscular dystrophy type 2H associated with mutation in TRIM32, a putative E3-ubiquitin-ligase gene. Am. J. Hum. Genet. *70*, 663–672.

Gaspard, N., Bouschet, T., Herpoel, A., Naeije, G., van den Ameele, J., and Vanderhaeghen, P. (2009). Generation of cortical neurons from mouse embryonic stem cells. Nat Protoc *4*, 1454–1463.

Gibbings, D.J., Ciaudo, C., Erhardt, M., and Voinnet, O. (2009). Multivesicular bodies associate with components of miRNA effector complexes and modulate miRNA activity. Nat Cell Biol *11*, 1143–1149.

Glickman, M.H., and Ciechanover, A. (2002). The ubiquitin-proteasome proteolytic pathway: destruction for the sake of construction. Physiol. Rev. *82*, 373–428.

Gonzalez-Cano, L., Hillje, A.-L., Fuertes-Alvarez, S., Marques, M.M., Blanch, A., Ian, R.W., Irwin, M.S., Schwamborn, J.C., and n, M.C.M.I. (2013). Regulatory feedback loop between TP73 and TRIM32. *4*, e704–e710.

Götz, M., and Huttner, W.B. (2005). The cell biology of neurogenesis. Nat Rev Mol Cell Biol *6*, 777–788.

Gregory, R.I., Chendrimada, T.P., Cooch, N., and Shiekhattar, R. (2005). Human RISC Couples MicroRNA Biogenesis and Posttranscriptional Gene Silencing. Cell *123*, 631–640.

Gregory, R.I., Yan, K.-P., Amuthan, G., Chendrimada, T., Doratotaj, B., Cooch, N., and Shiekhattar, R. (2004). The Microprocessor complex mediates the genesis of microRNAs. Nat Cell Biol *432*, 235–240.

Guo, H., Ingolia, N.T., Weissman, J.S., and Bartel, D.P. (2010). Mammalian microRNAs predominantly act to decrease target mRNA levels. Nature *466*, 835–840.

Guo, Y., Chen, Y., Ito, H., Watanabe, A., Ge, X., Kodama, T., and Aburatani, H. (2006). Identification and characterization of lin-28 homolog B (LIN28B) in human hepatocellular carcinoma. Gene *384*, 51–61.

Hammell, C.M., Lubin, I., Boag, P.R., Blackwell, T.K., and Ambros, V. (2009). nhl-2 Modulates MicroRNA Activity in Caenorhabditis elegans. Cell *136*, 926–938.

Han, J., Lee, Y., Yeom, K.-H., Kim, Y.-K., Jin, H., and Kim, N.V. (2004). The Drosha-DGCR8 complex in primary microRNA processing. Genes & Development *18*, 3016–3027.

Harris, R.E., Pargett, M., Sutcliffe, C., Umulis, D., and Ashe, H.L. (2011). Brat Promotes Stem Cell Differentiation via Control of a Bistable Switchthat Restricts BMP Signaling. Dev. Cell *20*, 72–83.

Hemmati-Brivanlou, A., and Melton, D. (1997). Vertebrate embryonic cells will become nerve cells unless told otherwise. Cell *88*, 13–17.

Heo, I., Joo, C., Cho, J., Ha, M., Han, J., and Kim, V.N. (2008). Short Article. Molecular Cell *32*, 276–284.

Herranz, H.E.C., Hong, X., rez, L.P.E., Ferreira, A., Olivieri, D., Cohen, S.M., and n, M.M.A. (2010). The miRNA machinery targets Mei-P26 and regulates Myc protein levels in the Drosophila wing. The EMBO Journal *29*, 1688–1698.

Hung, A.Y., Sung, C.C., Brito, I.L., and Sheng, M. (2010). Degradation of Postsynaptic Scaffold GKAP and Regulation of Dendritic Spine Morphology by the TRIM3 Ubiquitin Ligase in Rat Hippocampal Neurons. PLoS ONE *5*, e9842.

Huntzinger, E., and Izaurralde, E. (2011). Gene silencing by microRNAs: contributions of translational repression and mRNA decay. Nat. Rev. Genet. *12*, 99–110.

Hutvagner, G., McLachlan, J., Pasquinelli, A.E., Bálint, É., Tuschl, T., and Zamore, P.D. (2001). A Cellular Function for the RNA-Interference Enzyme Dicer in the Maturation of the let-7 Small Temporal RNA. Science *293*, 834–838.

Ibáñez-Ventoso, C., Vora, M., and Driscoll, M. (2008). Sequence Relationships among C. elegans, D. melanogaster and Human microRNAs Highlight the Extensive Conservation of microRNAs in Biology. PLoS ONE *3*, e2818.

Ichimura, T., Taoka, M., Shoji, I., Kato, H., Sato, T., Hatakeyama, S., Isobe, T., and Hachiya, N. (2013). 14-3-3 proteins sequester a pool of soluble TRIM32 ubiquitin ligase to repress autoubiquitylation and cytoplasmic body formation. Journal of Cell Science *126*, 2014–2026.

Jakymiw, A., Lian, S., Eystathioy, T., Li, S., Satoh, M., Hamel, J.C., Fritzler, M.J., and Chan, E.K.L. (2005). Disruption of GW bodies impairs mammalian RNA interference. Nat Cell Biol *7*, 1267–1274.

Joazeiro, C.A., Wing, S.S., Huang, H., Leverson, J.D., Hunter, T., and Liu, Y.C. (1999). The tyrosine kinase negative regulator c-Cbl as a RING-type, E2-dependent ubiquitin-protein ligase. Science *286*, 309–312.

Kano, S., Miyajima, N., Fukuda, S., and Hatakeyama, S. (2008). Tripartite Motif Protein 32 Facilitates Cell Growth and Migration via Degradation of Abl-Interactor 2. Cancer Research *68*, 5572–5580.

Khazaei, M.R., Bunk, E.C., Hillje, A.-L., Jahn, H.M., Riegler, E.M., Knoblich, J.A., Young, P., and Schwamborn, J.C. (2010). The E3-ubiquitin ligase TRIM2 regulates neuronal polarization. J. Neurochem. *117*, 29–37.

Knipscheer, P., and Sixma, T.K. (2007). Protein–protein interactions regulate Ubl conjugation. Current Opinion in Structural Biology *17*, 665–673.

Kriegstein, A., and Alvarez-Buylla, A. (2009). The Glial Nature of Embryonic and Adult Neural Stem Cells. Annu. Rev. Neurosci. *32*, 149–184.

Kudryashova, E., Struyk, A., Mokhonova, E., Cannon, S.C., and Spencer, M.J. (2011). The common missense mutation D489N in TRIM32 causing limb girdle muscular dystrophy 2H leads to loss of the mutated protein in knock-in mice resulting in a Trim32-null phenotype. Human Molecular Genetics *20*, 3925–3932.

Kudryashova, E., Wu, J., Havton, L.A., and Spencer, M.J. (2009). Deficiency of the E3 ubiquitin ligase TRIM32 in mice leads to a myopathy with a neurogenic component. Human Molecular Genetics *18*, 1353–1367.

Kudryashova, E., Kramerova, I., and Spencer, M.J. (2012). Satellite cell senescence underlies myopathy in a mouse model of limb-girdle muscular dystrophy 2H. J. Clin. Invest. *122*, 1764–1776.

Kudryashova, E., Kudryashov, D., Kramerova, I., and Spencer, M.J. (2005). Trim32 is a Ubiquitin Ligase Mutated in Limb Girdle Muscular Dystrophy Type 2H that Binds to Skeletal Muscle Myosin and Ubiquitinates Actin. Journal of Molecular Biology *354*, 413–424.

Kusek, G., Campbell, M., Doyle, F., Tenenbaum, S.A., Kiebler, M., and Temple, S. (2012). Asymmetric segregation of the double-stranded RNA binding protein Staufen2 during mammalian neural stem cell divisions promotes lineage progression. Cell Stem Cell *11*, 505–516.

Kwon, S.C., Yi, H., Eichelbaum, K., Föhr, S., Fischer, B., You, K.T., Castello, A., Krijgsveld, J., Hentze, M.W., and Kim, V.N. (2013). Nature Structural & Molecular Biology 2013 Kwo. Nature Structural & Molecular Biology *20*, 1122–1130.

La Torre, A., Georgi, S., and Reh, T.A. (2013). Conserved microRNA pathway regulates developmental timing of retinal neurogenesis. Proceedings of the National Academy of Sciences *110*, E2362–E2370.

Lagos-Quintana, M., Rauhut, R., Yalcin, A., Meyer, J., Lendeckel, W., and Tuschl, T. (2002). Identification of tissue-specific microRNAs from mouse. Curr. Biol. *12*, 735–739.

Lancaster, M.A., Renner, M., Martin, C.-A., Wenzel, D., Bicknell, L.S., Hurles, M.E., Homfray, T., Penninger, J.M., Jackson, A.P., and Knoblich, J.A. (2013). Cerebral organoids model human brain development and microcephaly. Nature *501*, 373–379.

Landgraf, P., Rusu, M., Sheridan, R., Sewer, A., Iovino, N., Aravin, A., Pfeffer, S., Rice, A., Kamphorst, A.O., Landthaler, M., *et al.* (2007). A mammalian microRNA expression atlas based on small RNA library sequencing. Cell *129*, 1401–1414.

Landthaler, M., Yalcin, A., and Tuschl, T. (2004). The Human DiGeorge Syndrome Critical

Region Gene 8 and Its D. melanogaster Homolog Are Required for miRNA Biogenesis. Current Biology *14*, 2162–2167.

Lee, Y., Ahn, C., Han, J., Choi, H., Kim, J., Yim, J., Lee, J., Provost, P., Rådmark, O., Kim, S., *et al.* (2003). The nuclear RNase III Drosha initiates microRNA processing. Nature *425*, 415–419.

Lee, Y., Kim, M., Han, J., Yeom, K.-H., Lee, S., Baek, S.H., and Kim, V.N. (2004). MicroRNA genes are transcribed by RNA polymerase II. The EMBO Journal *23*, 4051–4060.

Lee, Y.S., Pressman, S., Andress, A.P., Kim, K., White, J.L., Cassidy, J.J., Li, X., Lubell, K., Lim, D.H., Cho, I.S., et al. (2009). Silencing by small RNAs is linked to endosomal trafficking. Nat Cell Biol *11*, 1150–1156.

Li, W., Tu, D., Brunger, A.T., and Ye, Y. (2007). A ubiquitin ligase transfers preformed polyubiquitin chains from a conjugating enzyme to a substrate. Nature *446*, 333–337.

Lin, Y.-C., Hsieh, L.-C., Kuo, M.-W., Yu, J., Kuo, H.-H., Lo, W.-L., Lin, R.-J., Yu, A.L., and Li, W.-H. (2007). Human TRIM71 and its nematode homologue are targets of let-7 microRNA and its zebrafish orthologue is essential for development. Mol. Biol. Evol. *24*, 2525–2534.

Lindsay, A.J., and McCaffrey, M.W. (2011). Myosin Va Is Required for P Body but Not Stress Granule Formation. Journal of Biological Chemistry *286*, 11519–11528.

Lionel, A.C., Crosbie, J., Barbosa, N., Goodale, T., Thiruvahindrapuram, B., Rickaby, J., Gazzellone, M., Carson, A.R., Howe, J.L., Wang, Z., *et al.* (2011). Rare Copy Number Variation Discovery and Cross-Disorder Comparisons Identify Risk Genes for ADHD. Science Translational Medicine *3*, 95ra75–95ra75.

Liu, J., Rivas, F.V., Wohlschlegel, J., Yates, J.R., Parker, R., and Hannon, G.J. (2005a). A role for the P-body component GW182 in microRNA function. Nat Cell Biol *7*, 1261–1266.

Liu, J., Valencia-Sanchez, M.A., Hannon, G.J., and Parker, R. (2005b). MicroRNA-dependent localization of targeted mRNAs to mammalian P-bodies. Nat Cell Biol *7*, 719–723.

Locke, M., Tinsley, C.L., Benson, M.A., and Blake, D.J. (2009). TRIM32 is an E3 ubiquitin ligase for dysbindin. Human Molecular Genetics *18*, 2344–2358.

Loedige, I., Gaidatzis, D., Sack, R., Meister, G., and Filipowicz, W. (2012). The mammalian TRIM-NHL protein TRIM71/LIN-41 is a repressor of mRNA function. Nucleic Acids Research *41*, 518–532.

Lorick, K.L., Jensen, J.P., Fang, S., Ong, A.M., Hatakeyama, S., and Weissman, A.M. (1999). RING fingers mediate ubiquitin-conjugating enzyme (E2)-dependent ubiquitination. Proc. Natl. Acad. Sci. U.S.a. *96*, 11364–11369.

Lovat, P.E., Pearson, A.D., Malcolm, A., and Redfern, C.P. (1993). Retinoic acid receptor expression during the in vitro differentiation of human neuroblastoma. Neuroscience Letters *162*, 109–113.

Löer, B., Bauer, R., Bornheim, R., Grell, J., Kremmer, E., Kolanus, W., and Hoch, M. (2008). The NHL-domain protein Wech is crucial for the integrin–cytoskeleton link. Nat Cell Biol *10*, 422–428.

Lupas, A. (1996). Coiled coils: new structures and new functions. Trends in Biochemical Sciences *21*, 375–382.

Makeyev, E.V., Zhang, J., Carrasco, M.A., and Maniatis, T. (2007). The MicroRNA miR-124 Promotes Neuronal Differentiation by Triggering Brain-Specific Alternative Pre-mRNA Splicing. Molecular Cell *27*, 435–448.

Maller Schulman, B.R., Liang, X., Stahlhut, C., DelConte, C., Stefani, G., and Slack, F.J. (2008). The let-7 microRNA target gene, Mlin41/Trim71 is required for mouse embryonic survival and neural tube closure. Cell Cycle *7*, 3935–3942.

McCoy, A.J., Fucini, P., Noegel, A.A., and Stewart, M. (1999). Structural basis for dimerization of the Dictyostelium gelation factor (ABP120) rod. Nat. Struct. Biol. *6*, 836–841.

Miska, E.A., Alvarez-Saavedra, E., Townsend, M., Yoshii, A., Sestan, N., Rakic, P., Constantine-Paton, M., and Horvitz, H.R. (2004). Microarray analysis of microRNA expression in the developing mammalian brain. Genome Biol. *5*, R68.

Molyneaux, B.J., Arlotta, P., Menezes, J.R.L., and Macklis, J.D. (2007). Neuronal subtype specification in the cerebral cortex. Nat Rev Neurosci *8*, 427–437.

Monaghan, A.P., Grau, E., Bock, D., and Schütz, G. (1995). The mouse homolog of the orphan nuclear receptor tailless is expressed in the developing forebrain. Development *121*, 839–853.

Mooren, O.L., Galletta, B.J., and Cooper, J.A. (2012). Roles for Actin Assembly in Endocytosis. Annu. Rev. Biochem. *81*, 661–686.

Moss, E.G., Lee, R.C., and Ambros, V. (1997). The cold shock domain protein LIN-28 controls developmental timing in C. elegans and is regulated by the lin-4 RNA. Cell *88*, 637–646.

Moss, E.G., and Tang, L. (2003). Conservation of the heterochronic regulator Lin-28, its developmental expression and microRNA complementary sites. Developmental Biology *258*, 432–442.

Muguruma, K., and Sasai, Y. (2012). In vitro recapitulation of neural development using embryonic stem cells: from neurogenesis to histogenesis. Dev. Growth Differ. *54*, 349–357.

Napolitano, L.M., and Meroni, G. (2011). TRIM family: Pleiotropy and diversification through homomultimer and heteromultimer formation. IUBMB Life *64*, 64–71.

Napolitano, L.M., Jaffray, E.G., Hay, R.T., and Meroni, G. (2011). Functional interactions between ubiquitin E2 enzymes and TRIM proteins. Biochem. J. *434*, 309–319.

Nathan, J.A., Kim, H.T., Ting, L., Gygi, S.P., and Goldberg, A.L. (2013). Why do cellular proteins linked to K63-polyubiquitin chains not associate with proteasomes? The EMBO Journal *32*, 552–565.

Neumüller, R.A., Betschinger, J., Fischer, A., Bushati, N., Poernbacher, I., Mechtler, K., Cohen, S.M., and Knoblich, J.A. (2008). Mei-P26 regulates microRNAs and cell growth in the Drosophila ovarian stem cell lineage. Nature *454*, 241–245.

Newman, M.A., Thomson, J.M., and Hammond, S.M. (2008). Lin-28 interaction with the Let-7 precursor loop mediates regulated microRNA processing. Rna *14*, 1539–1549.

Nicklas, S., Otto, A., Wu, X., Miller, P., Stelzer, S., Wen, Y., Kuang, S., Wrogemann, K., Patel, K., Ding, H., *et al.* (2012). TRIM32 Regulates Skeletal Muscle Stem Cell Differentiation and Is Necessary for Normal Adult Muscle Regeneration. PLoS ONE *7*, e30445.

Nishino, J., Kim, I., Chada, K., and Morrison, S.J. (2008). Hmga2 Promotes Neural Stem Cell Self- Renewal in Young but Not Old Mice byReducing p16. Cell *135*, 227–239.

Nishino, J., Kim, S., Zhu, Y., Zhu, H., and Morrison, S.J. (2013). A network of heterochronic genes including Imp1 regulates temporal changes in stem cell properties. Elife *2*, e00924.

O'Farrell, F., Esfahani, S.S., Engström, Y., and Kylsten, P. (2008). Regulation of the Drosophila lin-41 homologue dappled by let-7 reveals conservation of a regulatory mechanism within the LIN-41 subclade. Dev. Dyn. *237*, 196–208.

Ohkawa, N., Kokura, K., Matsu-Ura, T., Obinata, T., Konishi, Y., and Tamura, T.A. (2001). Molecular cloning and characterization of neural activity-related RING finger protein (NARF): a new member of the RBCC family is a candidate for the partner of myosin V. J. Neurochem. *78*, 75–87.

Packer, A.N., Xing, Y., Harper, S.Q., Jones, L., and Davidson, B.L. (2008). The Bifunctional microRNA miR-9/miR-9* Regulates REST and CoREST and Is Downregulated in Huntington's Disease. Journal of Neuroscience *28*, 14341–14346.

Pasquinelli, A.E., Reinhart, B.J., Slack, F., Martindale, M.Q., Kuroda, M.I., Maller, B., Hayward, D.C., Ball, E.E., Degnan, B., Müller, P., *et al.* (2000). Conservation of the sequence and temporal expression of let-7 heterochronic regulatory RNA. Nature *408*, 86–89.

Peng, H., Begg, G.E., Schultz, D.C., Friedman, J.R., Jensen, D.E., Speicher, D.W., and Rauscher, F.J. (2000). Reconstitution of the KRAB-KAP-1 repressor complex: a model system for defining the molecular anatomy of RING-B box-coiled-coil domain-mediated protein-protein interactions. Journal of Molecular Biology *295*, 1139–1162.

Pozniak, C.D., Radinovic, S., Yang, A., McKeon, F., Kaplan, D.R., and Miller, F.D. (2000). An anti-apoptotic role for the p53 family member, p73, during developmental neuron death. Science *289*, 304–306.

Provance, D.W., Gourley, C.R., Silan, C.M., Cameron, L.C., Shokat, K.M., Goldenring, J.R., Shah, K., Gillespie, P.G., and Mercer, J.A. (2004). Chemical-genetic inhibition of a sensitized mutant myosin Vb demonstrates a role in peripheral-pericentriolar membrane traffic. Proc. Natl. Acad. Sci. U.S.a. *101*, 1868–1873.

Reddy, B.A., and Etkin, L.D. (1991). A unique bipartite cysteine-histidine motif defines a subfamily of potential zinc-finger proteins. Nucleic Acids Research *19*, 6330.

Reinhart, B.J., Slack, F.J., Basson, M., Pasquinelli, A.E., Bettinger, J.C., Rougvie, A.E., Horvitz, H.R., and Ruvkun, G. (2000). The 21-nucleotide let-7 RNA regulates developmental timing in Caenorhabditis elegans. Nature *403*, 901–906.

Reymond, A., Meroni, G., Fantozzi, A., Merla, G., Cairo, S., Luzi, L., Riganelli, D., Zanaria, E., Messali, S., Cainarca, S., *et al.* (2001). The tripartite motif family identifies cell compartments. The EMBO Journal *20*, 2140–2151.

Roy, K., Kuznicki, K., Wu, Q., Sun, Z., Bock, D., Schutz, G., Vranich, N., and Monaghan, A.P. (2004). The Tlx Gene Regulates the Timing of Neurogenesis in the Cortex. Journal of Neuroscience *24*, 8333–8345.

Ruberte, E., Dolle, P., Chambon, P., and Morriss-Kay, G. (1991). Retinoic acid receptors and cellular retinoid binding proteins. II. Their differential pattern of transcription during early morphogenesis in mouse embryos. Development *111*, 45–60.

Ruberte, E., Dolle, P., Krust, A., Zelent, A., Morriss-Kay, G., and Chambon, P. (1990). Specific spatial and temporal distribution of retinoic acid receptor gamma transcripts during mouse embryogenesis. Development *108*, 213–222.

Rudolf, R., Kögel, T., Kuznetsov, S.A., Salm, T., Schlicker, O., Hellwig, A., Hammer, J.A., and Gerdes, H.-H. (2003). Myosin Va facilitates the distribution of secretory granules in the F-actin rich cortex of PC12 cells. Journal of Cell Science *116*, 1339–1348.

Rüdel, S., Flatley, A., Weinmann, L., Kremmer, E., and Meister, G. (2008). A multifunctional human Argonaute2-specific monoclonal antibody. Rna *14*, 1244–1253.

Rybak, A., Fuchs, H., Hadian, K., Smirnova, L., Wulczyn, E.A., Michel, G., Nitsch, R., Krappmann, D., and Wulczyn, F.G. (2009). The let-7 target gene mouse lin-41 is a stem cell specific E3 ubiquitin ligase for the miRNA pathway protein Ago2. Nat Cell Biol *11*, 1411–1420.

Rybak, A., Fuchs, H., Smirnova, L., Brandt, C., Pohl, E.E., Nitsch, R., and Wulczyn, F.G. (2008). A feedback loop comprising lin-28 and let-7 controls pre-let-7 maturation during neural stem-cell commitment. Nat Cell Biol *10*, 987–993.

Saccone, V., Palmieri, M., Passamano, L., Piluso, G., Meroni, G., Politano, L., and Nigro, V. (2008). Mutations that impair interaction properties of TRIM32 associated with limb-girdle muscular dystrophy 2H. Hum. Mutat. *29*, 240–247.

Sato, T., Okumura, F., Kano, S., Kondo, T., Ariga, T., and Hatakeyama, S. (2011). TRIM32 promotes neural differentiation through retinoic acid receptor-mediated transcription. Journal of Cell Science *124*, 3492–3502.

Schmid, P., Lorenz, A., Hameister, H., and Montenarh, M. (1991). Expression of p53 during mouse embryogenesis. Development *113*, 857–865.

Schoser, B.G.H., Frosk, P., Engel, A.G., Klutzny, U., Lochm ller, H., and Wrogemann, K. (2005). Commonality ofTRIM32 mutation in causing sarcotubular myopathy and LGMD2H. Ann Neurol. *57*, 591–595.

Schulman, B.R.M., Esquela-Kerscher, A., and Slack, F.J. (2005). Reciprocal expression of lin-41 and the microRNAs let-7 and mir-125 during mouse embryogenesis. Dev. Dyn. *234*, 1046–1054.

Schwamborn, J.C., Berezikov, E., and Knoblich, J.A. (2009). The TRIM-NHL protein TRIM32 activates microRNAs and prevents self-renewal in mouse neural progenitors. Cell *136*, 913–925.

Schwartz, D.C., and Hochstrasser, M. (2003). A superfamily of protein tags: ubiquitin, SUMO and related modifiers. Trends in Biochemical Sciences *28*, 321–328.

Selbach, M., Schwanhäusser, B., Thierfelder, N., Fang, Z., Khanin, R., and Rajewsky, N. (2008). Widespread changes in protein synthesis induced by microRNAs. Nature *455*, 58–63.

Sempere, L.F., Freemantle, S., Pitha-Rowe, I., Moss, E., Dmitrovsky, E., and Ambros, V. (2004). Expression profiling of mammalian microRNAs uncovers a subset of brain-expressed microRNAs with possible roles in murine and human neuronal differentiation. Genome Biol. *5*, R13.

Sen, G.L., and Blau, H.M. (2005). Argonaute 2/RISC resides in sites of mammalian mRNA decay known as cytoplasmic bodies. Nat Cell Biol *7*, 633–636.

Siegenthaler, J.A., Ashique, A.M., Zarbalis, K., Patterson, K.P., Hecht, J.H., Kane, M.A., Folias, A.E., Choe, Y., May, S.R., Kume, T., et al. (2009). Retinoic acid from the meninges regulates cortical neuron generation. Cell *139*, 597–609.

Slack, F., and Ruvkun, G. (1998a). Heterochronic genes in development and evolution. Biol. Bull. *195*, 375–376.

Slack, F.J., and Ruvkun, G. (1998b). A novel repeat domain that is often associated with RING finger and B-box motifs. Trends in Biochemical Sciences *23*, 474–475.

Slack, F.J., Basson, M., Liu, Z., Ambros, V., Horvitz, H.R., and Ruvkun, G. (2000). The lin-41 RBCC gene acts in the C. elegans heterochronic pathway between the let-7 regulatory RNA and the LIN-29 transcription factor. Molecular Cell *5*, 659–669.

Smirnova, L., Gräfe, A., Seiler, A., Schumacher, S., Nitsch, R., and Wulczyn, F.G. (2005). Regulation of miRNA expression during neural cell specification. Eur. J. Neurosci. *21*, 1469–1477.

Spang, A. On the fate of early endosomes. Biological Chemistry *390*.

Streich, F.C., Ronchi, V.P., Connick, J.P., and Haas, A.L. (2013). Tripartite motif ligases catalyze polyubiquitin chain formation through a cooperative allosteric mechanism. Journal of Biological Chemistry *288*, 8209–8221.

Tahbaz, N., Kolb, F.A., Zhang, H., Jaronczyk, K., Filipowicz, W., and Hobman, T.C. (2004). Characterization of the interactions between mammalian PAZ PIWI domain proteins and Dicer. EMBO Rep *5*, 189–194.

Takahashi, K., and Yamanaka, S. (2006). Induction of Pluripotent Stem Cells from Mouse Embryonic and Adult Fibroblast Cultures by Defined Factors. Cell *126*, 663–676.

Tan, G.S., Garchow, B.G., Liu, X., Yeung, J., Morris, J.P., Cuellar, T.L., McManus, M.T., and Kiriakidou, M. (2009). Expanded RNA-binding activities of mammalian Argonaute 2. Nucleic Acids Research *37*, 7533–7545.

Tao, H., Simmons, B.N., Singireddy, S., Jakkidi, M., Short, K.M., Cox, T.C., and Massiah, M.A. (2008). Structure of the MID1 tandem B-boxes reveals an interaction reminiscent of intermolecular ring heterodimers. Biochemistry *47*, 2450–2457.

Thompson, S., Pearson, A.N., Ashley, M.D., Jessick, V., Murphy, B.M., Gafken, P., Henshall, D.C., Morris, K.T., Simon, R.P., and Meller, R. (2011). Identification of a Novel Bcl-2-interacting Mediator of Cell Death (Bim) E3 Ligase, Tripartite Motif-containing Protein 2 (TRIM2), and Its Role in Rapid Ischemic Tolerance-induced Neuroprotection. Journal of Biological Chemistry *286*, 19331–19339.

Thrower, J.S., Hoffman, L., Rechsteiner, M., and Pickart, C.M. (2000). Recognition of the polyubiquitin proteolytic signal. The EMBO Journal *19*, 94–102.

Traenckner, E.B., Pahl, H.L., Henkel, T., Schmidt, K.N., Wilk, S., and Baeuerle, P.A. (1995). Phosphorylation of human I kappa B-alpha on serines 32 and 36 controls I kappa B-alpha proteolysis and NF-kappa B activation in response to diverse stimuli. The EMBO Journal *14*, 2876–2883.

Trybus, K.M. (2008). Myosin V from head to tail. Cell. Mol. Life Sci. *65*, 1378–1389.

Urano, T., Saito, T., Tsukui, T., Fujita, M., Hosoi, T., Muramatsu, M., Ouchi, Y., and Inoue, S. (2002). Efp targets 14-3-3 sigma for proteolysis and promotes breast tumour growth. Nature *417*, 871–875.

Ventura, A., Young, A.G., Winslow, M.M., Lintault, L., Meissner, A., Erkeland, S.J., Newman, J., Bronson, R.T., Crowley, D., Stone, J.R., *et al.* (2008). Targeted Deletion Reveals Essential and Overlapping Functions of the miR-17~92 Family of miRNA Clusters. Cell *132*, 875–886.

Vertegaal, A.C.O. (2011). Uncovering Ubiquitin and Ubiquitin-like Signaling Networks. Chem. Rev. *111*, 7923–7940.

Viswanathan, S.R., Daley, G.Q., and Gregory, R.I. (2008). Selective Blockade of MicroRNA Processing by Lin28. Science *320*, 97–100.

Waterman, H., Levkowitz, G., Alroy, I., and Yarden, Y. (1999). The RING finger of c-Cbl mediates desensitization of the epidermal growth factor receptor. J. Biol. Chem. *274*, 22151–22154.

Winter, J., and Diederichs, S. (2011). Argonaute proteins regulate microRNA stability: Increased microRNA abundance by Argonaute proteins is due to microRNA stabilization. RNA Biol *8*, 1149–1157.

Worringer, K.A., Rand, T.A., Hayashi, Y., Sami, S., Takahashi, K., Tanabe, K., Narita, M., Srivastava, D., and Yamanaka, S. (2014). The let-7/LIN-41 Pathway Regulates Reprogramming to Human Induced Pluripotent Stem Cells by Controlling Expression of Prodifferentiation Genes.

Cell Stem Cell *14*, 40–52.

Wu, L., and Belasco, J.G. (2005). Micro-RNA Regulation of the Mammalian lin-28 Gene during Neuronal Differentiation of Embryonal Carcinoma Cells. Molecular and Cellular Biology *25*, 9198–9208.

Wulczyn, F.G., Smirnova, L., Rybak, A., Brandt, C., Kwidzinski, E., Ninnemann, O., Strehle, M., Seiler, A., Schumacher, S., and Nitsch, R. (2007). Post-transcriptional regulation of the let-7 microRNA during neural cell specification. The FASEB Journal *21*, 415–426.

Wulczyn, F.G., Cuevas, E., Franzoni, E., and Rybak, A. (2011). miRNAs Need a Trim : Regulation of miRNA Activity by Trim-NHL Proteins. Adv. Exp. Med. Biol. *700*, 85–105.

Xu, N., Papagiannakopoulos, T., Pan, G., Thomson, J.A., and Kosik, K.S. (2009). MicroRNA-145 regulates OCT4, SOX2, and KLF4 and represses pluripotency in human embryonic stem cells. Cell *137*, 647–658.

Yan, Q., Sun, W., Kujala, P., Lotfi, Y., Vida, T.A., and Bean, A.J. (2005). CART: an Hrs/actinin-4/BERP/myosin V protein complex required for efficient receptor recycling. Mol. Biol. Cell *16*, 2470–2482.

Yang, A., Walker, N., Bronson, R., Kaghad, M., Oosterwegel, M., Bonnin, J., Vagner, C., Bonnet, H., Dikkes, P., Sharpe, A., *et al.* (2000). p73-deficient mice have neurological, pheromonal and inflammatory defects but lack spontaneous tumours. Nature *404*, 99–103.

Yi, R., Qin, Y., Macara, I.G., and Cullen, B.R. (2003). Exportin-5 mediates the nuclear export of pre-microRNAs and short hairpin RNAs. Genes & Development *17*, 3011–3016.

Ying, Q.-L., Stavridis, M., Griffiths, D., Li, M., and Smith, A. (2003). Conversion of embryonic stem cells into neuroectodermal precursors in adherent monoculture. Nat Biotechnol *21*, 183–186.

Ylikallio, E., Poyhonen, R., Zimon, M., De Vriendt, E., Hilander, T., Paetau, A., Jordanova, A., Lonnqvist, T., and Tyynismaa, H. (2013). Deficiency of the E3 ubiquitin ligase TRIM2 in early-onset axonal neuropathy. Human Molecular Genetics *22*, 2975–2983.

Zeng, Y., and Cullen, B.R. (2005). Efficient Processing of Primary microRNA Hairpins by Drosha Requires Flanking Nonstructured RNA Sequences. Journal of Biological Chemistry *280*, 27595–27603.

Zhang, X., Zhao, H., Chen, Y., Liu, C., Meng, K., Yang, P., Wang, Y., Wang, G., and Bin Yao (2012). Fish & Shell. Fish and Shellfish Immunology *32*, 621–628.

Zhao, C., Sun, G., Li, S., and Shi, Y. (2009). A feedback regulatory loop involving microRNA-9 and nuclear receptor TLX in neural stem cell fate determination. Nature Structural & Molecular Biology *16*, 365–371.

Zhou, A.-X., Hartwig, J.H., and Akyürek, L.M. (2010). Filamins in cell signaling, transcription and organ development. Trends in Cell Biology *20*, 113–123.

Zou, Y., Chiu, H., Zinovyeva, A., Ambros, V., Chuang, C.-F., and Chang, C. (2013). Developmental decline in neuronal regeneration by the progressive change of two intrinsic timers. Science *340*, 372–376.